Chapter 6
Electroelastic Wave

Abstract In this chapter the electroelastic wave in piezoelectric and pyroelectric materials are discussed. In the electrically quasi-static approximation in an infinite space, there are three independent elastic waves for the piezoelectric material, and there is no independent electric wave. In the pyroelectric material a temperature wave has happened. In the reflection and transmission of waves, the inhomogeneous wave theory is effective; a quasi-surface wave is revealed in the electrically quasi-static approximation. In some particular cases the coupling between elastic equation and Maxwell electrodynamics equation needs to be studied together, and in these cases there are three elastic waves and two electric waves in the piezoelectric material. Surface acoustic waves (SAW) are extensively used in engineering. In order to improve performance of SAW devices, SAW devices may work in a biasing state. In this chapter a small perturbation superposed on finite generalized displacements is discussed in detail, and some surface waves under the biasing state are studied. The inertial entropy theory is used to derive the governing equation of the temperature wave with finite propagation velocity. The general dynamic analyses of interface cracks are given shortly, and some wave scattering problems from a crack tip are also discussed.

Keywords Electroelastic and temperature plane waves • Surface wave • Biasing state • Wave scattering

6.1 Electroelastic Waves in Piezoelectric Materials

6.1.1 Fundamental Equations in Electroelastic Wave

The elastic waves in isotropic and anisotropic materials and electroelastic waves in piezoelectric materials have been discussed in many literatures, such as Fischer (1955), Auld (1973), Dieulesaint and Royer (1980), and Nayfen (1995). Except Sect. 6.8 in this book, we discuss some linear problems in piezoelectric and

Z.-B. Kuang, *Theory of Electroelasticity*, DOI 10.1007/978-3-642-36291-0_6,

pyroelectric materials under the condition of quasi-static electric field. In the linear problem the Maxwell stress is not considered. The constitutive equations are shown in Eq. (3.2), and the generalized momentum equation without generalized body forces in terms of generalized displacements under electrically static condition is

$$C_{ijkl}u_{l,kj} + e_{kij}\varphi_{,kj} = \rho\ddot{u}_i, \quad e_{ikl}u_{l,ki} - \epsilon_{ij}\varphi_{,ji} = 0 \tag{6.1}$$

Equation (6.1) gives the elastic wave equation. The electric displacement does not have its own independent wave, but it propagates following the elastic waves through the constitutive equation.

In this book we only discuss the plane wave, which can be expressed in two forms.

For the generalized displacements $\boldsymbol{U} = [u_1, u_2, u_3, u_4]^{\mathrm{T}}, \quad u_4 = \varphi$ we have

$$\begin{aligned} &U_i = U_{0i}F(k_m x_m - \omega t) = U_{0i}F[k(n_m x_m - ct)], \quad \boldsymbol{U}_0 = [u_{01}, u_{02}, u_{03}, u_{04} = \varphi_0]^{\mathrm{T}} \\ &U_i = U_{0i}F[\omega(L_m x_m - t)], \quad k_m = kn_m, \quad L_m = n_m/c, \quad \omega = kc \end{aligned} \tag{6.2}$$

where $\boldsymbol{U}_0$ is the wave polarization vector or the amplitude vector and the ratio of its components represents the particle displacement direction, ω is the circular frequency, c is the phase velocity, $\boldsymbol{k}$ is the wave vector, $\boldsymbol{L}$ is the slowness vector, and $F(y)$ is a certain function of y. For an ideal piezoelectric material, the energy is not dissipative, so wave vector $\mathbf{k} = k\mathbf{n}$, where $k = 2\pi/\lambda$ is the wave number, λ is the wave length, $\boldsymbol{n}$ is the wave propagation direction Eq. (6.2) yields

$$\ddot{U}_i = U_{0i}\omega^2 F'', \quad u_{l,jk} = u_{0l}k_j k_k F'', \quad \varphi_{,jk} = \varphi_0 k_j k_k F'', \quad E_j = -\varphi_0 k_j F' \tag{6.3}$$

where $F'(y) = \partial F/\partial y$. Substituting Eq. (6.3) into (6.1) yields the Christoffel equation:

$$\begin{aligned} &\rho c^2 u_{0i} = \Gamma_{il}u_{0l} + e_i^*\varphi_0, \quad e_i^* u_{0i} - \epsilon^*\varphi_0 = 0 \\ &\Gamma_{il} = \Gamma_{li} = C_{ijkl}n_j n_k, \quad e_i^* = e_{kij}n_j n_k, \quad \epsilon^* = \epsilon_{jk}n_j n_k \end{aligned} \tag{6.4}$$

or

$$\boldsymbol{\Lambda}(\boldsymbol{k}, c)\boldsymbol{U}_0 = \boldsymbol{0}, \quad \boldsymbol{\Lambda} = \begin{bmatrix} \Gamma_{il} - \rho c^2\delta_{il} & e_i^* \\ e_l^* & -\epsilon^* \end{bmatrix} \tag{6.5}$$

In order for $\boldsymbol{U}_0$ to have nontrivial solution, $\boldsymbol{\Lambda}$ must satisfy the following secular equation:

$$|\boldsymbol{\Lambda}| = \begin{vmatrix} \Gamma_{il} - \rho c^2\delta_{il} & e_i^* \\ e_l^* & -\epsilon^* \end{vmatrix} = \begin{vmatrix} \Gamma_{11} - \rho c^2 & \Gamma_{12} & \Gamma_{13} & e_1^* \\ \Gamma_{21} & \Gamma_{22} - \rho c^2 & \Gamma_{23} & e_2^* \\ \Gamma_{31} & \Gamma_{32} & \Gamma_{33} - \rho c^2 & e_3^* \\ e_1^* & e_2^* & e_3^* & -\epsilon^* \end{vmatrix} = 0 \tag{6.6}$$

where $\boldsymbol{\Gamma}$ is symmetric and called Christoffel tensor. ρc^2 is the eigenvalue, and $\boldsymbol{U}_0$ is the corresponding eigenvector. Eliminating φ_0 from Eq. (6.4) yields

$$\rho c^2 u_{0i} = \bar{\Gamma}_{il} u_{0l}, \quad \left|\bar{\Gamma}_{il} - \rho c^2 \delta_{il}\right| = 0, \quad \bar{\Gamma}_{il} = \Gamma_{il} + e_i^* e_l^* / \epsilon^* \tag{6.7}$$

From Eq. (6.7) it is known that ρc^2 has three roots: $\rho c_1^2, \rho c_2^2, \rho c_3^2$. Corresponding to each ρc_i^2 there is an eigenvector $\boldsymbol{u}_0^{(i)}$ with one undetermined component. Sometimes for convenience we let the undetermined component equal to 1 or adopt the normalized eigenvector $\bar{\boldsymbol{u}}_0^{(i)} \boldsymbol{u}_0^{(j)} = \mathbf{I}$. Equation (6.7) yields

$$\rho c^2 = \frac{\bar{\Gamma}_{il} u_{0i} u_{0l}}{u_{0i} u_{0i}} = \frac{\bar{C}_{ijkl} n_j n_k u_{0i} u_{0l}}{u_{0i} u_{0i}}, \quad \bar{C}_{ijkl} = C_{ijkl} + \frac{(e_{pij} n_p)(e_{qkl} n_q)}{\epsilon_{jk} n_j n_k} \tag{6.8}$$

From Eq. (6.8) it is known that ρc^2 is real, because

$$\begin{aligned} \bar{C}_{ijkl} n_j n_k u_{0i} u_{0l} &= \bar{C}_{ijkl} \left[(u_{0i} n_j + u_{0j} n_i)(u_{0i} n_j - u_{0j} n_i) \right] \left[(u_{0l} n_k + u_{0k} n_l)(u_{0l} n_k - u_{0k} n_l) \right] / 4 \\ &= \bar{C}_{ijkl} (u_{0i} n_j + u_{0j} n_i)(u_{0l} n_k + u_{0k} n_l)/4 \geq 0 \end{aligned}$$

Because ρc^2 is real, there are three orthogonal plane waves. In general $\boldsymbol{u}_0^{(i)}$ is not parallel or perpendicular to the wave propagation direction $\boldsymbol{n}$. The wave $\boldsymbol{u}_0^{(1)}$ closest to $\boldsymbol{n}$ is called the quasi-longitudinal wave, which has the largest phase velocity c_1, while the other two waves $\boldsymbol{u}_0^{(2)}, \boldsymbol{u}_0^{(3)}$ are located on the plane close to the plane perpendicular to $\boldsymbol{n}$ and called the quasi-shear waves with slower velocity c_2 and $c_3 < c_2$.

6.1.2 *Energy Propagation*

According to Eqs. (1.57) and (1.58), the energy equation can be reduced to

$$\begin{aligned} &\frac{\mathrm{d}}{\mathrm{d}t} \int_V \mathfrak{A}_\mathrm{t} \, \mathrm{d}V = -\int_a P_j n_j \, \mathrm{d}a, \quad \mathfrak{A}_\mathrm{t} = \mathfrak{A} + K, \quad P_j = -\sigma_{ij} \dot{u}_i + \varphi \dot{D}_j \\ &\mathfrak{A} = (1/2) C_{ijkl} \varepsilon_{ij} \varepsilon_{kl} + (1/2) \beta_{ij} D_i D_j, \quad K = (1/2) \rho \dot{u}_i \dot{u}_i \\ &\int_a P_j n_j \, \mathrm{d}a = -\int_a (T_i \dot{u}_i + \varphi \sigma) \mathrm{d}a = \int_a (\sigma_{ij} \dot{u}_i - \varphi \dot{D}_j) n_j \, \mathrm{d}a \end{aligned} \tag{6.9}$$

where $\mathfrak{A}_\mathrm{t}$ is the total energy density, $\dot{\mathfrak{A}}_\mathrm{t}$ is the rate of the total energy, $\int_a P_j n_j \mathrm{d}a$ represents the rate of the traversing external energy through the boundary and $\boldsymbol{P}$ is the Poynting vector. In Eq. (6.9) the heat flow is not considered. If $\mathfrak{A}$ is expressed with ε and E, Eq. (6.9) becomes

$$\frac{\mathrm{d}}{\mathrm{d}t}\int_V \mathfrak{A}_\mathrm{t}\,\mathrm{d}V + \int_a P_j n_j\,\mathrm{d}a = 0, \quad P_j = -\sigma_{ij}\dot{u}_i - D_j\dot{\varphi}$$
$$\mathfrak{A} = (1/2)C_{ijkl}\varepsilon_{ij}\varepsilon_{kl} + (1/2)\epsilon_{ij}E_iE_j, \quad K = (1/2)\rho\dot{u}_i\dot{u}_i, \tag{6.10}$$

Define the energy transport velocity $\boldsymbol{V}^\mathrm{e}$ as

$$\boldsymbol{V}^\mathrm{e} = \boldsymbol{P}/g_\mathrm{t} \tag{6.11}$$

Equation (6.4) yields

$$\rho c^2 u_{0i}u_{0i} = \Gamma_{il}u_{0l}u_{0i} + e_i^*\varphi_0 u_{0i} = \Gamma_{il}u_{0l}u_{0i} + \epsilon^*\varphi_0\varphi_0, \quad e_i^*u_{0i}\varphi_0 - \epsilon^*\varphi_0\varphi_0 = 0 \tag{6.12}$$

Equations (6.4), (6.10), and (6.12) yield

$$\mathfrak{A} = (1/2)(C_{ijkl}u_{0i}u_{0l}n_jn_k + \epsilon_{ij}\varphi_0\varphi_0 n_in_j)\left(F'^2/c^2\right) = (1/2)\rho u_{0i}^2F'^2$$
$$K = (1/2)\rho u_{0i}^2F'^2, \quad K + \mathfrak{A} = \rho u_{0i}^2\, F'^2, \quad u_{0i}^2 = u_{0i}u_{0i}{}^2 \tag{6.13}$$
$$P_i = -\sigma_{ij}\dot{u}_j - D_i\dot{\varphi} = (C_{ijkl}u_{0j}u_{0l}n_k + \epsilon_{ij}\varphi_0\varphi_0 n_j)\left(F'^2/c\right)$$

Substitution of Eq. (6.13) into Eq. (6.11) yields

$$V_i^\mathrm{e} = (C_{ijkl}u_{0j}u_{0l}n_k + \epsilon_{ij}\varphi_0\varphi_0 n_j)/\rho u_{0m}^2 c, \quad V_i^\mathrm{e} n_i = c \tag{6.14a}$$

For the normalized displacement vector $(u_{0m}u_{0m} = 1)$, Eq. (6.14a) becomes

$$V_i^\mathrm{e} = (C_{ijkl}u_{0j}u_{0l}n_k + \epsilon_{ij}\varphi_0\varphi_0 n_j)/\rho c, \quad \boldsymbol{V}^\mathrm{e}\cdot\boldsymbol{n} = c \tag{6.14b}$$

where $\boldsymbol{V}^\mathrm{e}$ gives the energy transport direction, the direction of the acoustic ray. The projection of $\boldsymbol{V}^\mathrm{e}$ on $\boldsymbol{n}$ is equal to the phase velocity c, so $|\boldsymbol{V}^\mathrm{e}| \geq c$.

6.1.3 Group Velocity

Usually for a monochromatic wave, Eq. (6.2) is written in a complex number form:

$$u_i = u_{0i}\mathrm{e}^{\mathrm{i}(\boldsymbol{k}\cdot\boldsymbol{x}-\omega t)} = u_{0i}\mathrm{e}^{\mathrm{i}k(\boldsymbol{n}\cdot\boldsymbol{x}-ct)}, \quad \varphi = \varphi_0\mathrm{e}^{\mathrm{i}(\boldsymbol{k}\cdot\boldsymbol{x}-\omega t)} = \varphi_0\mathrm{e}^{\mathrm{i}k(\boldsymbol{n}\cdot\boldsymbol{x}-ct)} \tag{6.15}$$

A general plane wave is dealt with the superposition method. For a chromatic dispersion wave, the wave velocity is dependent to the frequency, and the group velocity is defined as

$$V_j^\mathrm{g} = \partial\omega/\partial k_j, \quad k_j = kn_j \tag{6.16}$$

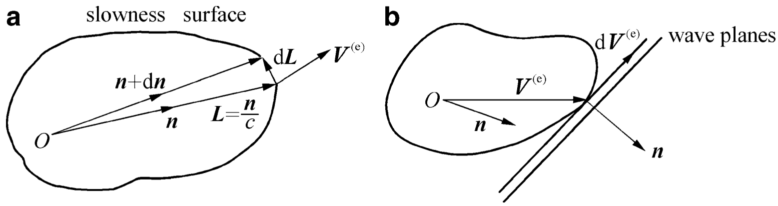

Fig. 6.1 (**a**) Energy velocity is orthogonal to slowness surface. (**b**) Wave surface and propagation direction

Multiplying Eq. (6.7) by k^2 yields

$$\left|\rho(kc)^2\delta_{il} - \left(C_{ijkl}kn_jkn_k + ke_i^*ke_l^*/\epsilon^*\right)\right| = 0 \tag{6.17}$$

It is found that the relation between c and $\left(n_j, e_i^*\right)$ is identical with the relation between $\omega = kc$ and $\left(kn_j, ke_i^*\right)$, so

$$V_j^{\mathrm{g}} = \partial\omega/\partial k_j = \partial(kc)/\partial(kn_j) = \partial c/\partial n_j = V_i^{\mathrm{e}} \tag{6.18}$$

where Eq. (6.12) has been used. Therefore, the energy transport velocity is identical with the group velocity for a non-dissipative plane wave, but for a dissipative plane wave, they may be different.

6.1.4 Characteristic Surfaces

In the illustration of the phenomena of an electroelastic wave propagation, the characteristic surfaces, including the velocity surface, slowness surface, and wave surface, are very useful.

1. *Velocity surface* When the propagation direction is varied, the locus of the ends of the phase velocity vector $\boldsymbol{c} = c\boldsymbol{n}$ forms a velocity surface. In a piezoelectric material there are three different velocities, so there are three velocity surfaces.

2. *Slowness surface* The end of the slowness vector $\boldsymbol{L} = \boldsymbol{n}/c$ draws a slowness surface. $\boldsymbol{L}$ is parallel to $\boldsymbol{c}$ and $Lc = 1, L = |\boldsymbol{L}|$. The slowness surface is important in dealing with reflection and transmission problem in crystals due to similarity with the index surface in optics. The energy transport velocity is always perpendicular to the slowness surface (Fig. 6.1a). In fact we have

$$\begin{aligned}
&\frac{\partial L_i}{\partial n_k} = \frac{\partial(n_i/c)}{\partial n_k} = \frac{\delta_{ik}}{c} - \frac{n_i}{c^2}\frac{\partial c}{\partial n_k} \\
&\boldsymbol{V}^{\mathrm{e}} \cdot \frac{\partial \boldsymbol{L}}{\partial n_k} = V_i^{\mathrm{e}}\frac{\partial L_i}{\partial n_k} = \frac{1}{c}\left(V_k^{\mathrm{e}} - \frac{V_i^{\mathrm{e}} n_i}{c}\frac{\partial c}{\partial n_k}\right) = \frac{1}{c}\left(V_k^{\mathrm{e}} - \frac{\partial c}{\partial n_k}\right) = 0
\end{aligned} \tag{6.19}$$

3. *Wave surface* The wave surface is the locus of the ends of the energy transport velocity. The propagation direction of a plane wave is perpendicular to the wave surface (Fig. 6.1b). In fact according to Eqs. (6.14b) and (6.19) from $\boldsymbol{V}^{\mathrm{e}} \cdot \boldsymbol{L} = 1$, $\boldsymbol{V}^{\mathrm{e}} \cdot \mathrm{d}\boldsymbol{L} = 0$, it can be derived as

$$\boldsymbol{L} \cdot \mathrm{d}\boldsymbol{V}^{\mathrm{e}} = 0, \quad \text{or} \quad \boldsymbol{n} \cdot \mathrm{d}\boldsymbol{V}^{\mathrm{e}} = 0 \tag{6.20}$$

6.1.5 Reflection and Transmission of the Plane Wave in Piezoelectric Materials

In order to save the size of this chapter, the wave propagation in an infinite space and the reflection and transmission problem of the plane wave in piezoelectric materials will be discussed with the thermo-electro-elastic wave in pyroelectric materials together.

6.2 Surface Wave

6.2.1 Surface Waves in Structures

Surface waves have been studied a long time (Gulyaev 1969; Auld 1973; Dieulesaint and Royer 1980; Nayfen 1995). Surface acoustic waves (SAW) including Rayleigh wave, Love wave, Lamb wave, and B-G wave are extensively used in transducers, actuators, filters, delay lines, oscillators, signal processing, acoustic imaging, mobile communication, nondestructive evaluation, biomedical ultrasound, and flow noise. Surface acoustic wave device includes a piezoelectric substrate, at least one interdigital transducer (IDT) disposed on the piezoelectric substrate, an input end and an output end connected to the IDT. The energy of the surface acoustic wave is mainly concentrated near the surface.

1. *Semi-infinite media* In 1885 Rayleigh found a surface wave at the surface of a semi-infinite medium, which is called Rayleigh wave. Rayleigh wave is a complex wave and attenuates along the normal direction of the surface. Its penetration depth is 2λ. In the isotropic media it is constituted of a longitudinal wave (L-wave) and a shear wave (S-wave) with $\pi/2$ phase shift. The transverse surface wave with polarization parallel to the surface cannot happen in an elastic media, but it can happen in a semi-infinite piezoelectric material and called B-G wave (Bleustein 1968; Biryukov et al. 1995), whose penetration depth is about 100λ larger than that in Rayleigh wave.

2. *Bi-semi-infinite media* In a bi-semi-infinite medium, Rayleigh wave can propagate on both sides of the interface and this surface wave is called Stoneley wave.

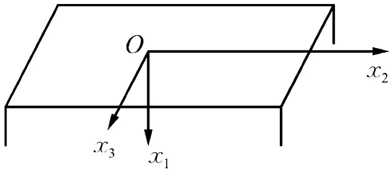

Fig. 6.2 Surface wave propagating in x_1x_2 plane

3. *Infinite plate* For a plate bounded by two parallel infinite planes, when the plate thickness is of the order of the wave length, one gets Lamb waves. Lamb wave possesses longitudinal and shear components, so it can be either symmetric or antisymmetric.

4. *Layer structures* Typically a layer structure is constituted of two or multiple layers of different materials, especially thin films deposited on a thick substrate. When the shear wave velocity of the film is larger than that in the substrate, the Love transverse shear surface wave will be happened.

6.2.2 General Procedure for Solving Surface Wave Problem

Let coordinates ox_i with its origin be at the free surface in a semi-infinite space. A surface wave propagates in (x_1, x_2) plane; x_1 is perpendicular to the free surface (Fig. 6.2). The generalized displacements decrease exponentially in direction x_1, i.e.,

$$u_i = u_{0i}\mathrm{e}^{-kbx_1}\mathrm{e}^{\mathrm{i}k(x_2n_2+x_3n_3-ct)}, \quad \varphi = \varphi_0\mathrm{e}^{-kbx_1}\mathrm{e}^{\mathrm{i}k(x_2n_2+x_3n_3-ct)} \tag{6.21}$$

where $b > 0$ is the unknown attenuated coefficient. Equation (6.21) can also be written as

$$u_i = u_{0i}\mathrm{e}^{\mathrm{i}k(x_jn_j-ct)}, \quad \varphi = \varphi_0\mathrm{e}^{\mathrm{i}k(x_jn_j-ct)}, \quad b = -\mathrm{i}n_1, \quad \mathrm{Im}\, n_1 > 0, \quad j = 1,2,3 \tag{6.22}$$

where n_1 is not the directional cosine, but an unknown related to the attenuated coefficient.

Substituting Eq. (6.22) into Eq. (6.1) yields Eq. (6.4) and the corresponding eigen-equation (6.6), but in the surface wave case, c and n_1 are unknown. Usually let c be a parameter and solve n_1 from the eigen-equation. Because the eigen-equation is an eight-order algebraic equation with real coefficients, n_1 has 4 pairs of complex roots. But there are 4 roots appropriate because Im $n_1 > 0$ is required. Corresponding 4 eigenvalues $n_1^{(r)}, r = 1,2,3,4$, there are 4 group eigenvectors $u_{0i}^{(r)}, \varphi_0^{(r)}$. The general solution is

$$\begin{aligned} u_i &= \sum_{r=1}^{4} A_r u_{0i}^{(r)}\mathrm{e}^{\mathrm{i}k\left(x_jn_j-ct\right)}, \quad \varphi = \sum_{r=1}^{4} A_r\varphi_0^{(r)}\mathrm{e}^{\mathrm{i}k\left(x_jn_j-ct\right)}, \quad j = 1,2,3 \\ u_i &= \sum_{r=1}^{4} A_r u_{0i}^{(r)}\mathrm{e}^{-kb_rx_1}\mathrm{e}^{\mathrm{i}k(x_2n_2+x_3n_3-ct)}, \quad \varphi = \sum_{r=1}^{4} A_r\varphi_0^{(r)}\mathrm{e}^{-kb_rx_1}\mathrm{e}^{\mathrm{i}k(x_2n_2+x_3n_3-ct)} \end{aligned} \tag{6.23}$$

Unknowns c and A_r in Eq. (6.23) are determined by the boundary conditions on the free surface. The boundary conditions on a free surface is

$$\sigma_{i1} = C_{i1kl}u_{k,l} + e_{ki1}\varphi_{,k} = \sum_{r=1}^{4} A_r \sigma_{i1}^{(r)} \mathrm{e}^{\mathrm{i}k(x_2 n_2 + x_3 n_3 - ct)} = 0; \quad \text{when} \quad x_1 = 0$$
$$\sigma_{i1}^{(r)} = -\mathrm{i}k\left(C_{i1kl}n_k u_{0l}^{(r)} + e_{ki1}n_k \varphi_0^{(r)}\right) \tag{6.24}$$

Let the environment of the piezoelectric material be air. In air $\nabla^2\varphi^c = 0$, we can assume

$$\varphi^c = \varphi_0^c \mathrm{e}^{\mathrm{i}k(x_j n_j - ct)}, \quad D_1^c = -\mathrm{i}k\epsilon_0\varphi_0^c \mathrm{e}^{\mathrm{i}k(x_j n_j - ct)} \quad x_1 \geq 0, \quad j = 1, 2, 3$$
$$\varphi^c = \varphi_0^c \mathrm{e}^{\mathrm{i}k(x_2 n_2 + x_3 n_3 - ct)}, \quad D_1^c = -\mathrm{i}k\epsilon_0\varphi_0^c \mathrm{e}^{\mathrm{i}k(x_2 n_2 + x_3 n_3 - ct)}; \quad x_1 = 0\ (n_1 = 1) \tag{6.25}$$

There are two kinds of the electric boundary conditions:

$$\text{Electrically open case}: \quad \varphi = \varphi^c, \quad D_1 = D_1^c, \quad \text{when} \quad x_1 = 0 \tag{6.26a}$$

$$\text{Electrically shorted case}: \quad \varphi^c = 0, \quad \text{when} \quad x_1 = 0 \tag{6.26b}$$

Combining Eqs. (6.24) and (6.26a) or (6.26b), five homogeneous equations with five unknowns A_r, φ_0^c are obtained. In order for A_r, φ_0^c to have nontrivial solutions, the determinant of coefficients before them must be zero. From this condition the wave velocity c and A_r, φ_0^c are obtained. Usually only one c can satisfy condition $\mathrm{Im}n_1 > 0$.

The coupling coefficient k_e is defined as (Laurent et al. 2000)

$$k_\mathrm{e}^2 = U_\mathrm{me}^2/U_\mathrm{m}U_\mathrm{e} = 2(c_\mathrm{f} - c_\mathrm{s})/c_\mathrm{f}(1 + \epsilon^c/\epsilon) \approx 2(c_\mathrm{f} - c_\mathrm{s})/c_\mathrm{f} \tag{6.27}$$

where c_f is the wave velocity under electrically open case and c_s is the wave velocity under electrically shorted case. $U_\mathrm{me}, U_\mathrm{m}, U_\mathrm{e}$ are the mutual electromechanical coupling energy, mechanical energy, and electric energy, respectively.

6.2.3 Surface Waves in a Semi-infinite Piezoelectric Material

Equation (6.23) has three displacement waves and an electric potential. It is a general 3D piezoelectric Rayleigh wave denoted by $\bar{R}_3$. In the material principle coordinate system, the number of the independent material constants will be obviously reduced by crystal symmetry. So the following simpler surface waves will happen:

1. $\Gamma_{13} = \Gamma_{23} = e_1^* = e_2^* = 0$, and Eq. (6.4) or (6.6) splits to the following two equations:

$$\begin{bmatrix} \Gamma_{11} - \rho c^2 & \Gamma_{12} \\ \Gamma_{21} & \Gamma_{22} - \rho c^2 \end{bmatrix} \begin{Bmatrix} u_{01} \\ u_{02} \end{Bmatrix} = \mathbf{0}, \quad \begin{bmatrix} \Gamma_{33} - \rho c^2 & e_3^* \\ e_3^* & -\epsilon^* \end{bmatrix} \begin{Bmatrix} u_{03} \\ \varphi_0 \end{Bmatrix} = \mathbf{0} \quad (6.28)$$

where the first equation represents the pure 2D elastic Rayleigh wave denoted by R_2 and the second equation represents the transverse piezoelectric wave denoted by B-G wave. According to $\Gamma_{13} = \Gamma_{23} = e_1^* = e_2^* = 0$, some relations between material constants can be derived.

2. $\Gamma_{13} = \Gamma_{23} = e_3^* = 0$, and Eq. (6.4) or (6.6) splits to the following two equations:

$$(\Gamma_{33} - \rho c^2) u_{03} = 0, \quad \begin{bmatrix} \Gamma_{11} - \rho c^2 & \Gamma_{12} & e_1^* \\ \Gamma_{21} & \Gamma_{22} - \rho c^2 & e_2^* \\ e_1^* & e_2^* & -\epsilon^* \end{bmatrix} \begin{Bmatrix} u_{01} \\ u_{02} \\ \varphi_0 \end{Bmatrix} = \mathbf{0} \quad (6.29)$$

where the first equation represents the pure elastic transverse shear wave and the second equation represents the 2D piezoelectric Rayleigh wave denoted by $\bar{R}_2$. According to $\Gamma_{13} = \Gamma_{23} = e_3^* = 0$, some relations between material constants can be derived.

Li et al. (2005b) and Li et al. (2005a) adopted the modified Mindlin (1968) polarization gradient theory to discuss the surface wave and showed that the gradient effect can make the surface wave dispersive which is different with the classical linear theory. This phenomenon may be meaningful in high-frequency short surface wave. In the later sections we mainly discuss the surface wave with initial stress or biasing electric field and a few problems about wave scattering from a crack.

6.3 Fundamental Theory of Layered Structure with Generalized Biasing Stresses

6.3.1 A Small Perturbation Superposed on Finite Generalized Displacements

In order to improve performance or select the most suitable operating conditions of SAW devices, such as selectivity of filters, stability of oscillators, and temperature compensation, the generalized biasing displacements or stresses are applied to the SAW devices to establish a biasing state. At the same time because of the material behaviors between the layer and substrate are different, the initial stresses and initial strains in the layer are produced unavoidably during manufacture process. Sometimes the initial stress is great with the magnitude of 1 GPa. The presence of initial stress causes changes in the speed of surface acoustic wave, frequency shift, controlling the selectivity of a filter and temperature compensation of devices, etc. A middle layer in the multilayered structure can be used to adjust the range of phase velocity of SAW and to improve its property (Khuri-Yakub and Kino 1974; Assour et al. 2000).

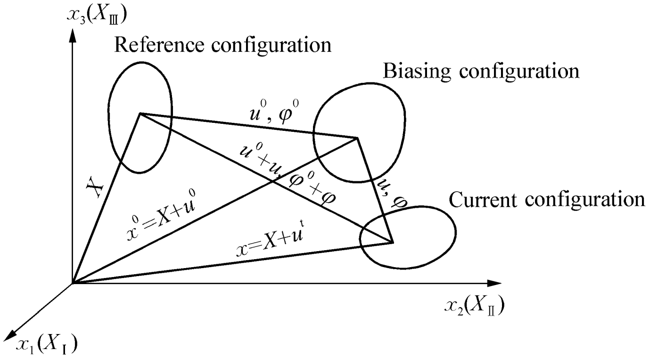

Fig. 6.3 Different configurations in finite deformation

The biasing stress and electric fields usually are large and assumed known, but the external signal or perturbation is small. So the problem is a small perturbation superposed on finite generalized displacements (Tiersten 1978; Sinha et al. 1985; Su et al. 2005). The fundamental theory of finite deformation can be seen in many books (Ogden 1984; Kuang 2002). Some fundamental formulas can be found in Sect. 1.3.4. Take the natural configuration without generalized stress as the reference configuration. In this theoretical part the notations shown in Sect. 1.3.4 are adopted. The same coordinate system in the current and initial configurations is taken, i.e., $x_I = x_i$, so that for the case without differential symbol, we have $\bar{\sigma}_{IJ} = \bar{\sigma}_{ij}$, but the differentiation with the capital or small letter subscript is different. Let $\bar{\boldsymbol{\sigma}}^0, \bar{\boldsymbol{\varepsilon}}^0, \bar{\boldsymbol{D}}^0, \bar{\boldsymbol{E}}^0, \boldsymbol{u}^0, \varphi^0, \bar{\boldsymbol{f}}^0, \bar{\boldsymbol{T}}^0, \bar{\rho}_{\mathrm{e}}^0, \bar{\sigma}^{*0}$ be variables in the biasing state. The small perturbation variables in the reference configuration are denoted with $\bar{\boldsymbol{\sigma}}, \bar{\boldsymbol{\varepsilon}}, \bar{\boldsymbol{D}}, \bar{\boldsymbol{E}}, \boldsymbol{u}, \varphi, \bar{\boldsymbol{f}}, \bar{\boldsymbol{T}}, \bar{\rho}_{\mathrm{e}}, \bar{\sigma}^*$ (Fig. 6.3), where $\bar{\boldsymbol{\sigma}}$ is the Kirchhoff stress and $\bar{\boldsymbol{\varepsilon}}$ is the Green strain. The current total variables described in the reference configuration are

$$\text{Generalized geometric equation:} \quad \bar{\varepsilon}_{KL}^t = (1/2)\left(u_{K,L}^t + u_{L,K}^t + u_{M,K}^t u_{M,L}^t\right); \quad \bar{E}_I^t = -\varphi_{,I}^t \tag{6.30}$$

$$\text{Generalized motion equation:} \quad \left(\bar{\sigma}_{KM}^t \delta_{lM} + \bar{\sigma}_{KM}^t u_{l,M}^t\right)_{,K} + \bar{f}_l^t = \bar{\rho}\ddot{u}_l^t; \quad \bar{D}_{I,I}^t = \bar{\rho}_{\mathrm{e}}^t \tag{6.31}$$

$$\text{Boundary conditions:} \quad x_{l,M}\bar{\sigma}_{KM}^t \bar{n}_K^t = \bar{T}_l^{*t}, \quad \bar{D}_K^t \bar{n}_K^t = -\bar{\sigma}^{*t}, \quad \text{or} \quad u_i^t = u_i^{t*}, \quad \varphi^t = \varphi^{t*} \tag{6.32}$$

where

$$\begin{aligned} &\bar{\boldsymbol{\sigma}}^t = \bar{\boldsymbol{\sigma}}^0 + \bar{\boldsymbol{\sigma}}, \quad \bar{\boldsymbol{D}}^t = \bar{\boldsymbol{D}}^0 + \bar{\boldsymbol{D}}, \quad \boldsymbol{u}^t = \boldsymbol{u}^0 + \boldsymbol{u}, \quad \boldsymbol{x} = \boldsymbol{X} + \boldsymbol{u}^t, \quad \boldsymbol{x}^0 = \boldsymbol{X} + \boldsymbol{u}^0 \\ &\bar{\boldsymbol{f}}^t = \bar{\boldsymbol{f}}^0 + \bar{\boldsymbol{f}}, \quad \bar{\boldsymbol{T}}^t = \bar{\boldsymbol{T}}^0 + \bar{\boldsymbol{T}}, \quad \bar{\rho}_{\mathrm{e}}^t = \bar{\rho}_{\mathrm{e}}^0 + \bar{\rho}_{\mathrm{e}}, \quad \bar{\sigma}^{*t} = \bar{\sigma}^{*0} + \bar{\sigma}^*, \quad \varphi^t = \varphi^0 + \varphi \end{aligned} \tag{6.33}$$

Because the biasing state is an equilibrium state, so

$$\begin{aligned}&(\bar{\sigma}^0_{KM}\delta_{lM} + \bar{\sigma}^0_{KM}u^0_{l,M})_{,K} + \bar{f}^0_l = 0, \quad \bar{D}^0_{I,I} = \bar{\rho}^0_e \\ &\left(\delta_{lM} + u^0_{l,M}\right)\bar{\sigma}^0_{KM}\bar{n}^0_K = \bar{T}^{*0}_l, \quad \bar{D}^0_K\bar{n}^0_K = -\bar{\sigma}^{*0}\end{aligned} \tag{6.34}$$

Subtracting the first equation in Eq. (6.34) from Eq. (6.31) and ignoring small terms in high order, such as $u_{m,K}u_{m,L}$, we find

$$\left(\bar{\sigma}_{KM}\delta_{lM} + \bar{\sigma}_{KM}u^0_{l,M} + \bar{\sigma}^0_{KM}u_{l,M}\right)_{,K} + \bar{f}_l = \rho_0\ddot{u}_l; \quad \bar{D}_{K,K} = \bar{\rho}_\mathrm{e} \tag{6.35}$$

Subtracting the second equation in Eq. (6.34) from Eq. (6.32) yields

$$\begin{aligned}&\left(\bar{\sigma}_{Kl} + \bar{\sigma}^0_{KM}u_{l,M} + u^0_{l,M}\bar{\sigma}_{KM}\right)\bar{n}^t_K + \left(\bar{n}^t_K - \bar{n}^0_K\right)\left(\bar{\sigma}^0_{Kl} + \bar{\sigma}^0_{KM}u^0_{l,M}\right) = \bar{T}_l \\ &\bar{D}_K\bar{n}^t_K + \bar{D}^0_K\left(\bar{n}^t_K - \bar{n}^0_K\right) = -\bar{\sigma}^*\end{aligned} \tag{6.36}$$

From Eq. (1.45) we can derive

$$\bar{n}^0_K = \left|\partial X_I \big/ \partial x^0_j\right|\left(\partial x^0_i/\partial X_K\right)n_i\mathrm{d}a\big/\mathrm{d}\bar{a}^0, \quad \bar{n}^t_K = \left|\partial X_I/\partial x_j\right|(\partial x_i/\partial X_K)n_i\mathrm{d}a/\mathrm{d}\bar{a}^t$$

The change of the normal of the boundary can only be obtained after solving the problem. But usually the difference between $\bar{n}^t_k$ and $\bar{n}^0_k$ is small and let $\bar{n}^t_k = \bar{n}^0_k$ to simplify the boundary conditions.

Sometimes the three-order coefficients in the constitutive equation are needed. Let

$$\begin{aligned}&\bar{\sigma}^t_{IJ} = C_{IJKL}\bar{\varepsilon}^t_{KL} + (1/2)C_{IJKLMN}\bar{\varepsilon}^t_{KL}\bar{\varepsilon}^t_{MN} - e_{MIJ}\bar{E}^t_M - e_{MIJKL}\bar{\varepsilon}^t_{KL}\bar{E}^t_M - (1/2)l_{MNIJ}\bar{E}^t_M\bar{E}^t_N \\ &\bar{D}^t_M = \epsilon_{MN}\bar{E}^t_N + (1/2)\epsilon_{MNJ}\bar{E}^t_N\bar{E}^t_J + e_{MIJ}\bar{\varepsilon}^t_{IJ} + (1/2)e_{MIJKL}\bar{\varepsilon}^t_{IJ}\bar{\varepsilon}^t_{KL} + l_{MNIJ}\bar{\varepsilon}^t_{IJ}\bar{E}^t_N\end{aligned} \tag{6.37}$$

Similarly for the biasing state, we have

$$\begin{aligned}&\bar{\sigma}^0_{IJ} = C_{IJKL}\bar{\varepsilon}^0_{KL} + (1/2)C_{IJKLMN}\bar{\varepsilon}^0_{KL}\bar{\varepsilon}^0_{MN} - e_{MIJ}\bar{E}^0_M - e_{MIJKL}\bar{\varepsilon}^0_{KL}\bar{E}^0_M - (1/2)l_{MNIJ}\bar{E}^0_M\bar{E}^0_N \\ &\bar{D}^0_M = \epsilon_{MN}\bar{E}^0_N + (1/2)\epsilon_{MNJ}\bar{E}^0_N\bar{E}^0_J + e_{MIJ}\bar{\varepsilon}^0_{IJ} + (1/2)e_{MIJKL}\bar{\varepsilon}^0_{IJ}\bar{\varepsilon}^0_{KL} + l_{MNIJ}\bar{\varepsilon}^0_{IJ}\bar{E}^0_N\end{aligned} \tag{6.38}$$

Subtracting Eq. (6.38) from (6.37) and neglecting the small terms in higher order, such as $u_{M,K}u_{M,L}$, $u^0_{P,N}u^0_{K,M}u_{K,L}$, then we get the results that are expressed in terms of generalized displacements:

$$\bar{\sigma}_{IJ} = \hat{C}_{IJKL}u_{K,L} + \hat{e}_{MIJ}\varphi_{,M}, \quad \bar{D}_K = e^*_{KIJ}u_{I,J} - \epsilon^*_{KN}\varphi_{,N} \tag{6.39}$$

where

$$
\begin{aligned}
&\hat{C}_{IJKL} = C_{IJKL} + C_{IJML}u^0_{K,M} + C_{IJKLMN}u^0_{K,L} + e_{MIJKL}\varphi^0_{,M} \\
&\hat{e}_{MIJ} = e_{MIJ} + e_{MIJKL}u^0_{K,L} - l_{MNIJ}\varphi^0_{,N} \\
&e^*_{MIJ} = e_{MIJ} + e_{MNJ}u^0_{I,N} + e_{MIJKL}u^0_{K,L} - l_{MNIJ}\varphi^0_{,N} \\
&\epsilon^*_{MN} = \epsilon_{MN} - \epsilon_{MNJ}\varphi^0_{,J} + l_{MNIJ}u^0_{I,J}
\end{aligned}
\tag{6.40}
$$

Substitution of Eq. (6.39) into Eqs. (6.35) and (6.36) finally yields

$$
\begin{aligned}
&\left(\bar{\sigma}^*_{Kl} + \bar{\sigma}^0_{KM}u_{l,M}\right)_{,K} + \bar{f}_l = \rho_0\ddot{u}_l, \quad \bar{D}_{K,K} = \bar{\rho}_{\mathrm{e}} \\
&\left(\sigma^*_{Kl} + \sigma^0_{KM}u_{l,M}\right)n_K = \bar{T}^*_l, \quad \bar{D}_K n_K = -\bar{\sigma}^*
\end{aligned}
\tag{6.41}
$$

where C^*_{KlPJ}, e^*_{KPJ}, etc. are effective material constants and

$$
\begin{aligned}
&\bar{\sigma}^*_{Kl} = \bar{\sigma}_{KM}\left(\delta_{lM} + u^0_{l,M}\right) = C^*_{KlPJ}u_{P,J}, \quad \bar{D}_K = e^*_{KPJ}u_{P,J}; \quad P = 1,2,3,4 \\
&C^*_{KlIJ} = \hat{C}_{KMIJ}\left(\delta_{lM} + u^0_{l,M}\right), \quad C^*_{Kl4J} = \hat{e}_{JKM}\left(\delta_{lM} + u^0_{l,M}\right), \quad u_{4,J} = \varphi_{,J} \\
&\bar{D}_K = e^*_{KPJ}u_{P,J}, \quad e^*_{KIJ} = e^*_{KIJ}, \quad e^*_{K4J} = -\epsilon^*_{KN}
\end{aligned}
\tag{6.42}
$$

where the capital letter subscript P takes the value $1, 2, 3, 4$. Equation (6.41) can also be rewritten as

$$
\begin{aligned}
&\left(C^{**}_{KlIJ}u_{I,J} + e^{**}_{NKl}\varphi_{,N}\right)_{,K} + \bar{f}_l = \rho_0\ddot{u}_l, \quad \left(e^*_{KIJ}u_{I,J} - \epsilon^*_{KN}\varphi_{,N}\right)_{,K} = \rho_{\mathrm{e}} \\
&\left(C^{**}_{KlIJ}u_{I,J} + e^{**}_{NKl}\varphi_{,N}\right)\bar{n}^t_K = \bar{T}_j, \quad \left(e^*_{KIJ}u_{I,J} - \epsilon^*_{KN}\varphi_{,N}\right)\bar{n}^t_K = -\bar{\sigma}^* \\
&C^{**}_{KlIJ} = C^*_{KlIJ} + \bar{\sigma}^0_{KJ}\delta_{Il}, \quad e^{**}_{NKl} = \hat{e}_{NKM}\left(\delta_{lM} + u^0_{l,M}\right) \approx e^*_{NKl}
\end{aligned}
\tag{6.43}
$$

When $\boldsymbol{u}, \varphi$ are solved, $\bar{\boldsymbol{\sigma}}, \bar{\boldsymbol{D}}$ is obtained; then from Eq. (1.45) the generalized Cauchy stresses $\boldsymbol{\sigma}, \boldsymbol{D}$ can be obtained.

6.3.2 *Simplifications of the Governing Equations for Some Cases*

1. *Initial stress configuration taken as reference configuration* If we use the configuration with initial stress as the reference configuration, then $\boldsymbol{u}^0, \varphi^0$ are not needed or let $\boldsymbol{u}^0 = \boldsymbol{0}, \varphi^0 = 0$ and $\bar{\sigma}^*_{Kl} = \bar{\sigma}_{KM} = \sigma_{kl}, \bar{D}_K = D_k$, so formulas are much simpler. But the material coefficients must take the "tangent modulus," or the constitutive equations are measured at the state with given generalized biasing

displacements and stresses. The total generalized stress and displacements are the sum of the initial values and the perturbation values.

2. *Small initial generalized displacements* If the initial generalized displacements and stresses are also small, i.e., $\boldsymbol{u}^0 + \boldsymbol{u}, \varphi^0 + \varphi$ are small compared with 1, the terms containing them can be neglected, so all generalized stress $\bar{\boldsymbol{\sigma}}^* = \boldsymbol{\sigma}, \bar{\boldsymbol{D}} = \boldsymbol{D}$.

6.4 Love Wave in ZnO/SiO$_2$/Si Structure with Initial Stresses

6.4.1 Transfer Matrix Method

Figure 6.4 shows a three-layer structure constituted of the substrate Si, the first layer SiO$_2$ of thickness h_1 and the second layer ZnO of thickness h_2 and $h_1 + h_2 = h$. The origin of the global coordinate system is located at interface of the substrate and first layer. The top surface of the layer $x_1 = -h$ is free of stress and the environment is air. Experiments show that the distribution of initial stresses along the depth x_1 in the layers is shown in Fig. 6.4. The thickness of the substrate is much larger than that of layers and can be treated as a half-space. The initial stresses in the substrate are negligible. In order to obtain more exact solution, the first layer is further divided into $1 \sim m$ sublayers, and the second layer is divided into $m + 1 \sim N$ sublayers. The substrate is denoted by layer 0 and the air is denoted by layer $N + 1$ (Fig. 6.5).

For a multilayer structure the transfer matrix method is a useful technique (Thomson 1950; Stewart and Yong 1994; Liu et al. 2003b; Su et al. 2005). The basis of the transfer matrix method is that for any sublayer k to establish, a transfer matrix maps the generalized stresses and displacements from its lower surface to upper surface. Successive application of the transfer method through sublayer 0 to $N + 1$ and invoking corresponding interface continuity conditions leads to a set of equations relating to the boundary conditions on the free surface. Combining the conditions at infinity, we can get enough equations to solve

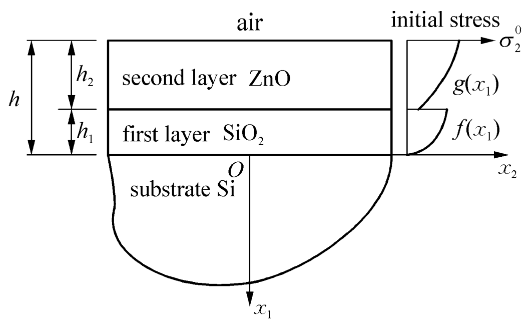

Fig. 6.4 Three-layer structure

Fig. 6.5 Layered structure divided into N sublayers

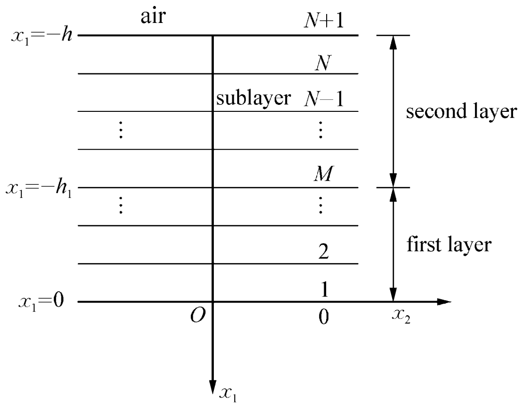

the problem. The state space approach with appropriate selected variables is a convenient method to establish the transfer matrix. Here $u_i, \varphi, \sigma_{i1}, D_1$ are used as state variables. For convenience in the following part, the subscripts all adopt the small letters except the capital letter P which takes the value 1, 2, 3, 4. It is noted that in this part the differentiation with a small letter is still considered in the reference configuration. According to the first equation in Eq. (6.41), in each sublayer we have

$$\bar{\sigma}^*_{i1,1} = \rho_0 \ddot{u}_i - \bar{\sigma}^*_{i2,2} - \bar{\sigma}^*_{i3,3} - \bar{\sigma}^0_{jk} u_{i,jk} - \bar{\sigma}^0_{jk,j} u_{i,k} \tag{6.44}$$

Assuming the incident wave is located in the plane x_2x_3, the solution of the generalized displacement U_P $(P = 1, 2, 3, 4)$ is

$$U_P = A_P(x_1) \exp[\mathrm{i}(k_2x_2 + k_3x_3 - \omega t)] = A_P(x_1) \exp[\mathrm{i}(k_\alpha x_\alpha - \omega t)], \quad \alpha = 2, 3 \tag{6.45}$$

Substitution of Eqs. (6.45) and (6.42) into Eq. (6.44) yields

$$\begin{aligned} \bar{\sigma}^*_{i1,1} = \Big\{ & -\rho_0 \omega^2 A_i - \mathrm{i}k_\beta \Big(C^*_{i\beta P1} A_{P,1} + \mathrm{i}k_\gamma C^*_{i\beta P\gamma} A_P \Big) - \bar{\sigma}^0_{11} A_{i,11} - 2\mathrm{i}k_\gamma \bar{\sigma}^0_{1\gamma} A_{i,1} \\ & + k_\beta k_\gamma \bar{\sigma}^0_{\beta\gamma} A_i - \bar{\sigma}^0_{j1,j} A_{i,1} - \mathrm{i}k_\beta \bar{\sigma}^0_{j\beta,j} A_i \Big\} \exp[\mathrm{i}(k_\alpha x_\alpha - \omega t)] \end{aligned} \tag{6.46}$$

Usually $\bar{\sigma}^0_{11}, \bar{\sigma}^0_{12}, \bar{\sigma}^0_{13}$ are small and can be dropped. Let

$$\bar{\sigma}^*_{ij} = \hat{\sigma}_{ij}(x_1) \exp[\mathrm{i}(k_\alpha x_\alpha - \omega t)], \quad \bar{D}_i = T_{i+6}(x_1) \exp[\mathrm{i}(k_\alpha x_\alpha - \omega t)] \tag{6.47}$$

Equation (6.46) can be rewritten as

$$\hat{\sigma}_{i1,1} + \mathrm{i}k_\beta C^*_{i\beta P1} A_{P,1} + \bar{\sigma}^0_{j1,j} A_{i,1} = \left(-\rho_0\omega^2 + k_\beta k_\gamma \bar{\sigma}^0_{\beta\gamma} - \mathrm{i}k_\beta \bar{\sigma}^0_{j\beta,j}\right) A_i + k_\beta k_\gamma C^*_{i\beta P\gamma} A_P \tag{6.48a}$$

The second equation in Eq. (6.41) and Eq. (6.42) can also be expressed as

$$\begin{aligned} &T_{7,1} + \mathrm{i}k_\beta e^*_{\beta p1} A_{P,1} = k_\beta k_\gamma e^*_{\beta p\gamma} A_P \\ &C^*_{1jP1} A_{P,1} = \hat{\sigma}_{j1} - \mathrm{i}k_\beta C^*_{1jP\beta} A_P, \quad e^*_{1P1} A_{P,1} = T_7 - \mathrm{i}k_\beta e^*_{1P\beta} A_P \end{aligned} \tag{6.48b}$$

Introduce (in Voigt notation)

$$\sigma_n = T_n(x_1)\exp[\mathrm{i}(k_\alpha x_\alpha - \omega t)], \quad n = 1, 2, \ldots, 6 \tag{6.49}$$

where $\sigma_n (n = 1, 2, \ldots, 6)$ represents $\sigma_{11}, \sigma_{22}, \sigma_{33}, \sigma_{32}, \sigma_{31}, \sigma_{12}$, respectively, and let $\hat{\sigma}_{i1} = T_1$, $\hat{\sigma}_{i2} = T_6$, and $\hat{\sigma}_{i3} = T_5$. Introduce an eight-dimensional vector $\boldsymbol{v}_m$:

$$\boldsymbol{v}_m(x_1) = [A_{1m}, A_{2m}, A_{3m}, A_{4m}, T_{1m}, T_{6m}, T_{5m}, T_{7m}]^{\mathrm{T}} \tag{6.50}$$

where A_{1m}, A_{2m}, A_{3m} are the amplitudes of u_1, u_2, u_3, respectively; A_{4m} is the amplitude of φ; T_{1m}, T_{6m}, T_{5m} are the amplitudes of $\sigma_{11}, \sigma_{21}, \sigma_{31}$, respectively; and T_{7m} is the amplitude of D_1. Using Eqs. (6.48a) and (6.48b) for any sublayer k, the eight-dimensional state equation with unknown vector $\boldsymbol{v}_m$ is

$$\left[\boldsymbol{B}_m(x_1)\frac{\mathrm{d}}{\mathrm{d}x_1} - \boldsymbol{F}_m(x_1)\right]\boldsymbol{v}_m(x_1) = \boldsymbol{0}, \quad \text{or} \quad \left[\frac{\mathrm{d}}{\mathrm{d}x_1} - \boldsymbol{B}_m^{-1}(x_1)\boldsymbol{F}_m(x_1)\right]\boldsymbol{v}_m(x_1) = \boldsymbol{0} \tag{6.51}$$

where $\boldsymbol{B}_m^{-1}(x_1)\boldsymbol{F}_m(x_1)$ is the state matrix of the sublayer k and

$$\boldsymbol{B}_m = \begin{bmatrix} B_m(11) & \mathrm{i}k_\beta C^*_{1\beta 21} & \mathrm{i}k_\beta C^*_{1\beta 31} & \mathrm{i}k_\beta C^*_{1\beta 41} & 1 & 0 & 0 & 0 \\ \mathrm{i}k_\beta C^*_{2\beta 11} & B_m(22) & \mathrm{i}k_\beta C^*_{2\beta 31} & \mathrm{i}k_\beta C^*_{2\beta 41} & 0 & 1 & 0 & 0 \\ \mathrm{i}k_\beta C^*_{3\beta 11} & \mathrm{i}k_\beta C^*_{3\beta 21} & B_m(33) & \mathrm{i}k_\beta C^*_{3\beta 41} & 0 & 0 & 1 & 0 \\ \mathrm{i}k_\beta e^*_{\beta 11} & \mathrm{i}k_\beta e^*_{\beta 21} & \mathrm{i}k_\beta e^*_{\beta 31} & \mathrm{i}k_\beta e^*_{\beta 41} & 0 & 0 & 0 & 1 \\ C^*_{1111} & C^*_{1121} & C^*_{1131} & C^*_{1141} & 0 & 0 & 0 & 0 \\ C^*_{1211} & C^*_{1221} & C^*_{1231} & C^*_{1241} & 0 & 0 & 0 & 0 \\ C^*_{1311} & C^*_{1321} & C^*_{1331} & C^*_{1341} & 0 & 0 & 0 & 0 \\ e^*_{111} & e^*_{121} & e^*_{131} & e^*_{141} & 0 & 0 & 0 & 0 \end{bmatrix}$$

$$B_m(11) = \sigma^0_{j1,j} + \mathrm{i}k_\beta c^*_{1\beta 11}, \quad B_m(22) = \sigma^0_{j1,j} + \mathrm{i}k_\beta c^*_{2\beta 21}, \quad B_m(33) = \sigma^0_{j1,j} + \mathrm{i}k_\beta c^*_{3\beta 31} \tag{6.52}$$

and

$$\boldsymbol{F}_m = \begin{bmatrix} F_m(11) & k_\beta k_\gamma C^*_{1\beta 2\gamma} & k_\beta k_\gamma C^*_{132\gamma} & k_\beta k_\gamma C^*_{1\beta 4\gamma} & 0 & 0 & 0 & 0 \\ k_\beta k_\gamma C^*_{2\beta 1\gamma} & F_m(22) & k_\beta k_\gamma C^*_{2\beta 3\gamma} & k_\beta k_\gamma C^*_{2\beta 4\gamma} & 0 & 0 & 0 & 0 \\ k_\beta k_\gamma C^*_{3\beta 1\gamma} & k_\beta k_\gamma C^*_{3\beta 2\gamma} & F_m(33) & k_\beta k_\gamma C^*_{3\beta 4\gamma} & 0 & 0 & 0 & 0 \\ k_\beta k_\gamma e^*_{\beta 1\gamma} & k_\beta k_\gamma e^*_{\beta 2\gamma} & k_\beta k_\gamma e^*_{\beta 3\gamma} & k_\beta k_\gamma e^*_{\beta 4\gamma} & 0 & 0 & 0 & 0 \\ -\mathrm{i}k_\beta C^*_{111\beta} & -\mathrm{i}k_\beta C^*_{112\beta} & -\mathrm{i}k_\beta C^*_{113\beta} & -\mathrm{i}k_\beta C^*_{114\beta} & 1 & 0 & 0 & 0 \\ -\mathrm{i}k_\beta C^*_{121\beta} & -\mathrm{i}k_\beta C^*_{122\beta} & -\mathrm{i}k_\beta C^*_{123\beta} & -\mathrm{i}k_\beta C^*_{124\beta} & 0 & 1 & 0 & 0 \\ -\mathrm{i}k_\beta C^*_{131\beta} & -\mathrm{i}k_\beta C^*_{132\beta} & -\mathrm{i}k_\beta C^*_{133\beta} & -\mathrm{i}k_\beta C^*_{134\beta} & 0 & 0 & 1 & 0 \\ -\mathrm{i}k_\beta e^*_{11\beta} & -\mathrm{i}k_\beta e^*_{12\beta} & -\mathrm{i}k_\beta e^*_{13\beta} & -\mathrm{i}k_\beta e^*_{14\beta} & 0 & 0 & 0 & 1 \end{bmatrix} \tag{6.53}$$

$$F_m(11) = -\rho_0\omega^2 + k_\beta k_\gamma \sigma^0_{\beta\gamma} - \mathrm{i}k_\beta \sigma^0_{j\beta,j} + k_\beta k_\gamma c^*_{1\beta 1\gamma}$$
$$F_m(22) = -\rho_0\omega^2 + k_\beta k_\gamma \sigma^0_{\beta\gamma} - \mathrm{i}k_\beta \sigma^0_{j\beta,j} + k_\beta k_\gamma c^*_{2\beta 2\gamma}$$
$$F_m(33) = -\rho_0\omega^2 + k_\beta k_\gamma \sigma^0_{\beta\gamma} - \mathrm{i}k_\beta \sigma^0_{j\beta,j} + k_\beta k_\gamma c^*_{3\beta 3\gamma}$$

The solution of Eq. (6.51) is

$$\begin{aligned} &\boldsymbol{v}_m(x_1) = \boldsymbol{Q}_m \boldsymbol{R}_m \boldsymbol{a}_m, \quad \boldsymbol{R}_m = \mathrm{diag}[\exp(b_{1m}x_1), \exp(b_{2m}x_1), \ldots, \exp(b_{8m}x_1)] \\ &\boldsymbol{Q}_m = [h_{1m}, h_{2m}, \ldots, h_{8m}], \quad \boldsymbol{a}_m = [a_{1m}, a_{2m}, \ldots, a_{8m}]^{\mathrm{T}} \end{aligned} \tag{6.54}$$

where b_{jm} and h_{jm} are the eigenvalue and eigenvector of the state matrix, respectively, and a_{jm} is an undetermined constant in the sublayer m. The generalized stresses and displacements at the bottom of the structure can be related to those at its top through the transfer matrix $\boldsymbol{P}_m(x_{1m} - d_m, x_{1m})$:

$$\boldsymbol{v}_m(x_{1m} - d_m) = \boldsymbol{P}_m(x_{1m} - d_m, x_{1m})\boldsymbol{v}_m(x_{1m}) \tag{6.55}$$

Equations (6.54) and (6.55) yield

$$\boldsymbol{P}_m(x_{1m} - d_m, x_{1m}) = \boldsymbol{Q}_m \boldsymbol{R}_m(-d_m)\boldsymbol{Q}_m^{-1} \tag{6.56}$$

where x_{1m} is the coordinate at the bottom surface of the sublayer m and d_m is its thickness. Using the basic relations of the transfer matrix, it is found

$$\boldsymbol{P}(x'_1, x_1) = \boldsymbol{P}\left(x'_1, x''_1\right)\boldsymbol{P}\left(x''_1, x_1\right) \tag{6.57}$$

This leads to

$$\boldsymbol{P}(-h, 0) = \prod_{m=1}^{N} \boldsymbol{P}_m(x_{1m} - d_m, x_{1m}), \quad \boldsymbol{v}_N(-h) = \boldsymbol{P}(-h, 0)\ \boldsymbol{v}_0(0) \tag{6.58}$$

where $\boldsymbol{v}_N(-h)$ and $\boldsymbol{v}_1(0)$ are the state vectors at the upper and lower surfaces of the structure, respectively.

6.4.2 Love Wave in Zno/SiO$_2$/Si Structure with Initial Stress

Figure 6.4 shows a ZnO/SiO$_2$/Si multilayer structure. SiO$_2$ and Si are isotropic elastic materials, and ZnO is a transverse isotropic piezoelectric material with poling direction along x_3. In a transversely isotropic piezoelectric material, the number of material constants is only ten: $C_{11} = C_{22}, C_{12}, C_{13} = C_{23}, C_{33}, C_{44} = C_{55}$, $C_{66} = (C_{11} - C_{12})/2, e_{31} = e_{32}, e_{15} = e_{24}, e_{33}, \epsilon_{11} = \epsilon_{22}, \epsilon_{33}$ Let the biasing stresses be $\sigma^0_{33}(x_1)$ and $\sigma^0_{22}(x_1)$. Other stress components and the biasing potential φ^0 is assumed to be zero. Love wave is a transverse shear wave, so only $u_3(x_1, x_2, t)$ and $\varphi(x_1, x_2, t)$ are not zero. Let Love wave propagate along the positive direction of x_2, so only $k_2 = k$ is not zero. In this case Eqs. (6.50), (6.52), and (6.53) are simplified to

$$
\begin{gathered}
\boldsymbol{v}_m(x_3) = [A_{3m}, A_{4m}, T_{5m}, T_{7m}]^{\mathrm{T}} \\
\boldsymbol{B}_m = \begin{bmatrix} \mathrm{i}kC^*_{45} & \mathrm{i}ke^*_{14} & 1 & 0 \\ \mathrm{i}ke^*_{25} & -\mathrm{i}k\,\epsilon^*_{21} & 0 & 1 \\ C^*_{55} & e^*_{15} & 0 & 0 \\ e^*_{15} & -\epsilon^*_{11} & 0 & 0 \end{bmatrix}, \quad \boldsymbol{F}_m = \begin{bmatrix} -\rho_0\omega^2 + \left(C^*_{44} + \sigma^0_{22}\right)k^2 & e^*_{24}k^2 & 0 & 0 \\ e^*_{24}k^2 & -\epsilon^*_{22}k^2 & 0 & 0 \\ -\mathrm{i}kC^*_{54} & -\mathrm{i}ke^*_{25} & 1 & 0 \\ -\mathrm{i}ke^*_{14} & \mathrm{i}k\,\epsilon^*_{12} & 0 & 1 \end{bmatrix}
\end{gathered} \tag{6.59}
$$

where effective material constants can be calculated from Eq. (6.42). For ZnO and SiO$_2$, $C_{45} = C_{54} = e_{14} = e_{25} = \epsilon_2 = \epsilon_1 = 0$, so for small initial stresses it yields

$$
\boldsymbol{B}_m = \begin{bmatrix} 0 & 0 & 1 & 0 \\ 0 & 0 & 0 & 1 \\ C^*_{55} & e^*_{15} & 0 & 0 \\ e^*_{15} & -\epsilon^*_{11} & 0 & 0 \end{bmatrix}, \quad \boldsymbol{F}_m = \begin{bmatrix} -\rho_0\omega^2 + \left(C^*_{44} + \sigma^0_{22}\right)k^2 & e^*_{24}k^2 & 0 & 0 \\ e^*_{24}k^2 & -\epsilon^*_{22}k^2 & 0 & 0 \\ 0 & 0 & 1 & 0 \\ 0 & 0 & 0 & 1 \end{bmatrix} \tag{6.60}
$$

For the $6mm$-type ceramics $C_{44} = C_{55}, e_{15} = e_{24}, \epsilon_{11} = \epsilon_{22}$, so the differences between c^*_{44} and c^*_{55}, e^*_{15} and e^*_{24}, and ϵ^*_{11} and ϵ^*_{22} can be neglected. In this case the eigenvalues of $\boldsymbol{B}^{-1}_m(x_1)\boldsymbol{F}_m(x_1)$ are obtained as

$$
\begin{gathered}
b_{1m,2m} = \pm k, \quad b_{3m,4m} = \pm kq_m, \quad q_m = \sqrt{1 - \left[\left(\rho c^2 - \sigma^0_{22}\right)/\bar{C}_{55}\right]} \\
\bar{C}_{55} = C^*_{55} + \left(e^*_{15}\right)^2/\epsilon^*_{11}, \quad c = \omega/k
\end{gathered} \tag{6.61}
$$

where c is the phase velocity. Correspondingly the eigenvector matrix $\boldsymbol{Q}_m$ is

$$
\boldsymbol{Q}_m = \begin{bmatrix} 0 & 0 & 1 & 1 \\ 1 & 1 & e^*_{15}/\epsilon^*_{11} & e^*_{15}/\epsilon^*_{11} \\ e^*_{15}k & -e^*_{15}k & \bar{C}_{55}q_mk & -\bar{C}_{55}q_mk \\ -\epsilon^*_{11}k & \epsilon^*_{11}k & 0 & 0 \end{bmatrix} \tag{6.62}
$$

Substitution of Eqs. (6.61) and (6.62) into Eq. (6.54) yields

$$\boldsymbol{v}_m(x_1) = \begin{bmatrix} 0 & 0 & 1 & 1 \\ 1 & 1 & e^*_{15}/\epsilon^*_{11} & e^*_{15}/\epsilon^*_{11} \\ e^*_{15}k & -e^*_{15}k & \bar{C}_{55}q_m k & -\bar{C}_{55}q_m k \\ -\epsilon^*_{11}k & \epsilon^*_{11}k & 0 & 0 \end{bmatrix} \times \begin{bmatrix} e^{kx_{1m}} & 0 & 0 & 0 \\ 0 & e^{-kx_{1m}} & 0 & 0 \\ 0 & 0 & e^{kq_m x_{1m}} & 0 \\ 0 & 0 & 0 & e^{-kq_m x_{1m}} \end{bmatrix} \begin{Bmatrix} a_{1m} \\ a_{2m} \\ a_{3m} \\ a_{4m} \end{Bmatrix} \tag{6.63}$$

According to Eq. (6.56) the transfer matrix of the sublayer m is

$$\begin{gathered} \boldsymbol{P}_m(x_{1m}-d_m, x_{1m}) \\ = \begin{bmatrix} \cosh(kq_m d_m) & 0 & -\dfrac{\sinh(kq_m d_m)}{\bar{C}_{55}q_m k} & -\dfrac{e^*_{15}\sinh(kq_m d_m)}{\bar{C}_{55}\epsilon^*_{11}q_m k} \\ P(21) & \cosh(kd_m) & -\dfrac{e^*_{15}\sinh(kq_m d_m)}{\bar{C}_{55}\epsilon^*_{11}q_m k} & P(24) \\ P(31) & -e^*_{15}k\sinh(kd_m) & \cosh(kq_m d_m) & P(34) \\ -e^*_{15}k\sinh(kd_m) & \epsilon^*_{11}k\sinh(kd_m) & 0 & \cosh(kd_m) \end{bmatrix} \\ P(21) = \frac{e^*_{15}}{\epsilon^*_{11}}[\cosh(kq_m d_m) - \cosh(kd_m)], \quad P(24) = \frac{\sinh(kd_m)}{\epsilon^*_{11}k} - \frac{e^{*2}_{15}\sinh(kq_m d_m)}{\bar{C}_{55}\epsilon^{*2}_{11}q_m k} \\ P(31) = -\bar{C}_{55}q_m k\sinh(kq_m d_m) + e^{*2}_{15}\sinh(kd_m)/\epsilon^*_{11} \\ P(34) = -\left(e^*_{15}/\epsilon^*_{11}\right)\cosh(kd_m) + \left(e^*_{15}/\epsilon^*_{11}\right)\cosh(kq_m d_m) \end{gathered} \tag{6.64}$$

Because the Love wave is confined to layers and near the substrate surface, the generalized displacements are attenuated in the substrate. In the substrate we have

$$\boldsymbol{v}_0(x_1) = \boldsymbol{Q}_0\left[0, a_{20}e^{b_{20}x_1}, 0, a_{40}e^{b_{40}x_1}\right]^{\mathrm{T}} \tag{6.65}$$

$\boldsymbol{Q}_0$ can be obtained by substituting material constants of the substrate into Eq. (6.62). At $x_1 = 0$ we have

$$\boldsymbol{v}_0(x_1) = \boldsymbol{Q}_0[0, a_{20}, 0, a_{40}]^{\mathrm{T}} \tag{6.66}$$

The electric potential φ_{N+1} and the electric displacement $D_{1(N+1)}$ in the air $x_1 < -h$ can be expressed as

$$\varphi_{N+1}(x_1,t) = a_{N+1}\exp(kx_1)\exp[\mathrm{i}(k_\alpha x_\alpha - \omega t)], \quad D_{1(N+1)} = -\epsilon_0\varphi_{N+1,1} \tag{6.67}$$

where ϵ_0 is the permittivity of air and a_{N+1} is an undetermined constant.

The mechanical boundary conditions are

$$\begin{aligned} &\sigma_{13} = 0, \quad \text{at} \quad x_1 = -h \\ &\sigma_{13}^{+} = \sigma_{13}^{-}, \quad u_3^{+} = u_3^{-}, \quad \text{at} \quad x_1 = 0 \end{aligned} \tag{6.68}$$

The electric boundary conditions between air and ZnO are divided into two kinds: electrically open and electrically shorted, i.e.,

$$\begin{aligned} &\varphi_N = \varphi_{N+1}, \quad D_{1\,(N)} = D_{1\,(N+1)}, \quad \text{at} \quad x_1 = -h \quad \text{(electrically open)} \\ &\varphi_N = 0, \quad \text{at} \quad x_1 = -h \quad \text{(electrically shorted)} \end{aligned} \tag{6.69}$$

The electric boundary conditions between the substrate and SiO$_2$ are

$$D_1^{+} = D_1^{-}, \quad \varphi^{+} = \varphi^{-}, \quad \text{at} \quad x_1 = 0 \tag{6.70}$$

The continuity condition at $x_1 = 0$ expressed by the state vector $\boldsymbol{v}(x_1)$ is

$$\boldsymbol{v}_0(x_1) = \boldsymbol{v}_1(x_1), \quad \text{at} \quad x_1 = 0 \tag{6.71}$$

From Eqs. (6.58), (6.66), and (6.71), the continuity condition of $\boldsymbol{v}(x_1)$ at $x_1 = -h$ is

$$\boldsymbol{v}_N(-h) = \boldsymbol{P}(-h, 0)\boldsymbol{v}_0(0) = \boldsymbol{M}[0, a_{20}, 0, a_{40}]^{\mathrm{T}}, \quad \boldsymbol{M} = \prod_{m=1}^{N} \boldsymbol{P}_m(x_{1m} - d_m, x_{1m})\boldsymbol{Q}_0 \tag{6.72}$$

According to the boundary conditions at $x_1 = -h$, $u_{3(N+1)}$ or u_{3air} is not needed, from the electrically open case we get

$$\begin{aligned} \begin{Bmatrix} A_{4N} \\ T_{5N} \\ T_{7N} \end{Bmatrix} &= \begin{bmatrix} M_{22} & M_{23} & M_{24} \\ M_{32} & M_{33} & M_{34} \\ M_{42} & M_{43} & M_{44} \end{bmatrix} \begin{Bmatrix} a_{20} \\ 0 \\ a_{40} \end{Bmatrix} = \begin{bmatrix} M_{22} & M_{24} \\ M_{32} & M_{34} \\ M_{42} & M_{44} \end{bmatrix} \begin{Bmatrix} a_{20} \\ a_{40} \end{Bmatrix} \\ &= \begin{Bmatrix} a_{N+1} \exp(-kh) \\ 0 \\ -\epsilon_0 a_{N+1} k \exp(-kh) \end{Bmatrix} \end{aligned} \tag{6.73}$$

or

$$\begin{bmatrix} M_{22} & M_{24} & -\exp(-kh) \\ M_{32} & M_{34} & 0 \\ M_{42} & M_{44} & \epsilon_0 k \exp(-kh) \end{bmatrix} \begin{Bmatrix} a_{20} \\ a_{40} \\ a_{N+1} \end{Bmatrix} = \begin{Bmatrix} 0 \\ 0 \\ 0 \end{Bmatrix} \tag{6.74}$$

In order to obtain nontrivial solutions for a_{20}, a_{40}, a_{N+1} the coefficient determinant in Eq. (6.74) should be vanished. So the equation to determine the phase velocity c_{f} in electrically open case is

$$(M_{42} + \epsilon_0 kM_{22})M_{34} - (M_{44} + \epsilon_0 kM_{24})M_{32} = 0 \tag{6.75}$$

Similarly for the electrically shorted case, the equation to determine the phase velocity c_{s} is

$$\begin{gathered} \begin{Bmatrix} A_{4N} \\ T_{5N} \end{Bmatrix} = \begin{bmatrix} M_{22} & M_{24} \\ M_{32} & M_{34} \end{bmatrix} \begin{Bmatrix} a_{20} \\ a_{40} \end{Bmatrix} = \begin{Bmatrix} 0 \\ 0 \end{Bmatrix}, \quad \text{or} \\ M_{22}M_{34} - M_{24}M_{32} = 0 \end{gathered} \tag{6.76}$$

There are many papers to discuss on the problem of Love wave, such as Danoyan and Pilliposian (2007) and Liu et al. (2001). Du et al. (2008) discussed the propagation of Love waves in prestressed piezoelectric layered structures loaded with viscous liquid.

6.4.3 *The Distribution of the Initial Stresses*

Because layers are very thin, the mechanical stresses have only occurred in layers, i.e., at $x_1 = -h_1, \bar{\sigma}_{i1}^0 = 0$; $x_1 = 0, \bar{\sigma}_{ij}^0 = 0$. The continuity conditions of the initial stresses at $x_1 = -h_1$ are that u_2^0 and u_3^0 are continuous, or

$$\bar{\varepsilon}^0_{2\mathrm{ZnO}} = \bar{\varepsilon}^0_{2\mathrm{SiO}_2} = \bar{\varepsilon}^0_2, \quad \bar{\varepsilon}^0_{3\mathrm{ZnO}} = \bar{\varepsilon}^0_{3\mathrm{SiO}_2} = \bar{\varepsilon}^0_3, \quad \bar{\varepsilon}^0_{23\mathrm{ZnO}} = \bar{\varepsilon}^0_{23\mathrm{SiO}_2} = \bar{\varepsilon}^0_{23}, \quad \text{at} \quad x_1 = -h_1 \tag{6.77}$$

Using the constitutive equation from Eq. (6.77), we can derive the following relation:

$$\begin{aligned} &\bar{\sigma}^0_{1\mathrm{ZnO}} = C_{11}\bar{\varepsilon}^0_{1\mathrm{ZnO}} + C_{12}\bar{\varepsilon}^0_{2\mathrm{ZnO}} + C_{13}\bar{\varepsilon}^0_{3\mathrm{ZnO}}, \quad \sigma^0_{2\mathrm{ZnO}} = C_{12}\bar{\varepsilon}^0_{1\mathrm{ZnO}} + C_{11}\bar{\varepsilon}^0_{2\mathrm{ZnO}} + C_{13}\bar{\varepsilon}^0_{3\mathrm{ZnO}} \\ &\bar{\sigma}^0_{3\mathrm{ZnO}} = C_{13}\bar{\varepsilon}^0_{1\mathrm{ZnO}} + C_{13}\bar{\varepsilon}^0_{2\mathrm{ZnO}} + C_{33}\bar{\varepsilon}^0_{3\mathrm{ZnO}}, \\ &Y\bar{\varepsilon}^0_{2\mathrm{SiO}_2} = \bar{\sigma}^0_{2\mathrm{SiO}_2} - \nu\bar{\sigma}^0_{3\mathrm{SiO}_2}, \quad Y\bar{\varepsilon}^0_{3\mathrm{SiO}_2} = \bar{\sigma}^0_{3\mathrm{SiO}_2} - \nu\bar{\sigma}^0_{2\mathrm{SiO}_2} \end{aligned} \tag{6.78}$$

where C_{ij} is the elastic constant of ZnO and Y, ν is the elastic constant of SiO_2. So at $x_1 = -h_1$, the initial stresses in ZnO and SiO_2 must satisfy the following relation:

$$\begin{aligned} YC_{11}\bar{\sigma}^0_{2\mathrm{ZnO}} = {} & \left[C_{11}^2 - C_{12}^2 - \nu C_{13}(C_{11} - C_{12})\right]\bar{\sigma}^0_{2\mathrm{SiO}_2} \\ & + \left[C_{13}(C_{11} - C_{12}) - \nu\left(C_{11}^2 - C_{12}^2\right)\right]\bar{\sigma}^0_{3\mathrm{SiO}_2} \end{aligned} \tag{6.79}$$

Similarly we can get $\bar{\sigma}^0_{3\mathrm{ZnO}}$, but it is not needed. It can be assumed that $\sigma^0_{2\mathrm{SiO_2}}, \sigma^0_{2\mathrm{ZnO}}$ are varied exponentially (Fig. 6.4), i.e.,

$$\begin{aligned}
&\bar{\sigma}^0_{2\mathrm{SiO_2}}(x_1) = f(x_1) = (\mathrm{e}^{x_1} - 1)\big/\big(\mathrm{e}^{-h_1} - 1\big)\bar{\sigma}^0_{2\mathrm{SiO_2}}(-h), \quad -h_1 \le x_1 \le 0 \\
&\bar{\sigma}^0_{2\mathrm{ZnO}}(x_1) = \mathrm{g}(x_1) = (\mathrm{e}^{x_1} - 1)\big/\big(\mathrm{e}^{-h} - 1\big)\bar{\sigma}^0_{2\mathrm{ZnO}}(-h), \quad -h \le x_1 \le -h_1
\end{aligned} \tag{6.80}$$

It is also noted that the generalized displacements and stresses at the initial state should be obtained directly by experiments or calculated by the updated Lagrange method which needs multiple steps from the natural state to initial state. The updated Lagrange method and other methods in plasticity can be utilized to the problems discussed here.

6.4.4 Numerical Example

In the paper of Su et al. (2005), they assumed $\sigma^0_{3\mathrm{SiO_2}} = L\sigma^0_{2\mathrm{SiO_2}}$ to simplify calculation, where L is a proportional coefficient. They adopted the following material constants:

$$\begin{aligned}
&\mathrm{ZnO}: \ \rho = 5{,}665\,\mathrm{kg/m^3}, \ C_{11} = 209.6, \ C_{12} = 120.5, \ C_{13} = 104.6, \ C_{44} = 242.3\,(\mathrm{MPa}); \\
&\qquad e_{15} = -0.48, \ e_{31} = -0.573, \ e_{33} = 1.32\,(\mathrm{C/m^2}); \ \epsilon_{11} = 0.67, \ \epsilon_{33} = 0.799\,(10^{-10}\mathrm{F/m}) \\
&\mathrm{SiO_2}: \ \rho = 2{,}200\,\mathrm{kg/m^3}, \ \lambda = 78.5, \ G = 31.2\,(\mathrm{MPa}); \ \epsilon_{11} = 0.33, \ \epsilon_{33} = 0.33\,(10^{-10}\mathrm{F/m}) \\
&\mathrm{Si}: \ \rho = 2{,}328\,\mathrm{kg/m^3}, \ \lambda = 165.75, \ G = 79.4\,(\mathrm{MPa}); \ \epsilon_{11} = 1.035, \ \epsilon_{33} = 1.035\,(10^{-10}\mathrm{F/m})
\end{aligned}$$

Figure 6.6 shows the change of the phase velocity c_{f0} of the Love wave with kh under the case that: electrically open, without initial stresses, $h_2 = 10^{-5}$ m and different h_1. It is seen that for all h_1 when $kh \to 0$, $c_{\mathrm{f0}} \to c_{\mathrm{Si}}$; c_{f0} decreases with increasing kh. When $kh \to \infty$ $c_{\mathrm{f0}} \to c_{\mathrm{ZnO}}$ if $h_1 < h_2$ and $h_1 \sim h_2$; or $c_{\mathrm{f0}} \to c_{\mathrm{SiO_2}}$ if $h_1 \gg h_2$. c_{f0} is in the following range:

$$\begin{aligned}
&(c_{\mathrm{ZnO}}, c_{\mathrm{SiO_2}}) < c_{\mathrm{f0}} < c_{\mathrm{Si}} \\
&c_{\mathrm{ZnO}} = \sqrt{\frac{C_{55} + e_{15}^2}{\rho_{\mathrm{ZnO}}}} = 2,841.5\,(\mathrm{m/s}), \quad c_{\mathrm{SiO_2}} = \sqrt{\frac{\mu_{\mathrm{SiO_2}}}{\rho_{\mathrm{SiO_2}}}} = 3,765.9(\mathrm{m/s}), \\
&c_{Si} = \sqrt{\frac{\mu_{Si}}{\rho_{Si}}} = 5,840\,(\mathrm{m/s})
\end{aligned} \tag{6.81}$$

Figure 6.7 shows the change of $\Delta c/c_{\mathrm{f0}}$ with kh under the case that: electrically open case, $\bar{\sigma}^0_{2\mathrm{ZnO}} = 200\,\mathrm{MPa}, L = 1, h_2 = 10^{-5}$ m and different h_1. Here $\Delta c = c_{\mathrm{f}} - c_{\mathrm{f0}}$ and c_{f} is the Love wave velocity with initial stress. From Figs. 6.6 and 6.7, it is seen that the middle layer has significant role.

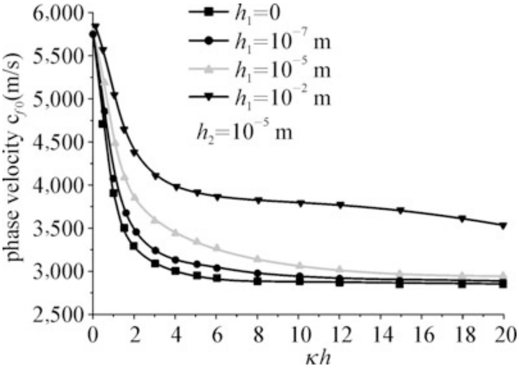

Fig. 6.6 Variation of phase velocity c_{f0} with kh under conditions: electrically open, without initial stress

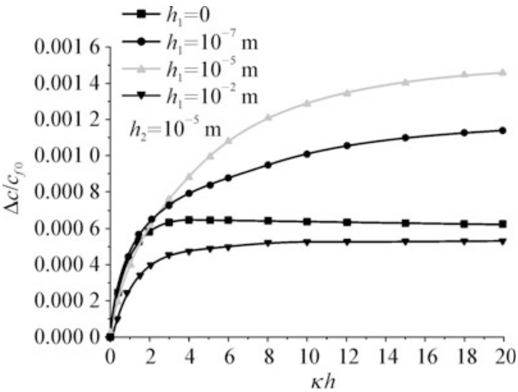

Fig. 6.7 Variation of $\Delta c/c_{f0}$ with kh under conditions: electrically open, $\sigma^0_{2\mathrm{ZnO}}(-h) = 200\,\mathrm{MPa}, \quad L = 1$

6.5 Other Surface Waves

6.5.1 B-G Wave in a Prestressed Piezoelectric Structure

Because the penetration depth of the B-G wave is about 10–100 λ, the application of B-G wave is limited in microwave techniques. However, the application of layered structures can significantly reduce the penetration depth. Jin et al. (2001) and Liu et al. (2003a) discussed the prestressed layered piezoelectric structures. The layer and substrate are all made by piezoelectric materials, and the poling directions of the layer and substrate are along the positive and negative axes x_3, respectively (see Fig. 6.2). The B-G wave in layered structure can also be considered as a kind of the Love wave. The basic equations have been discussed in Sect. 6.3 and governing equations can be seen in Eq. (6.43). In B-G wave only $u_3(x_1, x_2, t)$ and $\varphi(x_1, x_2, t)$ are not zero. Neglecting terms containing $u^0_{K,L}u^0_{M,N}$, Eq. (6.43) is reduced to

$$\begin{aligned}
&\left(C^*_{1331}+\sigma^0_{11}\right)u_{3,11}+\left(C^*_{1332}+C^*_{2331}+2\sigma^0_{12}\right)u_{3,12}+\left(C^*_{2332}+\sigma^0_{22}\right)u_{3,22}\\
&\quad+e^*_{131}\varphi_{,11}+\left(e^*_{132}+e^*_{231}\right)\varphi_{,12}+e^*_{232}\varphi_{,22}=\rho_0\ddot{u}_3\\
&e^*_{131}u_{3,11}+\left(e^*_{132}+e^*_{231}\right)u_{3,12}+e^*_{232}u_{3,22}-\epsilon^*_{11}\varphi_{,11}-2\,\epsilon^*_{12}\varphi_{,12}-\epsilon^*_{22}\varphi_{,22}=0
\end{aligned} \tag{6.82}$$

The variables in the substrate are denoted by a superscript "M." Because in the substrate $x_1>0$ there is no initial stress, the governing equations are

$$\begin{aligned}
&C^{\mathrm{M}}_{1331}u^{\mathrm{M}}_{3,11}+2C^{\mathrm{M}}_{1332}u^{\mathrm{M}}_{3,12}+C^{\mathrm{M}}_{2332}u^{\mathrm{M}}_{3,22}+e^{\mathrm{M}}_{131}\varphi^{\mathrm{M}}_{,11}+2e^{\mathrm{M}}_{132}\varphi^{\mathrm{M}}_{,12}+e^{\mathrm{M}}_{232}\varphi^{\mathrm{M}}_{,22}=\rho_0u^{\mathrm{M}}_3\\
&e^{\mathrm{M}}_{131}u^{\mathrm{M}}_{3,11}+2e^{\mathrm{M}}_{132}u^{\mathrm{M}}_{3,12}+e^{\mathrm{M}}_{232}u^{\mathrm{M}}_{3,22}-\epsilon^{\mathrm{M}}_{11}\varphi^{\mathrm{M}}_{,11}-2\,\epsilon^{\mathrm{M}}_{12}\varphi^{\mathrm{M}}_{,12}-\epsilon^{\mathrm{M}}_{22}\varphi^{\mathrm{M}}_{,22}=0
\end{aligned} \tag{6.83}$$

The boundary and the interface continuity conditions are

$$\begin{aligned}
&\bar{\sigma}^*_{13}+\sigma^0_{1k}u_{3,k}=0,\quad \text{at}\quad x_1=-h\\
&\varphi=\varphi^c,\quad D_1=D^c_1,\ \text{(electrically open)};\quad \varphi=0,\ \text{(electrically shorted)}\quad \text{at}\quad x_1=-h\\
&u_3=u^M_3,\quad \bar{\sigma}^*_{13}=\sigma^M_{13};\quad \varphi=\varphi^M,\quad \bar{D}_1=D^M_1,\quad \text{at}\quad x_1=0\\
&u_3,\quad \varphi\to 0,\quad \text{when}\quad x_1\to+\infty;\quad \varphi^c\to 0,\quad \text{when}\quad x_1\to-\infty
\end{aligned} \tag{6.84}$$

Let B-G wave propagate along positive x_2 direction. The generalized displacements in layer are assumed

$$u_3=\alpha_3\exp\left(\mathrm{i}kbx_1\right)\exp[\mathrm{i}k(x_2-ct)],\quad \varphi=\alpha_4\exp(\mathrm{i}kbx_1)\exp[\mathrm{i}k(x_2-ct)] \tag{6.85}$$

Substitution of Eq. (6.85) into Eq. (6.82) yields

$$\begin{bmatrix}
\left(c^*_{1331}+\sigma^0_{11}\right)b^2+\left(c^*_{1332}+c^*_{2331}+2\sigma^0_{12}\right)b+\left(c^*_{2332}+\sigma^0_{22}\right)-\rho_0c^2 & e^*_{131}b^2+\left(e^*_{132}+e^*_{231}\right)b+e^*_{232}\\
e^*_{131}b^2+\left(e^*_{132}+e^*_{231}\right)b+e^*_{232} & -\epsilon^*_{11}b^2-2\epsilon^*_{12}b-\epsilon^*_{22}
\end{bmatrix}\begin{Bmatrix}\alpha_3\\ \alpha_4\end{Bmatrix}=\begin{Bmatrix}0\\0\end{Bmatrix} \tag{6.86}$$

In order for α_3,α_4 to have nontrivial solutions, their coefficient determinate must be zero, or

$$A_4b^4+A_3b^3+A_2b^2+A_1b+A_0=0 \tag{6.87}$$

where A_i is determined by Eq. (6.86) and omitted here. Equation (6.87) has 4 eigenvalues $b_p(p=1,2,3,4)$ and a pair of eigenvectors α_3,α_4 corresponding to each b_p and

$$\beta_p = \frac{\alpha_4^{(p)}}{\alpha_3^{(p)}} = \frac{e_{131}^* b_p^2 + \left(e_{132}^* + e_{231}^*\right) b_p + e_{232}^*}{\epsilon_{11}^* b_p^2 + 2\epsilon_{12}^* b_p + \epsilon_{22}^*} \tag{6.88}$$

Substituting Eq. (6.88) into Eq. (6.85) yields the generalized displacements in layer

$$\begin{aligned} u_3 &= \sum_{p=1}^{4} \alpha_3^{(p)} \exp(\mathrm{i}kb_p x_1) \exp[\mathrm{i}k(x_2 - ct)] \\ \varphi &= \sum_{p=1}^{4} \beta_p \alpha_3^{(p)} \exp(\mathrm{i}kb_p x_1) \exp[\mathrm{i}k(x_2 - ct)] \end{aligned} \tag{6.89}$$

Similar to the layer and noting $u_3, \varphi \to 0$, when $x_1 \to \infty$, the generalized displacements in the substrate only have two eigenvalues $b_q^{\mathrm{M}} (q = 1, 2)$ with positive image parts, i.e.,

$$\begin{aligned} u_3^M &= \sum_{p=1}^{2} \alpha_3^{M(q)} \exp\left(\mathrm{i}kb_q^M x_1\right) \exp[\mathrm{i}k(x_2 - ct)] \\ \varphi^M &= \sum_{p=1}^{2} \beta_q^M \alpha_3^{M(q)} \exp\left(\mathrm{i}kb_q^M x_1\right) \exp[\mathrm{i}k(x_2 - ct)] \end{aligned} \tag{6.90}$$

From $\varphi_{,11}^c + \varphi_{,22}^c = 0$ and the connective conditions at $x_1 = -h$ in Eq. (6.84), it is assumed

$$\varphi^c = \sum_{p=1}^{4} \beta_p \alpha_3^{(p)} \exp(\mathrm{i}kb_p x_1) \exp[k(x_1 + h)] \exp[\mathrm{i}k(x_2 - ct)] \tag{6.91}$$

Substituting Eqs. (6.89), (6.90), and (6.91) into Eq. (6.84) yields six homogeneous equations for vector $\boldsymbol{\alpha}$:

$$\boldsymbol{P\alpha} = \mathbf{0}, \quad [P_{ij}]\{\alpha_j\} = \{0\}; \quad \boldsymbol{\alpha} = \left[\alpha_3^{(1)}, \alpha_3^{(2)}, \alpha_3^{(3)}, \alpha_3^{(4)}, \alpha_3^{M(1)}, \alpha_3^{M((1))}\right]^{\mathrm{T}} \tag{6.92}$$

In the electrically open case at $x_1 = -h$ for $j = 1, 2, 3, 4$, we have

$$\begin{aligned} &P_{1j} = \mathrm{i}k\left[\left(c_{1331}^* + \sigma_{11}^0 + e_{131}^*\beta_j\right)b_j + c_{1332}^* + \sigma_{12}^0 + e_{132}^*\beta_j\right] \exp(-\mathrm{i}kb_j h) \\ &P_{2j} = \mathrm{i}k\left[\left(e_{131}^* - \epsilon_{11}^*\beta_j\right)b_j + e_{132}^* - \left(\epsilon_{12}^* + i\,\epsilon^c\right)\beta_j\right] \exp(-\mathrm{i}kb_j h) \\ &P_{3j} = \mathrm{i}k\left[\left(c_{1331}^* + \sigma_{11}^0 + e_{131}^*\beta_j\right)b_j + c_{1332}^* + \sigma_{12}^0 + e_{132}^*\beta_j\right] \\ &P_{4j} = 1, \quad P_{5j} = \beta_j, \quad P_{6j} = \mathrm{i}k\left[\left(e_{131}^* - \epsilon_{11}^*\beta_j\right)b_j + e_{132}^* - \epsilon_{12}^*\beta_j\right] \end{aligned} \tag{6.93a}$$

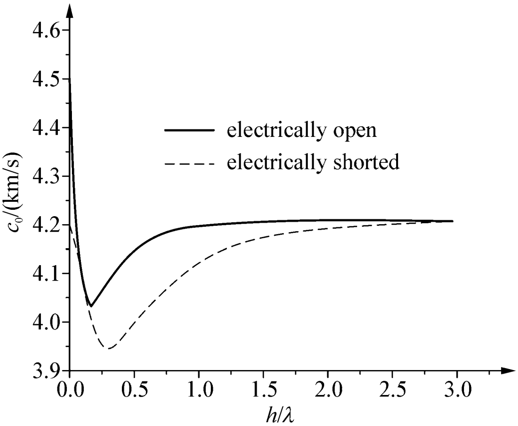

Fig. 6.8 Dispersion relations for the fundamental mode of B-G wave (without initial stress)

For $j = 5, 6$ we have

$$\begin{aligned} &P_{1j} = 0, \quad P_{2j} = 0, \quad P_{3j} = -\mathrm{i}k\left[\left(\hat{c}_{1331}^{M*} + e_{131}^{M*}\beta_{j-4}^{M}\right)b_{j-4}^{M} + \hat{c}_{1332}^{M*} + e_{132}^{*}\beta_{j-4}^{M}\right] \\ &P_{4j} = -1, \quad P_{5j} = -\beta_{j-4}^{M}, \quad P_{6j} = -\mathrm{i}k\left[\left(e_{131}^{M*} - \epsilon_{11}^{M*}\beta_{j-4}^{M}\right)b_{j-4}^{M} + e_{132}^{M*} - \epsilon_{12}^{M*}\beta_{j-4}^{M}\right] \end{aligned} \tag{6.93b}$$

The equation to determine the phase velocity of B-G wave under electrically open case is

$$|\boldsymbol{P}| = 0 \tag{6.94}$$

For the electrically shorted case at $x_1 = -h, P_{2j}$ in Eq. (6.93a) should be replaced by

$$P_{2j} = \beta_j \exp(-\mathrm{i}kb_jh), \quad \text{for} \quad j = 1-4 \tag{6.95}$$

In the paper of Liu et al. (2003a), they found that the penetration depth is dramatically reduced in a $LiNbO_3$ layer piezoelectric material and the effect of the third-order piezoelectric coefficients (Cho and Yamanouchi 1987) is meaningful for the low-frequency case. Figure 6.8 shows the dispersion relations for the fundamental mode of B-G surface wave in the absence of initial stress, where $c_0 = c_{f0}$ for electrically open case and $c_0 = c_{s0}$ for electrically shorted case. It is found that for a given value of h/λ, the phase velocity of the electrically open case is greater than that of electrically shorted case, i.e., $c_{f0} > c_{s0}$. In the low-frequency limit, $h/\lambda \to 0$, the wave mode tends to the B-G surface wave in a piezoelectric half-space, i.e., $c_{f0} \to 4.538\,\mathrm{km/s}, c_{s0} \to 4.203\,\mathrm{km/s}$. Figure 6.9 shows the variations of $\Delta c_f/c_{f0}$ and $\Delta c_s/c_{s0}$ with h/λ under the initial stress $\bar{\sigma}_{22}^0 = 40\,\mathrm{MPa}$, where c_f, c_s are the phase velocity in layer with initial stress and $\Delta c_f = c_f - c_{f0}$ or $\Delta c_s = c_s - c_{s0}$.

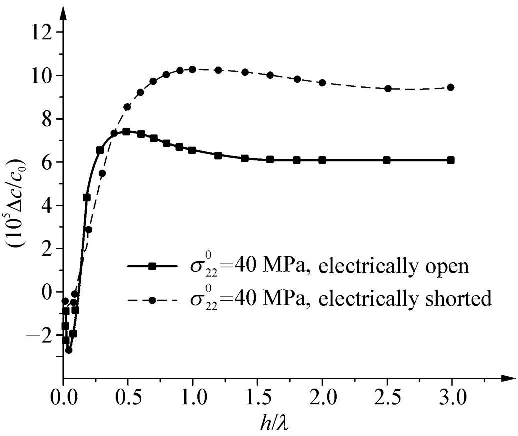

Fig. 6.9 Variations of $\Delta c/c_0$ with h/λ for different initial stresses

6.5.2 Rayleigh Wave in a Prestressed Structure

Discuss an approximately transversely isotropic $LiNbO_3$ piezoelectric film of thickness h polarized x_1-axis deposited on a sapphire substrate (see Fig. 6.2). Usually the thickness of the layer is some micrometers, so the substrate can be considered as semi-infinite. The basic equation Eq. (6.43) in the layer is reduced to

$$C^*_{KIlJ}u_{I,JK} + \bar{\sigma}^0_{KJ}u_{l,JK} + e^*_{NKl}\varphi_{,NK} = \rho_0\ddot{u}_l, \quad e^*_{KIJ}u_{I,JK} - \epsilon^*_{KN}\varphi_{,NK} = 0 \tag{6.96}$$

In the following the superscript * on material coefficients will be omitted. In the substrate the basic equation is

$$C^{\mathrm{M}}_{ijkl}u^{\mathrm{M}}_{k,li} + e^{\mathrm{M}}_{kij}\varphi^{\mathrm{M}}_{,ki} = \rho\ddot{u}^{\mathrm{M}}_j, \quad e^{\mathrm{M}}_{ikl}u^{\mathrm{M}}_{k,li} - \epsilon^{\mathrm{M}}_{ik}\varphi^{\mathrm{M}}_{,ik} = 0 \tag{6.97}$$

The boundary and the interface continuity conditions are

$$\begin{aligned}
&\bar{\sigma}^*_{1j} + \bar{\sigma}^0_{1k}u_{j,k} = 0, \quad x_1 = -h\\
&\varphi = \varphi^c, \quad D_1 = D^c_1, \quad \text{(electrically open)}; \quad \varphi = 0, \quad \text{(electrically shorted)} \quad \text{at} \quad x_1 = -h\\
&\bar{\sigma}^*_{1j} + \bar{\sigma}^0_{1k}u_{j,k} = \sigma^{\mathrm{M}}_{1j}, \quad u_j = u^{\mathrm{M}}_j, \quad \varphi = \varphi^{\mathrm{M}}, \quad \bar{D}_1 = D^{\mathrm{M}}_1; \quad \text{at} \quad x_1 = 0\\
&u_j, \varphi \to 0, \quad \text{when} \quad x_1 \to +\infty; \quad \varphi^c \to 0, \quad \text{when} \quad x_1 \to -\infty
\end{aligned} \tag{6.98}$$

Let the wave propagate along x_2 and take the form

$$u_i = B_i \mathrm{e}^{\mathrm{i}kbx_1}\mathrm{e}^{\mathrm{i}k(x_2-ct)}, \quad \varphi = B_4\mathrm{e}^{\mathrm{i}kbx_1}\mathrm{e}^{\mathrm{i}k(x_2-ct)} \tag{6.99}$$

where B_i is the amplitude of ith component. Substitution of Eq. (6.99) into Eq. (6.96) yields

$$
\begin{aligned}
&\boldsymbol{\Gamma B} = \mathbf{0}, \quad \text{or} \quad \left[\Gamma_{\alpha\beta}\right]\{B_\alpha\} = \{0\}; \quad \boldsymbol{B} = [B_1, B_2, B_3, B_4]^{\mathrm{T}}, \quad \alpha, \beta = 1-4 \\
&\Gamma_{jk} = C_{1jk1} + b(C_{3jk1} + C_{1jk3}) + b^2 C_{3jk3} + \delta_{jk}\left(\sigma_{11}^0 + 2b\sigma_{13}^0 + b^2\sigma_{33}^0 - \rho c^2\right) \\
&\Gamma_{j4} = e_{11j} + b(e_{13j} + e_{31j}) + b^2 e_{33j}, \quad \Gamma_{4j} = e_{1j1} + b(e_{1j3} + e_{3j1}) + b^2 e_{3j3} \\
&\Gamma_{44} = -(\epsilon_{11} + 2b\epsilon_{13} + b^2\epsilon_{33}); \quad i, j = 1, 2, 3
\end{aligned}
\tag{6.100}
$$

In order to get nontrivial solution of $\boldsymbol{B}$, its coefficient determinate need be zero, i.e.,

$$
A_8 b^8 + A_7 b^7 + A_6 b^6 + A_5 b^5 + A_4 b^4 + A_3 b^3 + A_2 b^2 + A_1 b^1 + A_0 = 0 \tag{6.101}
$$

where A_i is determined by Eq. (6.100). Equation (6.101) is the eighth-order equation of b with the Rayleigh wave velocity c as a parameter. From Eq. (6.101) eight b_q can be obtained and for each b_q an eigenvector with four components can be obtained. For convenience we let

$$
B_{iq} = \beta_{iq} B_{1q}, \quad \beta_{1q} = 1, \quad i = 1-4, \quad q = 1-8 \tag{6.102}
$$

After B_{iq} is obtained the generalized displacements in layer can be expressed as

$$
u_i = \sum_{q=1}^{8} \beta_{iq} B_{1q} \mathrm{e}^{\mathrm{i}kb_q x_1} \mathrm{e}^{\mathrm{i}k(x_2 - ct)}, \quad \varphi = \sum_{q=1}^{8} \beta_{4q} B_{1q} \mathrm{e}^{\mathrm{i}kb_q x_1} \mathrm{e}^{\mathrm{i}k(x_2 - ct)} \tag{6.103}
$$

Analogously the generalized displacements in substrate can be expressed as

$$
u_i^{\mathrm{M}} = \sum_{q=1}^{4} \beta_{iq}^{\mathrm{M}} \beta_{1q}^{\mathrm{M}} \mathrm{e}^{\mathrm{i}kb_q^{\mathrm{M}} x_1} \mathrm{e}^{\mathrm{i}k(x_2 - ct)}, \quad \varphi^{\mathrm{M}} = \sum_{q=1}^{4} \beta_{4q}^{\mathrm{M}} \beta_{1q}^{\mathrm{M}} \mathrm{e}^{\mathrm{i}kb_q^{\mathrm{M}} x_1} \mathrm{e}^{\mathrm{i}k(x_2 - ct)} \tag{6.104}
$$

Analogous to Eq. (6.91) for the electrically open case, the electric potential in the air is

$$
\varphi^c = \sum_{q=1}^{8} \beta_{4q} B_{1q} \mathrm{e}^{-\mathrm{i}kb_q h} \mathrm{e}^{k(h + x_1)} \mathrm{e}^{\mathrm{i}k(x_2 - ct)} \tag{6.105}
$$

Substitution of Eqs. (6.103), (6.104), and (6.105) into Eq. (6.98) yields

$$
\boldsymbol{PB} = \mathbf{0}, \quad \boldsymbol{P} = [P_{mn}], \quad \boldsymbol{B} = \left\{B_{1q}, B_{1q}^{M}\right\}^{\mathrm{T}}; \quad m, n = 1-12 \tag{6.106}
$$

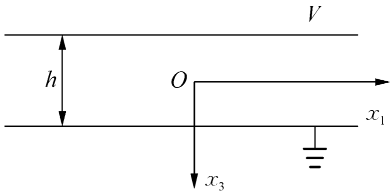

Fig. 6.10 Lamb wave in piezoelectric plate with biasing electric field

where for $j, k = 1, 2, 3;\ n = 1 - 8$ we have

$$\begin{aligned}
&P_{jn} = \mathrm{i}k\left\{\left[C_{3jk1} + C_{3jk3}b_n + \delta_{jk}\left(\sigma_{13}^0 + \sigma_{33}^0 b_n\right)\right]\beta_{kn} + (e_{13j} + e_{33j}b_n)\beta_{4n}\right\}\mathrm{e}^{-\mathrm{i}kb_n h} \\
&P_{4n} = \mathrm{i}k\{(e_{3k1} + e_{3k3}b_n)\beta_{kn} - (\epsilon_{31} + \epsilon_{33}b_n + \mathrm{i}\epsilon_0)\beta_{4n}\}\mathrm{e}^{-\mathrm{i}kb_n h} \\
&P_{j+4,n} = \mathrm{i}k\left\{\left[C_{3jk1} + C_{3jk3}b_n + \delta_{jk}\left(\sigma_{13}^0 + \sigma_{33}^0 b_n\right)\right]\beta_{kn} + \left(e_{13j} + e_{33j}b_n\right)\beta_{4n}\right\} \\
&P_{k+7,n} = \beta_{kn}, \quad P_{11,n} = \beta_{4n}, \quad P_{12,n} = \mathrm{i}k\{(e_{3k1} + e_{3k3}b_n)\beta_{kn} - (\epsilon_{31} + \epsilon_{33}b_n)\beta_{4n}\}
\end{aligned} \tag{6.107a}$$

and for $j, k = 1, 2, 3;\ n = 9 - 12$ we have

$$\begin{aligned}
&P_{jn} = 0, \quad P_{4n} = 0, \quad P_{j+4,n} = -\mathrm{i}k\left\{\left[C_{3jk1}^M + C_{3jk3}^M b_n^M\right]\beta_{kn}^M + (e_{13j}^M + e_{33j}^M b_n^M)\beta_{4n}^M\right\} \\
&P_{k+7,n} = -\beta_{k,n-8}^M, \quad P_{11,n} = -\beta_{4,n-8}^M, \\
&P_{12,n} = -\mathrm{i}k\left\{\left(e_{3k1}^M + e_{3k3}^M b_{n-8}^M\right)\beta_{kn}^M - \left(\epsilon_{31}^M + \epsilon_{33}^M b_{n-8}^M\right)b_{4,n-8}^M\right\}
\end{aligned} \tag{6.107b}$$

The phase velocity c of the Rayleigh wave $\bar{R}_3$ should satisfy Eqs. (6.100) and (6.106) simultaneously. From this condition c can be obtained by iteration method.

For the electrically shorted case, the fourth row in $[P_{mn}]$ should be changed to

$$P_{4n} = \beta_{4n}\mathrm{e}^{-\mathrm{i}kb_n h}, \quad n = 1 - 8; \quad P_{4n} = 0, \quad n = 9 - 12 \tag{6.108}$$

Liu et al. (2003d) discussed the phase velocity and the electromechanical coupling coefficient, $k^2 = 2(c_\mathrm{f} - c_\mathrm{s})/c_\mathrm{f}$. The results show that for a given value of h/λ, the phase velocity of the electrically open case is greater than that of the shorted case. The phase velocity approaches the Rayleigh wave velocity of the substrate when $h/\lambda \to 0$ and tends to the Rayleigh wave velocity of the layer for large $h/\lambda > 1.5$.

Babich and Lukyanov (1998) discussed the surface wave in a curved layered structure. Liu et al. (2003c, d) discussed the Love wave in a layered structure with functionally graded isotropic substrate.

6.5.3 Lamb Waves in Piezoelectric Plate with Biasing Electric Field

Lamb waves were researched a long time (Joshi and Jin 1991), it shows a large sensitivity to mass loading, and the zero-order antisymmetric mode can be applied in contact with a liquid with a small attenuation (Laurent et al. 2000). Figure 6.10 shows a thin infinite transversely isotropic piezoelectric plate of thickness h polarized x_3-axis. Liu et al. (2002a, b) assumed that a small biasing voltage V is applied to the electrode deposited on the upper surface and the electrode on the lower surface is grounded. The deference between the natural and initial configurations is neglected in their analysis. The electric field $\boldsymbol{E}^0 = (V/h)\mathbf{i}_3$, $\mathbf{i}_3$ is the unit vector on the axis x_3. According to the external loading, the generalized stresses can be assumed as constants. In this section the Voigt notations are used. The static electric force acted on the upper and lower surfaces of the piezoelectric material produced by the electric charges on the electrodes is neglected. The boundary conditions are assumed

$$\begin{aligned}&\boldsymbol{T}^0 = \mathbf{0}, \quad \text{on} \quad x_3 = \pm h/2; \quad \varepsilon^0_{1j} = 0, \quad x_1 = \pm\infty; \quad \varepsilon^0_{2j} = 0, \quad x_2 = \pm\infty \\ &\varphi^0 = V, \quad \text{on} \quad x_3 = -h/2; \quad \varphi^0 = 0, \quad \text{on} \quad x_3 = h/2, \quad x_1 = \pm\infty, \quad x_2 = \pm\infty\end{aligned} \tag{6.109}$$

A transversely isotropic material polarized x_3-axis only has ten independent constants. From Eq. (6.109) and the constitutive equation (3.2), it is obtained

$$\begin{aligned}&\sigma^0_1 = \eta_\sigma E^0_3, \quad \sigma^0_2 = \eta'_\sigma E^0_3, \quad D^0_3 = \eta_D E^0_3; \quad E^0_3 = (V/h); \quad \text{other} \quad \sigma^0_i = D^0_i = 0 \\ &\eta_\sigma = C_{13}e_{33}/C_{33} - e_{31}, \quad \eta'_\sigma = C_{23}e_{33}/C_{33} - e_{23}, \quad \eta_D = e^2_{33}/C_{33} + \epsilon_{33}\end{aligned} \tag{6.110}$$

According to Eq. (6.41) for the small perturbation in a 2D problem, we have

$$\begin{aligned}&\sigma_{1,1} + \sigma_{5,3} + \sigma^0_1 u_{1,11} = \rho_0 \ddot{u}_1, \quad \sigma_{5,1} + \sigma_{3,3} + \sigma^0_1 u_{3,11} = \rho_0 \ddot{u}_3 \\ &D_{1,1} + D_{3,3} = 0\end{aligned} \tag{6.111}$$

And the constitutive equation

$$\begin{aligned}&\sigma_1 = C_{11}\varepsilon_1 + C_{13}\varepsilon_3 - e_{31}E_3, \quad \sigma_3 = C_{13}\varepsilon_1 + C_{33}\varepsilon_3 - e_{33}E_3 \\ &\sigma_5 = C_{44}\varepsilon_5 - e_{15}E_1, \quad D_1 = e_{15}\varepsilon_5 + \epsilon_{11}E_1, \quad D_3 = e_{31}\varepsilon_1 + e_{33}\varepsilon_3 + \epsilon_{33}E_3\end{aligned} \tag{6.112}$$

Substitution of Eqs. (6.110) and (6.112) into Eq. (6.111) yields

$$\begin{aligned}&\left(C_{11} + \eta_\sigma E^0_3\right)u_{1,11} + C_{44}u_{1,33} + (C_{13} + C_{44})u_{3,13} + (e_{31} + e_{15})\varphi_{,13} = \rho_0 \ddot{u}_1 \\ &(C_{13} + C_{44})u_{1,13} + \left(C_{44} + \eta_\sigma E^0_3\right)u_{3,11} + C_{33}u_{3,33} + e_{15}\varphi_{,11} + e_{33}\varphi_{,33} = \rho_0 \ddot{u}_3 \\ &(e_{31} + e_{15} + \eta_D E^0_3)u_{1,13} + e_{15}u_{3,11} + (e_{33} + \eta_D E^0_3)u_{3,33} - \epsilon_{11}\varphi_{,11} - \epsilon_{33}\varphi_{,33} = 0\end{aligned} \tag{6.113}$$

It is assumed that the solutions of the antisymmetric Lamb waves are (Liu et al. 2002a)

$$\begin{aligned}&u_1 = B_1 \sin(kbx_3)\exp[\mathrm{i}k(x_1 - ct)], \quad u_3 = B_2 \cos(kbx_3)\exp[\mathrm{i}k(x_1 - ct)] \\ &\varphi = B_3 \cos(kbx_3)\exp[\mathrm{i}k(x_1 - ct)]\end{aligned} \tag{6.114}$$

and assumed that the solutions of the symmetric Lamb waves are (Liu et al. 2002b)

$$\begin{aligned} &u_1 = B_1\cos(kbx_3)\exp[\mathrm{i}k(x_1-ct)], \quad u_3 = B_2\sin(kbx_3)\exp[\mathrm{i}k(x_1-ct)] \\ &\varphi = B_3\sin(kbx_3)\exp[\mathrm{i}k(x_1-ct)] \end{aligned} \tag{6.115}$$

where B_i is the undetermined constant. Substitution of Eqs. (6.114) and (6.115) into Eq. (6.113) yields

$$\begin{aligned} &\pm\left[C_{11}-\rho_0c^2+C_{44}b^2+\eta_\sigma E_3^0\right]B_1+(C_{13}+C_{44})\mathrm{i}bB_2+(e_{31}+e_{15})\mathrm{i}bB_3=0 \\ &(C_{13}+C_{44})\mathrm{i}bB_1\mp\left[C_{44}-\rho_0c^2+C_{33}b^2+\eta_\sigma E_3^0\right]B_2\mp(e_{15}+e_{33}b^2)B_3=0 \\ &(e_{31}+e_{15}+\eta_DE_3^0)\mathrm{i}bB_1\mp\left[e_{15}+(e_{33}+\eta_DE_3^0)b^2\right]B_2\pm(\epsilon_{11}+\epsilon_{33}b^2)B_3=0 \end{aligned} \tag{6.116}$$

where the upper and lower symbols in "$\pm$" and "$\mp$" are used for the antisymmetric and symmetric solutions, respectively. In order to get nontrivial solutions of B_1, B_2, B_3, their coefficient determinant must be zero. So we get a third-order equation of b^2 containing phase velocity c as an unknown parameter:

$$A_1(c)b^6+A_2(c)b^4+A_3(c)b^2+A_4(c)=0 \tag{6.117}$$

Solving Eq. (6.117) we get three solutions of b^2 and select appreciate one $b_l(l=1,2,3)$ in b^2. Substituting $b_l(l=1,2,3)$ into Eq. (6.114) or (6.115) yields the amplitude ratios B_{1l}/B_{3l}, $B_{2l}/B_{3l}, l=1,2,3$. Substituting $b_l, B_{1l}/B_{3l}, B_{2l}/B_{3l}$ $(l=1,2,3)$ back into Eq. (6.114) or (6.115) and then into boundary conditions, we can finally get three homogeneous equations of B_{31}, B_{32}, B_{33}. Let the determinant of the coefficients of B_{31}, B_{32}, B_{33} equal to zero; the equation to determine c is obtained. The details can be seen in the original papers.

Sharma and Pal (2004) also discussed propagation of Lamb waves in a transversely isotropic piezo-thermo-elastic plate. Li et al. (2005b) discussed the spatial dispersion of short surface acoustic waves in piezoelectric ceramics.

6.6 Waves in Pyroelectrics

6.6.1 Generalized Thermodynamics of Temperature Wave in Thermoelasticity

The infinite wave speed problem (Banerjee and Bao 1974) and the Landau second sound speed in liquid helium and in some solids at low temperatures (Landau 1941; Jackson and Walker 1971) induced the development of the generalized heat, thermoelastic, and thermo-piezoelectric wave theories. The temperature wave from heat pulses at low temperature propagates with a finite phase velocity. The main simpler generalized theories with a finite velocity are Kaliski (1965)-Lord-Shulman (K-L-S) theory (1967), Green-Lindsay (G-L) theory (1972), and inertial entropy theory (Kuang 2009). The temperature wave equation can also be established on the extended irreversible thermodynamics and can be found in Joseph and Preziosi's papers (1989, 1990). In the K-L-S theory for an isotropic thermoelastic material, the following Cattaneo-Vernotte heat conduction formula (Vernotte 1958; Cattaneo 1958) was used to replace the Fourier's law, but the classical entropy equation and the Helmholtz free energy are kept, i.e.,

$$\begin{aligned} &q_i + \tau_0 \dot{q}_i = -\lambda \vartheta_{,i}, \quad T\dot{s} = \dot{r} - q_{i,i}, \quad g(\varepsilon_{kl}, \vartheta) = \mathfrak{A}(\varepsilon_{kl}, s) - \vartheta s \\ &\sigma_{ij} = \partial g / \partial \varepsilon_{ij} = C_{ijkl}\varepsilon_{kl} - \alpha_{ij}\vartheta, \quad s = -\partial g / \partial \vartheta = \alpha_{ij}\varepsilon_{ij} + C\vartheta / T_0 \end{aligned} \tag{6.118}$$

where τ_0 represents the relaxation time and is a material parameter. From Eq. (6.118) we find

$$\begin{aligned} &q_{i,i} = -T\dot{s} = T\left[(\partial^2 g/\partial \vartheta^2)\dot{\vartheta} + (\partial^2 g/\partial \vartheta \partial \varepsilon_{ij})\dot{\varepsilon}_{ij}\right] \\ &\lambda \vartheta_{,ii} = T\left[(\partial^2 g/\partial \vartheta^2)(\dot{\vartheta} + \tau_0 \ddot{\vartheta}) + (\partial^2 g/\partial \vartheta \partial \varepsilon_{ij})(\dot{\varepsilon}_{ij} + \tau_0 \ddot{\varepsilon}_{ij})\right] \end{aligned}$$

Then neglecting many small terms, finally, they got

$$\begin{aligned} &\lambda \vartheta_{,ii} = C(\dot{\vartheta} + \tau_0 \ddot{\vartheta}) + \alpha T_0(\dot{\varepsilon}_{kk} + \tau_0 \ddot{\varepsilon}_{kk}) \\ &[G/(1-2\nu)]u_{j,ij} + Gu_{i,jj} - [2G(1+\nu)/(1-2\nu)]\alpha \vartheta_{,i} = \rho \ddot{u}_i \end{aligned} \tag{6.119}$$

where $\alpha_{ij} = \alpha \delta_{ij}$. The second equation in Eq. (6.119) is the momentum equation.

The G-L theory (1972) was based on modifying the Clausius-Duhemin inequality and the energy equation; They used a new temperature function $\phi(T, \dot{T})$ instead of the usual temperature T. i.e.,

$$\begin{aligned} &\int_V \dot{s}\,\mathrm{d}V - \int_V (r/\phi)\,\mathrm{d}V + \int_a (q_i/\phi)n_i\,\mathrm{d}a \geq 0, \quad \phi = \phi(T, \dot{T}), \quad T = \phi(T, 0) \\ &g = \mathfrak{A} - \phi s, \quad g = g(T, \dot{T}, \varepsilon_{ij}) \end{aligned} \tag{6.120}$$

Substituting Eq. (6.120) into the momentum and energy equations, after complex manipulation and linearization and neglecting small terms finally get (here we take the form in small deformation for an isotropic material)

$$\begin{aligned} &\lambda T_{,ii} = C(\dot{T} + \tau_0 \ddot{T}) + \gamma T_0 \dot{\varepsilon}_{jj}, \quad \sigma_{ji,j} + \rho f_i = \rho \ddot{u}_i \\ &\sigma_{ij} = [2G\nu/(1-2\nu)]\varepsilon_{kk}\delta_{ij} + 2G\varepsilon_{ij} - \gamma(\theta + \tau_1 \dot{\theta}) \end{aligned} \tag{6.121}$$

where τ_0, τ_1, and γ are material constants.

The derivation of the governing equations is very complex when using K-L-S or G-L theory, but the derivation is very simple when the inertial entropy theory is used as shown at the next section.

6.6.2 The Inertial Entropy Theory of Temperature Wave

In Sect. 1.7.2 the inertial entropy theory (Kuang 2009) is introduced. Equation (1.84) gives

$$T\dot{s} + T\dot{s}^{(\mathrm{a})} = \dot{r} - q_{i,i}; \quad \dot{s}^{(\mathrm{a})} = \rho_{\mathrm{s}}\ddot{T}, \quad \rho_{\mathrm{s}} = \rho_{\mathrm{s}0}C/T \tag{6.122}$$

The Fourier's law given in Eqs. (1.71) or (5.107) is

$$q_i = -\lambda_{ij}T_{,j}, \quad T_{,j} = \vartheta_{,j} = -\lambda_{ji}^{-1}q_i; \quad -q_{i,i} = T\dot{s} - \dot{r} \tag{6.123}$$

The constitutive (or state) and evolution equations given in (5.106) are

$$\begin{aligned} &\sigma_{ij} = C_{ijkl}\varepsilon_{kl} - e_{kij}E_k - \alpha_{ij}\vartheta, \quad D_i = \epsilon_{ij}E_j + e_{ikl}\varepsilon_{kl} + \tau_i\vartheta \\ &s = \alpha_{ij}\varepsilon_{ij} + \tau_i E_i + C\vartheta/T_0, \quad \vartheta = T - T_0 \end{aligned} \tag{6.124}$$

where α_{ij} is the stress-temperature coefficient. Equations (6.122), (6.123), and (6.124) yield

$$(\alpha_{ij}\varepsilon_{ij} + \tau_i E_i + C\vartheta/T_0)^{\cdot} + \rho_{\mathrm{s}0}(C/T)\ddot{\vartheta} = \dot{r}/T + (\lambda_{ij}T_{,j})_{,i}/T \tag{6.125}$$

When material coefficients are all constants and the variation of temperature is not large from (6.125) we have

$$(C/T_0)(\rho_{\mathrm{s}0}\ddot{\vartheta} + \dot{\vartheta}) - \lambda_{ij}\vartheta_{,ji}/T_0 = \dot{r}/T_0 - \alpha_{ij}\dot{u}_{i,j} + \tau_i\dot{\varphi}_{,i} \tag{6.126}$$

Equation (6.126) is a temperature wave equation with finite phase velocity.

The generalized momentum equations are

$$\begin{aligned} &\sigma_{ij,j} + f_i = \rho\ddot{u}_i, \quad \text{or} \quad \rho\ddot{u}_i = C_{ijkl}u_{k,lj} + e_{kij}\varphi_{,kj} - \alpha_{ij}\vartheta_{,j} + f_i \\ &D_{i,i} = \rho_{\mathrm{e}}, \quad \text{or} \quad e_{ikj}u_{k,ji} - \epsilon_{ij}\varphi_{,ji} + \tau_i\vartheta_{,i} = \rho_{\mathrm{e}} \end{aligned} \tag{6.127}$$

It is obvious that the experimental studies for the inertial entropy theories are very important.

6.6.3 The Homogeneous Thermo-electro-elastic Wave in Pyroelectric Material

Under the quasi-static electric approximation, the governing equations of the waves in pyroelectric material in the inertial entropy theory are shown in Eqs. (6.126) and (6.125). Like Eq. (6.119), using Eq. (6.118) in a piezoelectric material, the extended K-L-S equation can also be obtained. When $f_j^{\mathrm{m}}, f_j^{\mathrm{e}}, \rho_{\mathrm{e}}, r$ are not considered and assuming the variation of temperature is small (i.e., let $T \approx T_0$), the inertial entropy theory, the K-L-S theory can be expressed in a unified equation system:

$$\begin{aligned} &C_{ijkl}u_{k,lj} + e_{kij}\varphi_{,kj} - \alpha_{ij}\vartheta_{,j} = \rho\ddot{u}_i, \quad e_{ikj}u_{k,ji} - \epsilon_{ij}\varphi_{,ji} + \tau_i\vartheta_{,i} = 0 \\ &T_0\alpha_{ij}(\dot{u}_{i,j} + \xi_1\ddot{u}_{i,j}) - T_0\tau_i(\dot{\varphi}_{,i} + \xi_2\ddot{\varphi}_{,i}) + C(\dot{\vartheta} + \xi_0\ddot{\vartheta}) = \lambda_{ij}\vartheta_{,ji} \end{aligned} \tag{6.128}$$

When $\xi_1 = \xi_2 = 0, \xi_0 = \rho_{s0}$, Eq. (6.128) represents the inertial entropy theory and $\xi_1 = \xi_2 = \xi_0 = \tau_0$ represents the K-L-S theory. In Sect. 1.6.2 we have pointed out that there are some questions in the K-L-S theory. Here we can also show that (1) from Eq. (6.118) we get $T\dot{s} - \tau_0 T\ddot{s} = \lambda_{ij}T_{,ji} + (\dot{r} + \tau_0\ddot{r})$, so it is difficult to consider that s is a state function. (2) It is difficult to physically explain why Eq. (6.128) also has the inertial terms $\tau_0 T_0(-\tau_i\ddot{\varphi}_{,i}, \alpha_{ij}\ddot{u}_{i,j})$. (3) The Fourier thermal conductive equation is substantially an irreversible phenomenon, which is in the same level with the mechanical viscous effect, as seen from the equation of the entropy production. So the viscous effect in elasticity produced by the Cattaneo-Vernotte heat conductive equation is a second effect.

For a plane wave Eq. (6.2) becomes

$$u_k = U_k \mathrm{e}^{\mathrm{i}(kn_m x_m - \omega t)}, \quad \varphi = \Phi \mathrm{e}^{\mathrm{i}(kn_m x_m - \omega t)}, \quad \vartheta = \Theta \mathrm{e}^{\mathrm{i}(kn_m x_m - \omega t)} \tag{6.129}$$

or

$$u_k = U_k \mathrm{e}^{i\omega(L_m x_m - t)}, \quad \varphi = \Phi \mathrm{e}^{i\omega(L_m x_m - t)}, \quad \vartheta = \Theta \mathrm{e}^{i\omega(L_m x_m - t)}; \quad L_m = kn_m/\omega = n_m/c \tag{6.130}$$

where U, Φ, Θ are the amplitudes of the displacement, electric potential, and temperature, respectively. In general k is a complex number:

$$k = \alpha + \mathrm{i}\beta, \quad \mathrm{e}^{\mathrm{i}(kn_m x_m - \omega t)} = \mathrm{e}^{-\beta n_m x_m}\mathrm{e}^{\mathrm{i}(\alpha n_m x_m - \omega t)}, \quad c = \omega/\alpha, \quad \boldsymbol{c} = (\omega/\alpha)\boldsymbol{n} \tag{6.131}$$

where c is the phase velocity and β is the attenuation coefficient. Substituting Eq. (6.129) into (6.128) and dropping the common factor $\exp[\mathrm{i}(kn_m x_m - \omega t)]$ we obtain the Christoffel equation:

$$
\begin{aligned}
&(\Gamma_{ik}^{*}k^{2}-\rho\omega^{2}\delta_{ik})U_{k}+e_{i}^{*}k^{2}\Phi+\mathrm{i}\alpha_{i}^{*}k\Theta=0\\
&e_{k}^{*}k^{2}U_{k}-\epsilon^{*}k^{2}\Phi-\mathrm{i}\tau^{*}k\Theta=0\\
&T_{0}\alpha_{k}^{*}k\omega(1-\mathrm{i}\xi_{1}\omega)U_{k}-T_{0}\tau^{*}k\omega(1-\mathrm{i}\xi_{2}\omega)\Phi+(\lambda^{*}k^{2}-C\xi_{0}\omega^{2}-\mathrm{i}C\omega)\Theta=0
\end{aligned}
\tag{6.132}
$$

or

$$
\boldsymbol{\Lambda}(k,\omega,\boldsymbol{n})\boldsymbol{U}=\mathbf{0},\quad \boldsymbol{U}=[U_1,U_2,U_3,\Phi,\Theta]^{\mathrm{T}}
\tag{6.133}
$$

where

$$
\boldsymbol{\Lambda}=\begin{bmatrix}
\Gamma_{11}^{*}k^{2}-\rho\omega^{2} & \Gamma_{12}^{*}k^{2} & \Gamma_{13}^{*}k^{2} & e_{1}^{*}k^{2} & \mathrm{i}\alpha_{1}^{*}k\\
\Gamma_{21}^{*}k^{2} & \Gamma_{22}^{*}k^{2}-\rho\omega^{2} & \Gamma_{23}^{*}k^{2} & e_{2}^{*}k^{2} & \mathrm{i}\alpha_{2}^{*}k\\
\Gamma_{31}^{*}k^{2} & \Gamma_{32}^{*}k^{2} & \Gamma_{33}^{*}k^{2}-\rho\omega^{2} & e_{3}^{*}k^{2} & \mathrm{i}\alpha_{3}^{*}k\\
e_{1}^{*}k^{2} & e_{2}^{*}k^{2} & e_{3}^{*}k^{2} & -\epsilon^{*}k^{2} & -\mathrm{i}\tau^{*}k\\
\alpha_{1}^{*}k\omega\eta_{1} & \alpha_{2}^{*}k\omega\eta_{1} & \alpha_{3}^{*}k\omega\eta_{1} & -\tau^{*}k\omega\eta_{2} & T_{0}^{-1}(\lambda^{*}k^{2}-C\eta_{3})
\end{bmatrix}
\tag{6.134}
$$

with

$$
\begin{aligned}
&\Gamma_{ik}^{*}=C_{ijkl}n_{j}n_{l},\quad e_{i}^{*}=e_{kij}n_{k}n_{j},\quad \alpha_{i}^{*}=\alpha_{ij}n_{j}\\
&\tau^{*}=\tau_{j}n_{j},\quad \epsilon^{*}=\epsilon_{jk}n_{k}n_{j},\quad \lambda_{j}^{*}=\lambda_{ij}n_{i},\quad \lambda^{*}=\lambda_{j}^{*}n_{j}\\
&\eta_{1}=1-\mathrm{i}\xi_{1}\omega,\quad \eta_{2}=1-\mathrm{i}\xi_{2}\omega,\quad \eta_{3}=\xi_{0}\omega^{2}+\mathrm{i}\omega
\end{aligned}
\tag{6.135}
$$

In order to get the nontrivial solution of $\boldsymbol{U}$, it is necessary that

$$
\det\Lambda(k,\omega,\boldsymbol{n})=0
\tag{6.136a}
$$

Equation (6.136) is called the secular equation and can be expanded to

$$
\left[F_{8}(\omega,\mathbf{n})k^{8}+F_{6}(\omega,\mathbf{n})k^{6}+F_{4}(\omega,\mathbf{n})k^{4}+F_{2}(\omega,\mathbf{n})k^{2}+F_{0}(\omega,\mathbf{n})\right]k^{2}=0
\tag{6.136b}
$$

where $F_i(\omega,\boldsymbol{n})$ is known functions of $(\omega,\boldsymbol{n})$. So one k^2 is zero in Eq. (6.136), i.e., the wave velocity of the electric potential is infinite or the electric potential does not have its own independent wave mode. From Eq. (6.136) we can solve four independent eigenvalues or wave velocity, and for each wave velocity an independent mode from Eq. (6.133) is obtained. There are total four independent modes: the quasi-longitudinal (QL) wave with highest wave velocity, fast quasi-transverse wave (FT), slow quasi-transverse wave (ST), and a temperature wave (T).

From Eq. (6.132) we can also eliminate $\boldsymbol{\Phi}$ to get equations with independent variables U_k, ϑ.

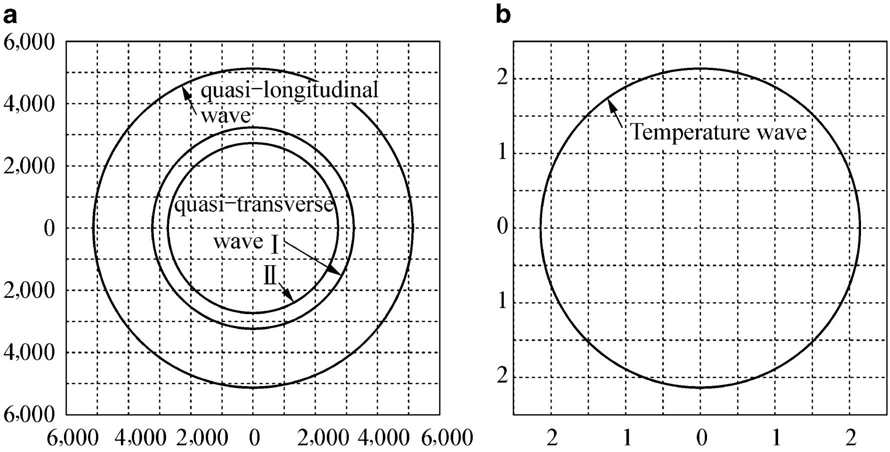

Fig. 6.11 Cross sections of the velocity surfaces in an isotropic plane (x_1, x_2): (**a**) elastic waves and (**b**) temperature wave

6.6.4 An Example

Now we discuss the character surfaces for material $BaTiO_3$ under $\omega = 2\pi \times 10^6\,s^{-1}$, $\gamma = 0$. Material constants of $BaTiO_3$ with poling axis x_3 are

$$
\begin{aligned}
&C_{11} = 150, \quad C_{12} = 66, \quad C_{13} = 66, \quad C_{33} = 146, \quad C_{44} = 44, \quad C_{66} = 43(\mathrm{MPa});\\
&e_{13} = -4.35, \quad e_{33} = 17.5, \quad e_{15} = 11.4(\mathrm{C/m^2});\\
&\epsilon_{11} = 9.87, \quad \epsilon_{33} = 11.15(10^{-9}\mathrm{C/Vm}); \quad \lambda_{11} = 1.1, \quad \lambda_{33} = 3.5\mathrm{J/mKs};\\
&\alpha_{11}^{\varepsilon} = 8.53, \quad \alpha_{33}^{\varepsilon} = 1.99(10^{-6}/\mathrm{K}); \quad \tau = 5.53(10^{-3}\mathrm{C/m^2K})\\
&\alpha_{11} = \alpha_{22} = (C_{11} + C_{12})\alpha_{11}^{\varepsilon} + (C_{13} + e_{31})\alpha_{33}^{\varepsilon}, \quad \alpha_{33} = 2C_{13}\alpha_{11}^{\varepsilon} + (C_{33} + e_{33})\alpha_{33}^{\varepsilon}
\end{aligned}
$$

where $\alpha_{11}^{\varepsilon}$, $\alpha_{33}^{\varepsilon}$ are the usual thermal expansion coefficients. Figure 6.11 (a) and (b) gives the velocity surfaces of the elastic waves and temperature wave in the isotropic plane (x_1, x_2), respectively; Fig. 6.12 (a) and (b) gives the velocity surfaces of the elastic waves and temperature wave in the anisotropic plane (x_1, x_3), respectively; Fig. 6.13 (a) and (b) gives the slowness surfaces of the elastic waves and temperature wave in the anisotropic plane (x_1, x_3), respectively. The dotted lines in the Fig. 6.13 represent the velocity or slowness surfaces for purely elastic material. The numerical results show that the attenuation of the temperature wave is large, but for the elastic waves, they are small and may be negative for certain ρ_{s0}. The results of Ezzat et al. (2002) and Yuan and Kuang (2008) also showed that the temperature wave can enforce the elastic wave when the temperature is decreased. It means that the term containing ρ_{s0} enforces the elastic wave, or when the temperature decreased, the released inertial heat is partly transformed to the elastic wave. It may be a restriction of ρ_{s0}. This phenomenon has been discussed in Sect. 1.7.5.

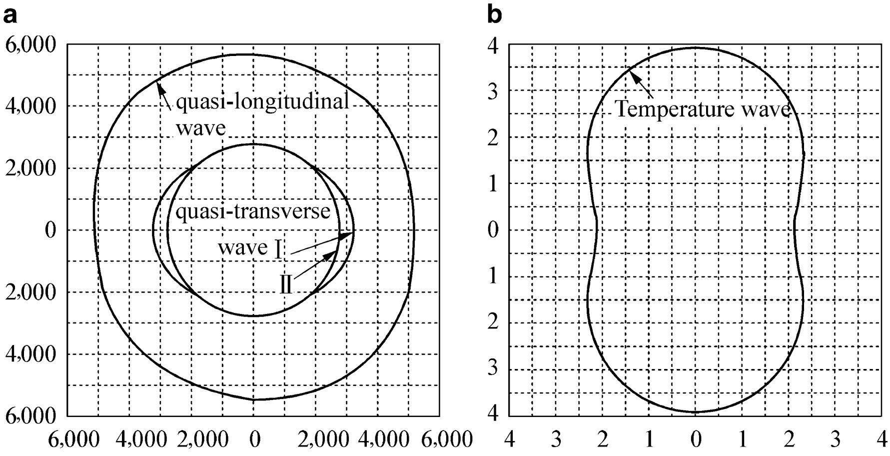

Fig. 6.12 Cross sections of the velocity surfaces in an anisotropic plane (x_1, x_3): (**a**) elastic waves and (**b**) temperature wave

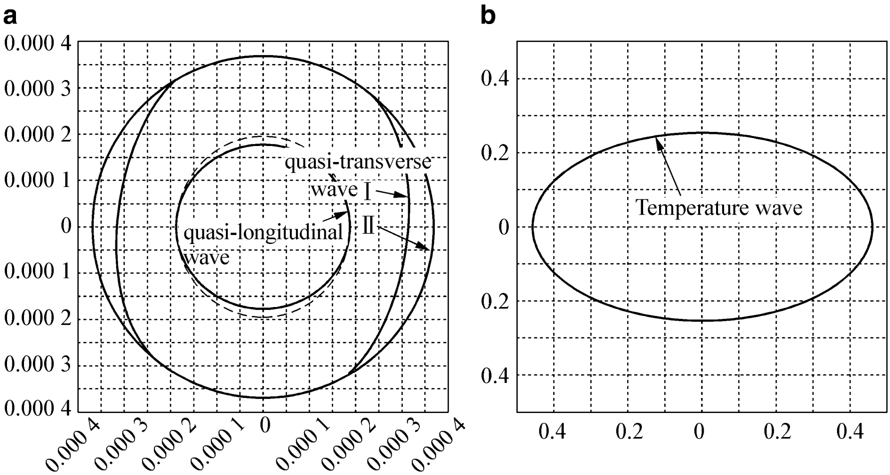

Fig. 6.13 Cross sections of the slowness surfaces in an anisotropic plane (x_1, x_3): (**a**) elastic waves and (**b**) temperature wave

6.6.5 Inhomogeneous Wave

In the framework of the inhomogeneous wave theory generally, the wave vector is $\boldsymbol{k} = \boldsymbol{P} + \mathrm{i}\boldsymbol{A}$, where $\boldsymbol{P}$ and $\boldsymbol{A}$ are two real vectors (Buchen 1971; Borcherdt 1973). The vector $\boldsymbol{n} = \boldsymbol{P}/|\boldsymbol{P}|$ represents the wave propagation direction which is perpendicular to the wave surface with equal phase, and $\boldsymbol{m} = \boldsymbol{A}/|\boldsymbol{A}|$ represents the maximum

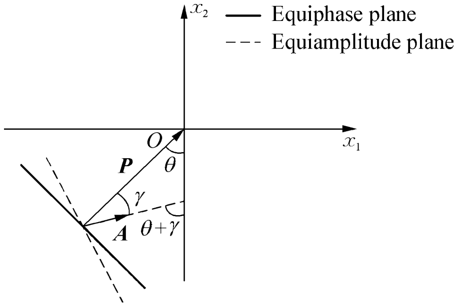

Fig. 6.14 Inhomogeneous wave

attenuation direction which is perpendicular to the equal-amplitude surface. The angle γ between $\boldsymbol{n}$ and $\boldsymbol{m}$ is called the attenuation angle (Fig. 6.14). The surface wave may be considered as an inhomogeneous wave with $\gamma = \pi/2$ and P is parallel to the surface. In general case how to determine γ is not very clear (Krebes 1983). For an inhomogeneous plane wave, we have (Yuan and Kuang 2010)

$$\begin{aligned} &f = f_0 \mathrm{e}^{\mathrm{i}(\boldsymbol{k}\cdot\boldsymbol{x}-\omega t)} = f_0 \mathrm{e}^{\mathrm{i}(k_m x_m - \omega t)}, \quad \boldsymbol{k} = \boldsymbol{P} + \mathrm{i}\boldsymbol{A}, \quad \boldsymbol{P} = P\boldsymbol{n}, \quad \boldsymbol{A} = A\boldsymbol{m} \\ &k_j = P_j + \mathrm{i}A_j = Pn_j + \mathrm{i}Am_j, \quad P = \sqrt{P_1^2 + P_2^2}, \quad A = \sqrt{A_1^2 + A_2^2} \end{aligned} \tag{6.137}$$

Let θ denote the angle between $\boldsymbol{n}$ and the ordinate, so

$$\boldsymbol{n} = [\sin\theta, \cos\theta]^{\mathrm{T}}, \quad \boldsymbol{m} = [\sin(\theta+\gamma), \cos(\theta+\gamma)]^{\mathrm{T}}, \quad \boldsymbol{n}\cdot\boldsymbol{m} = \cos\gamma \tag{6.138}$$

For an inhomogeneous wave we need four variables (P, A, θ, γ) to describe it, but for a homogeneous wave we only need three variables (P, A, θ) due to $\boldsymbol{n} = \boldsymbol{m}, \gamma = 0$ and $k_1 = (P + \mathrm{i}A)\sin\theta,\ k_2 = (P + \mathrm{i}A)\cos\theta$. So $\boldsymbol{k}$ can be expressed by one complex number.

An inhomogeneous plane wave can be written as

$$u_k = U_k \mathrm{e}^{\mathrm{i}(k_m x_m - \omega t)}, \quad \varphi = \Phi \mathrm{e}^{\mathrm{i}(k_m x_m - \omega t)}, \quad \vartheta = \Theta \mathrm{e}^{\mathrm{i}(k_m x_m - \omega t)} \tag{6.139}$$

Substituting Eq. (6.139) into (6.129) and dropping the common factor we get the Christoffel equation:

$$\begin{aligned} &\boldsymbol{\Lambda}(\boldsymbol{k},\omega)\boldsymbol{U} = \boldsymbol{0}, \quad \boldsymbol{U} = [U_1, U_2, U_3, \Phi, \Theta]^{\mathrm{T}} \\ &\boldsymbol{\Lambda} = \begin{bmatrix} \Gamma_{11}^*(\boldsymbol{k}) - \rho\omega^2 & \Gamma_{12}^*(\boldsymbol{k}) & \Gamma_{13}^*(\boldsymbol{k}) & e_1^*(\boldsymbol{k}) & \mathrm{i}\alpha_1^*(\boldsymbol{k}) \\ \Gamma_{21}^*(\boldsymbol{k}) & \Gamma_{22}^*(\boldsymbol{k}) - \rho\omega^2 & \Gamma_{23}^*(\boldsymbol{k}) & e_2^*(\boldsymbol{k}) & \mathrm{i}\alpha_2^*(\boldsymbol{k}) \\ \Gamma_{31}^*(\boldsymbol{k}) & \Gamma_{32}^*(\boldsymbol{k}) & \Gamma_{33}^*(\boldsymbol{k}) - \rho\omega^2 & e_3^*(\boldsymbol{k}) & \mathrm{i}\alpha_3^*(\boldsymbol{k}) \\ e_1^*(\boldsymbol{k}) & e_2^*(\boldsymbol{k}) & e_3^*(\boldsymbol{k}) & -\epsilon^*(\boldsymbol{k}) & -\mathrm{i}\tau^*(\boldsymbol{k}) \\ T_0\alpha_1^*(\boldsymbol{k})\eta_1 & T_0\alpha_2^*(\boldsymbol{k})\eta_1 & T_0\alpha_3^*(\boldsymbol{k})\eta_1 & -T_0\tau^*(\boldsymbol{k})\eta_2 & \lambda^* - C\eta_3 \end{bmatrix} \end{aligned} \tag{6.140}$$

where

$$\begin{aligned}&\Gamma_{ik}^{*}(\boldsymbol{k})=C_{ijkl}k_jk_l,\quad e_i^{*}(\boldsymbol{k})=e_{kij}k_kk_j,\quad \alpha_i^{*}(\boldsymbol{k})=\alpha_{ij}k_j\\&\tau^{*}(\boldsymbol{k})=\tau_jk_j,\quad \epsilon^{*}(\boldsymbol{k})=\epsilon_{jk}k_kk_j,\quad \lambda_j^{*}=\lambda_{ij}n_i,\quad \lambda^{*}(\boldsymbol{k})=\lambda_{ij}k_ik_j\\&\eta_1=1-\mathrm{i}\xi_1\omega,\quad \eta_2=1-\mathrm{i}\xi_2\omega,\quad \eta_3=\xi_0\omega^2+\mathrm{i}\omega\end{aligned} \tag{6.141}$$

The secular equation corresponding to Eq. (6.140) is

$$|\boldsymbol{\Lambda}|=0 \tag{6.142a}$$

Substituting $k_j=Pn_j+iAm_j$ and decomposing $|\boldsymbol{\Lambda}|=0$ into real and imaginary parts we get two coupling real equations of (P,A,θ,γ):

$$\mathrm{Re}|\boldsymbol{\Lambda}|=0,\quad \mathrm{Im}|\boldsymbol{\Lambda}|=0 \tag{6.142b}$$

Giving (θ,γ), (P,A) can be obtained from Eq. (6.142), so (k_1,k_2). It means that k_1 and k_2 are obtained simultaneously. In order to (P,A) are not negative it needs $-\pi/2<\gamma<\pi/2$.

Similar to the homogeneous wave, Eq. (6.142) only has four independent eigenvalues $\boldsymbol{k}_i=P_i\boldsymbol{n}+\mathrm{i}A_i\boldsymbol{m}$ $(i=1,2,3,4)$ corresponding four phase velocities:

$$c_i=\omega/P_i,\quad P_i=\sqrt{(P_in_1)^2+(P_in_2)^2} \tag{6.143}$$

Corresponding each complex $\boldsymbol{k}_i$, from Eq. (6.142) we can get the amplitude vectors or eigenvectors $\boldsymbol{U}_i$. In each $\boldsymbol{U}_i$, $U_{1i}:U_{2i}:U_{3i}:\Phi_i(=U_{4i}):\Theta_i(=U_{5i})$ is determined, i.e., only one component, say, $U_{j1}=\beta_j$, is undetermined. So there are only four undetermined amplitude components, and the general solution of the wave propagation problem is

$$\begin{aligned}&u_k=\sum_{j=1}^{4}\beta_jU_k^{(j)}\mathrm{e}^{\mathrm{i}(k_m^{(j)}x_m-\omega t)},\quad \varphi=\sum_{j=1}^{4}\beta_j\Phi^{(j)}\mathrm{e}^{\mathrm{i}(k_m^{(j)}x_m-\omega t)},\quad \vartheta=\sum_{j=1}^{4}\beta_j\Theta^{(j)}\mathrm{e}^{\mathrm{i}(k_m^{(j)}x_m-\omega t)}\\&\mathrm{e}^{\mathrm{i}(k_m^{(j)}x_m-\omega t)}=\mathrm{e}^{\mathrm{i}\left[(P^{(j)}\boldsymbol{n}+\mathrm{i}A^{(j)}\boldsymbol{m})\cdot\boldsymbol{x}-\omega t\right]}=\mathrm{e}^{-A^{(j)}\boldsymbol{m}\cdot\boldsymbol{x}}\mathrm{e}^{\mathrm{i}(P^{(j)}\boldsymbol{n}\cdot\boldsymbol{x}-\omega t)}\end{aligned} \tag{6.144}$$

where $\beta_j(i=1,2,3,4)$ is an undetermined coefficient.

The numerical calculations for $BaTiO_3$ show that the effect of γ on the velocity surfaces of elastic waves is limited and there is a certain effect on the velocity surfaces of the temperature. There are certain effects on the attenuation coefficients of all waves.

6.7 Reflection and Transmission of Waves in Pyroelectric and Piezoelectric Materials

6.7.1 General Theory

Consider the problem of two semi-infinite pyroelectric materials I and II bounded on the interface $x_2 = 0$ subjected to an inhomogeneous harmonic incident wave of frequency ω with an incident angle θ from the lower semi-plane I, $x_2 < 0$, (Fig. 6.15) (Kuang and Yuan 2011; Zhou et al. 2012). In Fig. 6.15 only one reflection wave and one transmission wave are drawn for clarity. The mechanical, electrical, and thermal continuity conditions on the interface are (MCC), (ECC), and (TCC), respectively

$$\begin{array}{llll} \text{MCC}: & u_i^I = u_i^{II}, & \sigma_{ij}^I n_i^I + \sigma_{ij}^{II} n_i^{II} = 0, & (6\text{ conditions}) \\ \text{ECC}: & \varphi^I = \varphi^{II}, & D_i^I n_i^I + D_i^{II} n_i^{II} = 0, & (2\text{ conditions}) \\ \text{TCC}: & \vartheta^{\mathrm{I}} = \vartheta^{\mathrm{II}}, & \lambda_{ij}^{\mathrm{I}} \vartheta_{,j}^{\mathrm{I}} n_i^{\mathrm{I}} + \lambda_{ij}^{\mathrm{II}} \vartheta_{,j}^{\mathrm{II}} n_i^{\mathrm{II}} = 0, & (2\text{ conditions}) \end{array} \tag{6.145}$$

where $n_i^{\mathrm{II}} = -n_i^{\mathrm{I}}$. There are totally ten continuity conditions on the interface.

Let an incident wave with a wave vector $\boldsymbol{k}^{(0)}$ be in the semi-infinite plane I, $x_2 \le 0$, and corresponding displacement, electric potential, and relative temperature can be expressed by

$$u_k^{(0)} = U_k^{(0)} \mathrm{e}^{\mathrm{i}\left(k_m^{(0)} x_m - \omega t\right)}, \quad \varphi^{(0)} = \Phi^{(0)} \mathrm{e}^{\mathrm{i}\left(k_m^{(0)} x_m - \omega t\right)}, \quad \vartheta^{(0)} = \Theta^{(0)} \mathrm{e}^{\mathrm{i}\left(k_m^{(0)} x_m - \omega t\right)}, \tag{6.146}$$

where $U_k^{(0)}$, $\Phi^{(0)}$, $\Theta^{(0)}$ and $k_m^{(0)}$ are all known. The reflection wave in the semi-infinite plane I, $x_2 \le 0$, can be expressed by

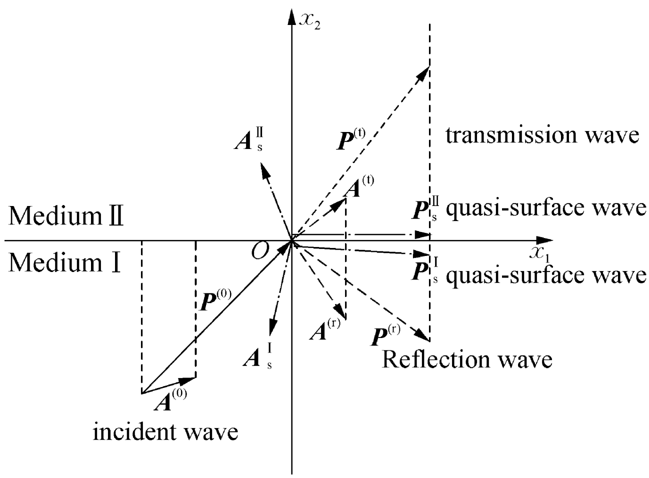

Fig. 6.15 A sketch of reflection and transmission of inhomogeneous waves

$$
\begin{aligned}
u_k^{(r)} &= \sum_{j=1}^{N} \beta_j^{(r)} U_k^{(r,j)} \mathrm{e}^{\mathrm{i}\left(k_m^{(r,j)} x_m - \omega t\right)}, \quad \varphi^{(r)} = \sum_{j=1}^{N} \beta_j^{(r)} \Phi^{(r,j)} \mathrm{e}^{\mathrm{i}\left(k_m^{(r,j)} x_m - \omega t\right)} \\
\vartheta^{(r)} &= \sum_{j=1}^{N} \beta_j^{(r)} \Theta^{(r,j)} \mathrm{e}^{\mathrm{i}\left(k_m^{(r,j)} x_m - \omega t\right)}
\end{aligned}
\tag{6.147}
$$

and the transmission wave in the semi-infinite plane II, $x_2 \geq 0$, can be expressed by

$$
\begin{aligned}
u_k^{(t)} &= \sum_{j=1}^{N} \beta_j^{(t)} U_k^{(t,j)} \mathrm{e}^{\mathrm{i}\left(k_m^{(t,j)} x_m - \omega t\right)}, \quad \varphi^{(t)} = \sum_{j=1}^{N} \beta_j^{(t)} \Phi^{(t,j)} \mathrm{e}^{\mathrm{i}\left(k_m^{(t,j)} x_m - \omega t\right)} \\
\vartheta^{(t)} &= \sum_{j=1}^{N} \beta_j^{(t)} \Theta^{(t,j)} \mathrm{e}^{\mathrm{i}\left(k_m^{(t,j)} x_m - \omega t\right)}
\end{aligned}
\tag{6.148}
$$

In Eqs. (6.147) and (6.148), N is the number of the independent waves. It is obvious that

$$
\begin{aligned}
&u_k^{\mathrm{I}} = u_k^{(0)} + u_k^{(r)}, \quad u_k^{\mathrm{II}} = u_k^{(t)}, \quad \varphi^{\mathrm{I}} = \varphi^{(0)} + \varphi^{(r)}, \quad \varphi^{\mathrm{II}} = \varphi^{(t)}, \quad \vartheta^{\mathrm{I}} = \vartheta^{(0)} + \vartheta^{(r)}, \quad \vartheta^{\mathrm{II}} = \vartheta^{(t)} \\
&\sigma_{ij}^{\mathrm{I}} = \sigma_{ij}^{(0)} + \sigma_{ij}^{(r)}, \quad \sigma_{ij}^{\mathrm{II}} = \sigma_{ij}^{(t)}, \quad D_i^{\mathrm{I}} = D_i^{(0)} + D_i^{(r)}, \quad D_i^{\mathrm{II}} = D_i^{(t)}
\end{aligned}
\tag{6.149}
$$

When waves propagate in the x_1-x_2 plane, the following synchronism condition should be held:

$$
k_1^{(0)} = k_1^{(r,j)} = k_1^{(t,j)}, \quad k_1^{(\alpha,j)} = k^{(\alpha,j)} n_1^{(\alpha,j)}, \quad (\alpha = r, t;\ j = 1 - N) \tag{6.150}
$$

Decomposing Eq. (6.150) into real and imaginary parts yields

$$
\begin{aligned}
&P^{(0)} \sin\theta^{(0)} = P^{(r,j)} \sin\theta^{(r,j)} = P^{(t,j)} \sin\theta^{(t,j)} \\
&A^{(0)} \sin\left(\theta^{(0)} + \gamma^{(0)}\right) = A^{(r,j)} \sin\left(\theta^{(r,j)} + \gamma^{(r,j)}\right) = A^{(t,j)} \sin\left(\theta^{(t,j)} + \gamma^{(t,j)}\right)
\end{aligned}
\tag{6.151}
$$

From Eqs. (6.137) and (6.151), we can get the generalized Snell's law from the real part:

$$
\begin{aligned}
&\frac{\sin\theta^{(0)}}{c^{(0)}} = \frac{\sin\theta^{(r,j)}}{c^{(r,j)}} = \frac{\sin\theta^{(t,j)}}{c^{(t,j)}}, \quad c^{(0)} = \frac{\omega}{P^{(0)}}, \quad c^{(r,j)} = \frac{\omega}{P^{(r,j)}}, \\
&\quad c^{(t,j)} = \frac{\omega}{P^{(t,j)}};\ (j = 1 - N)
\end{aligned}
\tag{6.152}
$$

From Eq. (6.152), $\theta^{(r,j)}, \theta^{(t,j)}, \gamma^{(r,j)}, \gamma^{(t,j)}$ can be solved when $\theta^{(0)}, \gamma^{(0)}, c^{(0)}$ and $c^{(r,j)}$, $c^{(t,j)}$ are known. In the reflection and transmission wave case, $k_1^{(0)} = k_1^{(r,j)} = k_1^{(t,j)}$ are known and unknowns are $k_2^{(r,j)}, k_2^{(t,j)}$ in Eq. (6.142). In this case except four bulk waves as that in the infinite space, a new kind of wave will be revealed. The numerical examples show that this new wave propagates almost parallel to the interface, but the maximum attenuation direction is almost perpendicular to the interface. So we call it quasi-surface wave or QS wave. The similar waves called evanescent wave in the previous literatures for piezoelectric by Auld (1973) and Every and Neiman (1992) had been discussed. Sharma et al. (2008) discussed also the wave reflection and transmission in pyroelectric materials.

Substituting Eqs. (6.146), (6.147), (6.148), and (6.149) into Eq. (6.145), the ten boundary conditions on the interface can be expressed as

$$\begin{aligned}
&U_k^{(0)} + \sum_{j=1}^{5} \beta_j^{(r)} U_k^{(r,j)} = \sum_{j=1}^{5} \beta_j^{(t)} U_k^{(t,j)}, k = 1-3,\\
&C_{2iml}^{(r)} k_l^{(0)} U_m^{(0)} + e_{m2i}^{(r)} k_m^{(0)} \Phi^{(0)} + \mathrm{i}\alpha_{i2}^{(r)} \Theta^{(0)} + \sum_{j=1}^{5} \beta_j^{(r)} (C_{2iml}^{(r)} k_l^{(r,j)} U_m^{(r,j)} + e_{m2i}^{(r)} k_m^{(r,j)} \Phi^{(r,j)}\\
&\quad + \mathrm{i}\alpha_{i2}^{(r)} \Theta^{(r,j)} = \sum_{j=1}^{5} \beta_j^{(t)} \left(C_{2iml}^{(t)} k_l^{(t,j)} U_m^{(t,j)} + e_{m2i}^{(t)} k_m^{(t,j)} \Phi^{(t,j)} + \mathrm{i}\alpha_{i2}^{(t)} \Theta^{(t,j)} \right), \quad i = 1-3
\end{aligned} \tag{6.153a}$$

$$\begin{aligned}
&\Phi^{(0)} + \sum_{j=1}^{5} \beta_j^{(r)} \Phi^{(r,j)} = \sum_{j=1}^{5} \beta_j^{(t)} \Phi^{(t,j)}\\
&\quad - \epsilon_{2m}^{(r)} k_m^{(0)} \Phi^{(0)} + e_{2pm}^{(r)} k_m^{(0)} U_p^{(0)} - \mathrm{i}\tau_i^{(r)} \Theta^{(0)} + \sum_{j=1}^{5} \beta_j^{(r)} \left(e_{2pm}^{(r)} k_m^{(r,j)} U_p^{(r,j)} - \epsilon_{2m}^{(r)} k_m^{(r,j)} \Phi^{(r,j)} \right.\\
&\left. -\mathrm{i}\tau_i^{(r)} \Theta^{(r,j)} \right) = \sum_{j=1}^{5} \beta_j^{(t)} \left(e_{2pm}^{(t)} k_m^{(t,j)} U_p^{(t,j)} - \epsilon_{2m}^{(t)} k_m^{(t,j)} \Phi^{(t,j)} - \mathrm{i}\tau_i^{(t)} \Theta^{(t,j)} \right)
\end{aligned} \tag{6.153b}$$

$$\begin{aligned}
&\Theta^{(0)} + \sum_{j=1}^{5} \beta_j^{(r)} \Theta^{(r,j)} = \sum_{j=1}^{5} \beta_j^{(t)} \Theta^{(t,j)}\\
&\lambda_{2m}^{(r)} k_m^{(0)} \Theta^{(0)} + \lambda_{2m}^{(r)} \sum_{j=1}^{5} \beta_j^{(r)} k_m^{(r,j)} \Theta^{(r,j)} = \lambda_{2m}^{(t)} \sum_{j=1}^{5} \beta_j^{(t)} k_m^{(t,j)} \Theta^{(t,j)}
\end{aligned} \tag{6.153c}$$

Therefore, in the reflection and transmission waves, there are ten complex unknown amplitude coefficients $\beta_j^{(r)}$ and $\beta_j^{(t)}$ $(j = 1-5)$ with total ten complex interface continuity conditions. This shows that the reflection and transmission waves are solvable.

The general expression of the wave energy flow and its ratio of the reflection and transmission are defined as

$$\dot{W}_i = -\sigma_{kl}\dot{u}_k + \varphi\dot{D}_i - \lambda_{ik}\vartheta_{,k}\vartheta/T_0, \quad e^{(j)} = < \dot{W}_2^{(j)} > / < \dot{W}_2^{(0)} >, \tag{6.154}$$

where the symbol $<>$ expresses the average value over one period of a physical variable and $\dot{W}_2^{(j)}$ is the energy flow component corresponding to $\beta^{(j)}$ along x_2 direction.

Omitting the terms related to temperature, the governing equations of the piezoelectric materials are obtained.

The above theory of acoustic wave in piezoelectric materials is based on the quasi-electrostatic description, because the sound speed c_a is several orders smaller than the electromagnetic wave speed c_e. The precision of this approximation is very high. The electromagnetic corrections to the surface acoustic speeds only have the order $(c_a/c_e)^2 \approx 10^{-8}$. The exceptional case is the incidence under small angle of the order of c_a/c_e to the normal of the interface, due to the generalized Snell's law or the synchronism condition (Darinskii et al. 2008). In this case the incident elastic wave can be converted into the electromagnetic waves. However, the magnitudes of the tangential components of the wave amplitudes are in order of c_a/c_e, so very small due to the small incident angle.

6.7.2 Numerical Example

As an example, we discuss 2D propagation waves in PZT-6B/BaTiO$_3$ material combination, which are transversely isotropic materials with poling axis x_3 (Zhou et al. 2012). In 2D case there is only one transverse wave QT.

The material data for BaTiO$_3$ are given in 6.6.4. The material data for PZT-6B are given as

$$\begin{aligned}
&C_{11} = 168\times10^9,\ \ C_{13} = 60\times10^9,\ \ C_{33} = 163\times10^9,\ \ C_{44} = 27.1\,(\text{MPa}),\\
&e_{13} = -0.9,\ \ e_{33} = 7.1,\ \ e_{15} = 4.6\,(\text{C/m}^2),\ \ \epsilon_{11} = 3.6\times10^{-9},\ \ \epsilon_{33} = 3.4\times10^{-9}(\text{C/Vm}),\\
&\alpha_{11}^{\varepsilon} = 7\times10^{-6},\ \ \alpha_{33}^{\varepsilon} = 7(10^{-6}/\text{K}),\ \ \lambda_{11} = 1.2,\ \ \lambda_{33} = 1.2(\text{J/msK}),\ \ \tau = 3.7(10^{-4}\text{C/m}^2\text{K}),\\
&\rho = 7{,}600\,(\text{kg/m}^3),\ \ \omega = 2\pi\times10^6\text{s}^{-1},\ \ C = 420\,(\text{J/kgK}),\ \ \rho_{s0} = 10^{-14}\text{s}^{-1}.
\end{aligned}$$

Figure 6.16 shows the variations of the amplitude coefficients $|\beta_i|$ and the energy flow ratios $e^{(j)}$ of the reflection and transmission waves with the incident angle θ of the QL incident wave from PZT-6B to BaTiO$_3$. Figure 6.16a gives the amplitude coefficients for reflected waves Ref-QL and Ref-QT and transmitted wave Tran-QL and Tran-QT. It is found that when the incident angle θ exceeds the critical angle θ_{cr} $(\theta_{cr} \approx 61.2°)$, the Tran-QL wave becomes evanescent propagating along the interface. Figure 6.16b shows the energy flow ratios normal to the interface for the Ref-QL, Ref-QT, Tran-QL, and Tran-QT. It is found that the sum of Ref-QL

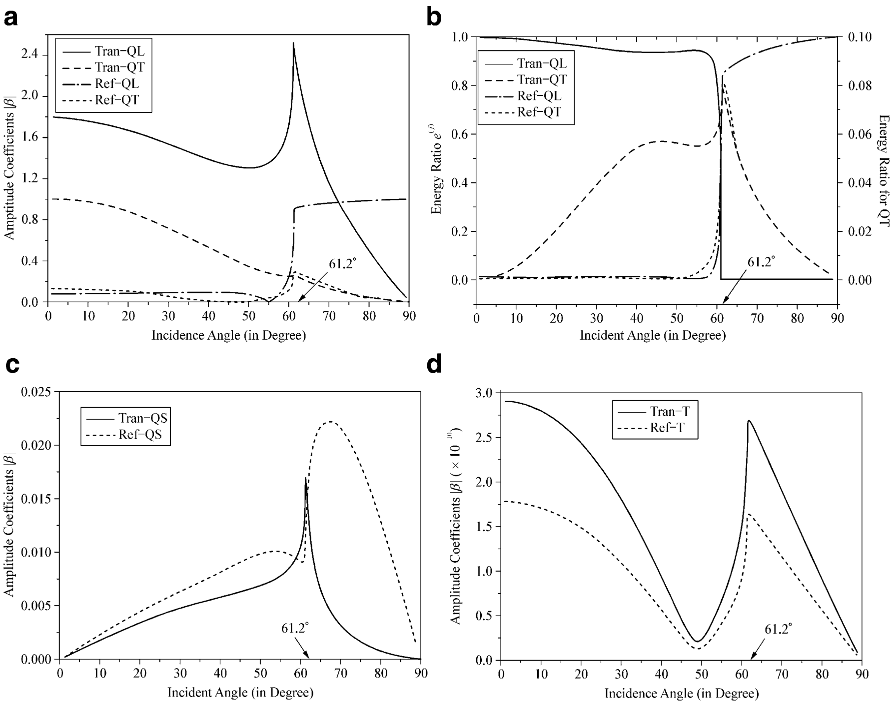

Fig. 6.16 Variations of $|\beta_i|$ and $e^{(j)}$ with the incident angle θ of QL incident wave from PZT-6B to $BaTiO_3$: (**a**) coefficients of QL and QT waves, (**b**) energy flow ratios of QL and QT waves, (**c**) coefficients of QS wave, and (**d**) coefficients of T wave

and Tran-QL waves is far larger than the sum of Ref-QT and Tran-QT waves. Figure 6.16c gives the amplitude coefficients for the quasi-surface (QS) waves. The amplitude coefficients of QS waves are much less than those of other elastic waves. Figure 6.16d shows the amplitude coefficients of the reflected and transmitted temperature T waves. The amplitude coefficients of temperature waves are far less than those of other waves discussed in the example. The energy flow normal to the interface for the temperature wave is also very little and dissipates quickly.

Kuang and Yuan (2011) discussed the 2D reflection problem from the interface of $BiTiO_3$/vaccum with the boundary conditions

$$\sigma_{2j}^{(o)} + \sigma_{2j}^{(r)} = 0, \quad D_2^{(o)} + D_2^{(r)} = 0, \quad \lambda_{2j}\left(\vartheta_j^{(o)} + \vartheta_j^{(r)}\right) = 0, \quad j = 1, 2$$

In this case there are no transmitted waves. The quasi-surface wave becomes surface wave. They found that the wave velocity of the quasi-surface wave is significantly dependent to the incident angle due to the generalized Snell's law. When the incident wave is the elastic wave, the reflected wave is mainly the elastic wave, the quasi-surface wave is weaker, and the reflected temperature wave is very limited. The effect of the attenuation angle γ is very limited.

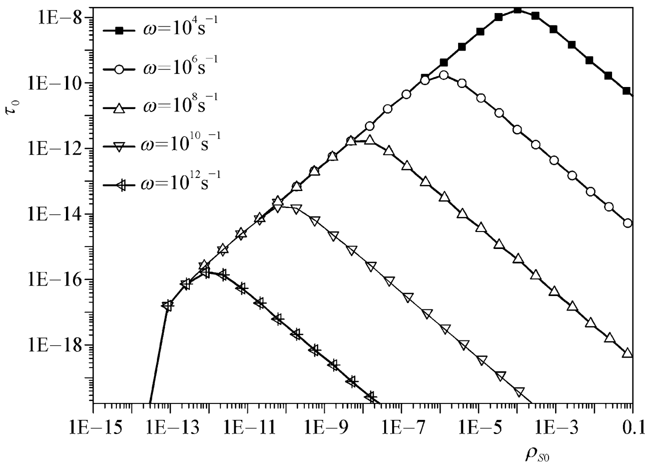

Fig. 6.17 Phase diagram of the attenuation coefficient

6.7.3 Viscous Effect

The experimental results showed that the viscous relaxation times are about $10^{-6}-10^{-8}$s for various metals under shock-loading conditions (Mineev and Mineev 1997; Ma et al. 2011). Ezzat et al. (2002) discussed the generalized thermo-viscoelasticity with G-L theory. Lionetto et al. (2005) studied the boundary value problem of one-dimensional semi-infinite piezoelectric rod subjected to a sudden heat based on K-L-S theory. They found that the thermal relaxation and the viscous effects were evident in short time for the thermal shock in viscoelastic-piezoelectric material. Kuang (2011) and Kuang and Zhou (2012) introduced material constant β_{ijkl} to discuss tentatively the viscoelastic effect in the inertial entropy theory. The constitutive equation (6.124) is changed to

$$\begin{aligned} &\sigma_{ij} = C_{ijkl}\varepsilon_{kl} + \beta_{ijkl}\dot{\varepsilon}_{kl} - e_{kij}E_k - \alpha_{ij}\vartheta, \quad D_i = \epsilon_{ij}E_j + e_{ikl}\varepsilon_{kl} + \tau_i\vartheta, \\ &\quad s = \alpha_{ij}\varepsilon_{ij} + \tau_i E_i + C\vartheta/T_0 \end{aligned} \tag{6.155}$$

The governing equation (6.128) becomes

$$\begin{aligned} &C_{ijkl}u_{k,lj} + \beta_{ijkl}\dot{\varepsilon}_{kl} + e_{kij}\varphi_{,kj} - \alpha_{ij}\vartheta_{,j} = \rho\ddot{u}_i, \quad e_{ikj}u_{k,ji} - \epsilon_{ij}\varphi_{,ji} + \tau_i\vartheta_{,i} = 0 \\ &\alpha_{ij}\dot{u}_{i,j} - \tau_i\dot{\varphi}_{,i} + (C/T_0)(\dot{\vartheta} + \rho_{s0}\ddot{\vartheta}) = \lambda_{ij}\vartheta_{,ji}/T \end{aligned} \tag{6.156}$$

Figure 6.17 gives the phase diagram of attenuation coefficient of QL wave for various ρ_{s0}, τ_0 for a plane wave with $\gamma = 0$ for various ω, where $\beta_{ijkl} = \tau_0 C_{ijkl}$ is assumed. In Fig. 6.17 the attenuation coefficient is positive if the region is above the lines and negative if the region is below the lines. In the region with negative attenuation coefficient, there is an enlarged factor before the elastic wave amplitudes. However, it is not to say that on the propagation path the elastic waves are enhanced, because the elastic wave amplitudes are proportional to the temperature wave amplitude (see Sect. 1.7.6).

It is found that if $\tau_0 = 0$, negative damping occurred, but for $\rho_{s0} = 0$ there is no damping region. How to explain and use the negative damping it is also a meaningful problem.

In the shock problem it is better to take the integral-type viscoelastic constitutive equation (Kuang 2002; Ezzat et al. 2002).

6.7.4 Waves in Piezoelectric Materials

The governing equations in the piezoelectric materials can be obtained by omitting the terms containing temperature in the governing equations of the pyroelectric materials. For the plane wave from Eq. (6.132) the Christoffel equation is

$$(\Gamma^*_{ik}k^2 - \rho\omega^2\delta_{ik})U_k + e^*_i k^2 \Phi = 0, \quad e^*_k k^2 U_k - \epsilon^* k^2 \Phi = 0 \tag{6.157}$$

or

$$\begin{gathered}
\boldsymbol{\Lambda}(k,\omega,\boldsymbol{n})\boldsymbol{U} = \boldsymbol{0}, \quad \boldsymbol{U} = [U_1, U_2, U_3, \Phi]^{\mathrm{T}} \\
\boldsymbol{\Lambda}(k,\omega,\boldsymbol{n}) = \begin{bmatrix} \Gamma^*_{11}k^2 - \rho\omega^2 & \Gamma^*_{12}k^2 & \Gamma^*_{13}k^2 & e^*_1 k^2 \\ \Gamma^*_{21}k^2 & \Gamma^*_{22}k^2 - \rho\omega^2 & \Gamma^*_{23}k^2 & e^*_2 k^2 \\ \Gamma^*_{31}k^2 & \Gamma^*_{32}k^2 & \Gamma^*_{33}k^2 - \rho\omega^2 & e^*_3 k^2 \\ e^*_1 k^2 & e^*_2 k^2 & e^*_3 k^2 & -\epsilon^* k^2 \end{bmatrix}
\end{gathered} \tag{6.158}$$

where $\Gamma^*_{ij}, e^*_j, \epsilon^*$ are shown in Eq. (6.135). Other theories can be discussed similarly.

Pang et al. (2008) discussed the reflection of plane waves at the interface between piezoelectric piezomagnetic media.

6.8 Coupling Problem of Elastic and Electromagnetic Waves in Piezoelectric Material

6.8.1 Governing Equations in Pyroelectric Materials

In this section we shall discuss the coupling of elastic wave with electromagnetic wave shortly. It is assumed that there are no body force and body electric charge in the material. According to Eq. (1.4) the independent Maxwell equations for the case without electric current are

$$\nabla \times \boldsymbol{E} = -\dot{\boldsymbol{B}}, \quad \nabla \times \boldsymbol{H} = \dot{\boldsymbol{D}} \tag{6.159}$$

It is assumed that the material is nonmagnetic, so the constitutive equations are

$$\begin{aligned} &\boldsymbol{\sigma} = \boldsymbol{C} : \boldsymbol{\varepsilon} - \boldsymbol{e} \cdot \boldsymbol{E} - \boldsymbol{\alpha}\theta, \quad s = \boldsymbol{\alpha} : \boldsymbol{\varepsilon} + \boldsymbol{\tau} \cdot \boldsymbol{E} + C\vartheta/T_0, \\ &\boldsymbol{D} = \boldsymbol{\epsilon} \cdot \boldsymbol{E} + \boldsymbol{e} : \boldsymbol{\varepsilon} + \boldsymbol{\tau}\vartheta, \quad \boldsymbol{B} = \boldsymbol{\mu} \cdot \boldsymbol{H} \end{aligned} \tag{6.160}$$

Equations (6.159) and (6.160) yield the electromagnetic wave equation

$$\ddot{\boldsymbol{D}} = \nabla \times \dot{H} = -\nabla \times (\boldsymbol{\mu}^{-1} \cdot \nabla \times \boldsymbol{E}); \quad \text{or} \quad \epsilon_{ij}\ddot{E}_j + e_{ikl}\ddot{\varepsilon}_{kl} + \tau_i\ddot{\vartheta} = -\varpi_{lkj}\varpi_{pni}\mu_{nj}^{-1}E_{k,lp} \tag{6.161}$$

where ϖ_{ijk} is the permutation notation. The momentum and thermal equations are

$$C_{ijkl}u_{k,lj} - e_{kij}E_{k,j} - \alpha_{ji}\vartheta_{,j} = \rho\ddot{u}_i, \quad \alpha_{ij}\dot{u}_{i,j} + \tau_i\dot{E}_i + (C/T_0)(\dot{\vartheta} + \rho_{s0}\ddot{\vartheta}) = \lambda_{ij}\vartheta_{,ji}/T \tag{6.162}$$

The continuity conditions on an interface for a wave reflection and transmission problem are

$$\begin{aligned} &\boldsymbol{u}^{\mathrm{I}} = \boldsymbol{u}^{\mathrm{II}}, \boldsymbol{\sigma}^{\mathrm{I}} \cdot \boldsymbol{n} = \boldsymbol{\sigma}^{\mathrm{II}} \cdot \boldsymbol{n}, \boldsymbol{n} \times \boldsymbol{E}^{\mathrm{I}} = \boldsymbol{n} \times \boldsymbol{E}^{\mathrm{II}}, \\ &\boldsymbol{n} \times \boldsymbol{H}^{\mathrm{I}} = \boldsymbol{n} \times \boldsymbol{H}^{\mathrm{II}}, \vartheta^{\mathrm{I}} = \vartheta^{\mathrm{II}}, \boldsymbol{q}^{\mathrm{I}} \cdot \boldsymbol{n} = \boldsymbol{q}^{\mathrm{II}} \cdot \boldsymbol{n} \end{aligned} \tag{6.163}$$

Equations (6.161), (6.162), and (6.163) are the electroelastic coupling governing equations in pyroelectric materials.

6.8.2 *Coupling Problem of Plane Wave in Piezoelectric Materials*

Kyame (1949), Auld (1973), and Every and Neiman (1992) discussed the electroelastic coupling waves in piezoelectric materials. From Eqs. (6.160), (6.161), and (6.162), the governing equations in piezoelectric materials with isotropic magnetic behavior are

$$\begin{aligned} &\nabla \cdot (\boldsymbol{C} : \boldsymbol{\varepsilon}) - \nabla \cdot (\boldsymbol{e} \cdot \boldsymbol{E}) = \rho\ddot{\boldsymbol{u}} \\ &\mu_0(\boldsymbol{\epsilon} \cdot \ddot{\boldsymbol{E}} + \boldsymbol{e} : \ddot{\boldsymbol{\varepsilon}}) = -\nabla \times (\nabla \times \boldsymbol{E}) = -\nabla(\nabla \cdot \boldsymbol{E}) + \nabla^2\boldsymbol{E}; \quad \text{or} \\ &C_{ijkl}u_{k,lj} - e_{kij}E_{k,j} = \rho\ddot{u}_i, \quad \mu_0\left(e_{ikl}\ddot{u}_{k,l} + \epsilon_{ij}\ddot{E}_j\right) = E_{i,mm} - E_{m,mi} \end{aligned} \tag{6.164}$$

In the coupling problem it is convenient to use the velocity instead of displacement. For a plane wave it is assumed

$$v_k = \dot{u}_k = V_k e^{i(k_m x_m - \omega t)}, \quad E_i = E_{0i} e^{i(k_m x_m - \omega t)}; \quad u_k = U_k e^{i(k_m x_m - \omega t)}, \quad V_k = -i\omega U_k \tag{6.165}$$

Substituting Eq. (6.165) into Eq. (6.164) yields the Christoffel equation

$$\begin{aligned} &\left(C_{ijkl}k_l k_j - \rho\omega^2 \delta_{ik}\right)V_k + e_{kij}\omega k_j E_{0k} \\ &e_{ikl}\mu_0 \omega k_l V_k + \left[(k_j k_j \delta_{im} - k_m k_i) - \omega^2 \mu_0 \epsilon_{im}\right]E_{0m} \end{aligned} \tag{6.166}$$

or

$$\boldsymbol{\Lambda}(\boldsymbol{k})\boldsymbol{U} = \boldsymbol{0}, \quad \boldsymbol{U} = [V_1, V_2, V_3, E_{01}, E_{02}, E_{03}]^{\mathrm{T}}$$

$$\boldsymbol{\Lambda} = \begin{bmatrix} \Gamma^*_{11} - \rho\omega^2 & \Gamma^*_{12} & \Gamma^*_{13} & e^*_{11} & e^*_{21} & e^*_{31} \\ \Gamma^*_{21} & \Gamma^*_{22} - \rho\omega^2 & \Gamma^*_{23} & e^*_{12} & e^*_{22} & e^*_{32} \\ \Gamma^*_{31} & \Gamma^*_{32} & \Gamma^*_{33} - \rho\omega^2 & e^*_{13} & e^*_{23} & e^*_{33} \\ e^{**}_{11} & e^{**}_{12} & e^{**}_{13} & \gamma^*_{11} & \gamma^*_{12} & \gamma^*_{13} \\ e^{**}_{21} & e^{**}_{22} & e^{**}_{23} & \gamma^*_{21} & \gamma^*_{22} & \gamma^*_{23} \\ e^{**}_{31} & e^{**}_{32} & e^{**}_{33} & \gamma^*_{31} & \gamma^*_{32} & \gamma^*_{33} \end{bmatrix} \tag{6.167}$$

where

$$\Gamma^*_{ik} = C_{ijkl}k_l k_j, \quad e^*_{ki} = e_{kij}\omega k_j, \quad e^{**}_{ki} = \mu_0 e^*_{ki}, \quad \gamma^*_{ik} = \left[(k_j k_j \delta_{ik} - k_i k_k) - \omega^2 \mu_0 \epsilon_{ik}\right] \tag{6.168}$$

The corresponding secular equation $\det\boldsymbol{\Lambda} = 0$ is a 6×6 determinant of the coefficients including V_m and E_{0m}. Every and Neiman (1992) discussed the approximate solution.

Now discuss a plane wave propagating along x_1 axis (so $k_1 = k, k_2 = k_3 = 0$) in a transversely isotropic piezoelectric material with x_3 polarization. In a transversely isotropic piezoelectric material, the material constants in Voigt notations are $e_{31} = e_{32}, e_{15} = e_{24}, e_{33}, \epsilon_{11} = \epsilon_{22}, \epsilon_{33}$, $C_{11} = C_{22}, C_{12}, C_{13} = C_{23}, C_{33}, C_{44} = C_{55}, C_{66} = (C_{11} - C_{12})/2$. Therefore, the secular equation is

$$\begin{aligned} |\boldsymbol{\Lambda}| &= \begin{vmatrix} C_{11}k^2 - \rho\omega^2 & 0 & 0 & 0 & 0 & e_{31}\omega k \\ 0 & C_{66}k^2 - \rho\omega^2 & 0 & 0 & 0 & 0 \\ 0 & 0 & C_{44}k^2 - \rho\omega^2 & e_{15}\omega k & 0 & 0 \\ 0 & 0 & \mu_0 e_{15}\omega k & -\omega^2\mu_0\epsilon_{11} & 0 & 0 \\ 0 & 0 & 0 & 0 & k^2 - \omega^2\mu_0\epsilon_{11} & 0 \\ \mu_0 e_{31}\omega k & 0 & 0 & 0 & 0 & k^2 - \omega^2\mu_0\epsilon_{33} \end{vmatrix} \\ &= (C_{66}k^2 - \rho\omega^2)(k^2 - \omega^2\mu_0\epsilon_{11})\left[(C_{11}k^2 - \rho\omega^2)(k^2 - \omega^2\mu_0\epsilon_{33}) - \mu_0 e_{31}^2\omega^2 k^2\right] \\ &\quad \times \left[-\omega^2\mu_0\epsilon_{11}(C_{44}k^2 - \rho\omega^2) - \mu_0 e_{15}\omega k e_{15}\omega k\right] = 0 \end{aligned} \tag{6.169}$$

Equations (6.169) and (6.167) can be decomposed into four groups. The modes and the corresponding wave velocities $c_i = \omega/k_i$ can be given as follows:

Purely acoustic wave: mode, $(C_{66}k^2 - \rho\omega^2)V_2 = 0$; velocity, $c_{s6} = \sqrt{C_{66}/\rho}$

Purely electromagnetic wave: mode, $(k^2 - \omega^2\mu_0\epsilon_{11})E_{02} = 0$; velocity, $c_e = \sqrt{1/\mu_0\epsilon_{11}}$.

Stiffened acoustic wave (electrically quasi-static): modes, $(C_{44}k^2 - \rho\omega^2)V_3 + e_{15}\omega k E_{01} = 0$, $\mu_0 e_{15}\omega k V_3 - \omega^2\mu_0\epsilon_{11}E_{01} = 0$; velocity, $c_s^* = \sqrt{\left(C_{44} + e_{15}^2/\epsilon_{11}\right)/\rho}$

Quasi-acoustic and quasi-electromagnetic coupling wave:

$$\text{modes,}\ (C_{11}k^2 - \rho\omega^2)V_1 - e_{31}\omega k E_{03} = 0, \quad \mu_0 e_{31}\omega k V_1 + (k^2 - \omega^2\mu_0\epsilon_{33})E_{03} = 0$$

$$\text{velocities,}\ \begin{Bmatrix} c_{q\,\text{elctr.}} \\ c_{q\,\text{acust.}} \end{Bmatrix} = \frac{1}{2}\left(\frac{1}{\mu_0\epsilon_{33}} + \frac{C_{11}}{\rho} + \frac{e_{31}^2}{\rho\epsilon_{33}}\right)\left[1 \pm \sqrt{1 - \frac{4\rho\mu_0\epsilon_{33}C_{11}}{\left(\rho + \mu_0\epsilon_{33}C_{11} + \mu_0 e_{31}^2\right)^2}}\right]$$

6.9 Transverse Wave Scattering from a Semi-infinite Conducting Crack

6.9.1 Fundamental Theory

Discuss a transversely isotropic piezoelectric material with isotropic magnetic behavior and isotropic plane $x_1 - x_2$. Assume the electromechanical coupling occurred between antiplane displacement $\boldsymbol{u}(0, 0, u_3)$ and in-plane electric field $\boldsymbol{E}(E_1, E_2, 0)$. For mode-III problem Eq. (6.164) becomes

$$\begin{aligned} &C_{44}\nabla^2 u_3 - e_{15}\boldsymbol{\nabla}\cdot\boldsymbol{E} = \rho\ddot{u}_3, \quad \boldsymbol{\nabla}(\,) = \mathbf{i}_1(\,)_{,1} + \mathbf{i}_2(\,)_{,2} \\ &\ddot{\boldsymbol{D}} = \epsilon_{11}\ddot{\boldsymbol{E}} + e_{15}\boldsymbol{\nabla}\ddot{u}_3 = \boldsymbol{\nabla}\times\dot{\boldsymbol{H}} = -\mu_0^{-1}\boldsymbol{\nabla}\times(\boldsymbol{\nabla}\times\boldsymbol{E}) \end{aligned} \tag{6.170}$$

Let

$$\boldsymbol{E} = -\boldsymbol{\nabla}\varphi - \dot{\boldsymbol{A}}/c_e; \quad c_e = 1/\sqrt{\mu_0\epsilon_{11}}, \quad \boldsymbol{\nabla}\cdot\boldsymbol{A} + \dot{\varphi}/c_e = 0 \tag{6.171}$$

The last one in Eq. (6.171) is a gauge condition to make $\boldsymbol{A}$ unique.

For a general mode-III case from Eq. (6.170), we obtained the electromagneto-acoustic wave equations:

$$C_{44}\nabla^2 u_3 + e_{15}\left(\nabla^2\varphi - \ddot{\varphi}/c_e^2\right) = \rho\ddot{u}_3, \quad \boldsymbol{\nabla}^2\boldsymbol{A} - \ddot{\boldsymbol{A}}/c_e^2 = -\,\mu_0 e_{15}c_e\boldsymbol{\nabla}\dot{u}_3 \tag{6.172}$$

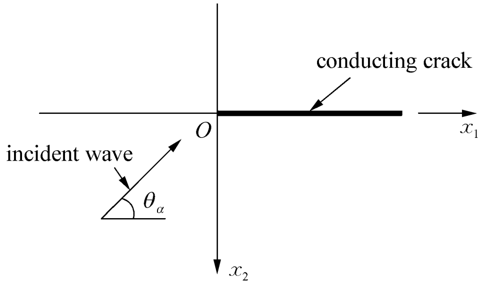

Fig. 6.18 Transverse wave scattering from a semi-infinite conducting crack

where $\boldsymbol{\nabla} \cdot \boldsymbol{E} = -\boldsymbol{\nabla}^2\varphi + \ddot{\varphi}/c_e^2$ has been used. For the electrically quasi-stationary (EQS) case, we have $\boldsymbol{\nabla} \times \boldsymbol{E} = -\dot{\boldsymbol{B}} = \boldsymbol{0}$, so Eq. (6.170) yields

$$C_{44}\nabla^2 u_3 + e_{15}\left(\nabla^2\varphi - \ddot{\varphi}/c_e^2\right) = \rho\ddot{u}_3, \quad e_{15}\nabla^2 u_3 = \epsilon_{11}\left(\nabla^2\varphi - \ddot{\varphi}/c_e^2\right) \quad (6.173)$$

In EQS case the electroelastic wave does not couple with magnetic field. Let

$$\psi = \varphi - (e_{15}/\epsilon_{11})\hat{c}u_3, \quad \hat{c} = c_e^2/\left(c_e^2 - c_s^{*2}\right), \quad c_s^* = \sqrt{\left(C_{44} + e_{15}^2/\epsilon_{11}\right)/\rho} \quad (6.174)$$

Using Eq. (6.174), Eq. (6.173) can be reduced to

$$\nabla^2 u_3 - L_s^{*2}\ddot{u}_3 = 0, \quad \nabla^2\psi - L_e^2\ddot{\psi} = 0; \quad L_s^* = 1/c_s^*, \quad L_e = 1/c_e \ll L_s^* \quad (6.175)$$

If term $\ddot{\varphi}/c_e^2$ is neglected, Eq. (6.173) is reduced to Eq. (4.239) for the electrically static problem. So the difference between the electrically quasi-stationary and static problems is very small, but Eq. (6.175) forms two hyperbolic equations, which may sometimes solve the problem easier. The constitutive equations are

$$\begin{aligned} &\sigma_{13} = C_{44}^* u_{3,1} + e_{15}\psi_{,1}, \quad \sigma_{23} = C_{44}^* u_{3,2} + e_{15}\psi_{,2}; \quad C_{44}^* = C_{44} + \hat{c}e_{15}^2/\epsilon_{11} \\ &D_1 = e_{15}(1-\hat{c})u_{3,1} - \epsilon_{11}\psi_{,1}, \quad D_2 = e_{15}(1-\hat{c})u_{3,2} - \epsilon_{11}\psi_{,2} \end{aligned} \quad (6.176)$$

6.9.2 Transverse Wave Scattering from a Semi-infinite Conducting Crack

Figure 6.18 shows the diffraction of an incident shear wave through a semi-infinite conducting crack in a transversely isotropic piezoelectric material. Li (1996) used the governing equations Eq. (6.175) to solve this problem and called it "quasi-hyperbolic approximation" method. The generalized displacement in the material is

$$u_3(x_1,x_2,t)=u_3^{(i)}+u_3^{(s)},\quad \psi(x_1,x_2,t)=\psi^{(i)}+\psi^{(s)},\quad \left(\varphi(x_1,x_2,t)=\varphi^{(i)}+\varphi^{(s)}\right) \tag{6.177}$$

where the superscripts "(i)" and "(s)" denote the incident and scattering fields, respectively. The incident acoustic wave is assumed in the following form:

$$u_3^{(i)}(x_1,x_2,t)=u_{30}^{(i)}G\left(t-L_s^*n_mx_m\right),\quad G(t)=H(t)\int_0^t \mathrm{g}(\tau)\mathrm{d}\tau \tag{6.178}$$

where $\mathrm{g}(\tau)$ is a given real function, $H(t)$ is the Heaviside function, $U_0^{(i)}$ is the amplitudes of incident acoustic wave, and $n_1=\cos\theta_\alpha,\ n_2=-\sin\theta_\alpha$. For convenience the field variables in the upper half-space ($x_2<0$) and lower space ($x_2>0$) are labeled by supermarks " $-$ " and " $+$," respectively. In order to apply the Wiener-Hopf technique an artificial interface $x_2=0, x_1<0$ is introduced. Using Eq. (6.176) the boundary conditions on the crack and the artificial surfaces are

$$\begin{aligned}&\sigma_{23}^{\pm}(x_1,0,t)=\sigma_{23}^{(i)}+\sigma_{23}^{\pm(s)}=0,\quad \varphi^{\pm}(x_1,0,t)=\varphi^{(i)}+\varphi^{\pm(s)}=0;\quad 0\le x_1<\infty;\\&u_3^{+}(x_1,0,t)=u_3^{-}(x_1,0,t),\quad D_2^{+}(x_1,0,t)=D_2^{-}(x_1,0,t);\quad x_1<0\end{aligned} \tag{6.179}$$

The initial and radiation conditions are as follows:

$$\begin{aligned}&u_3^{(s)}(x_1,x_2,t)=\dot u_3^{(s)}(x_1,x_2,t)=0,\quad \varphi^{(s)}(x_1,x_2,t)=\dot\varphi^{(s)}(x_1,x_2,t)=0;\quad t<0\\&\lim_{|x|\to\infty}\left[u_3^{(s)}(x_1,x_2,t),\quad \dot u_3^{(s)}(x_1,x_2,t),\quad \varphi^{(s)}(x_1,x_2,t),\quad \dot\varphi^{(s)}(x_1,x_2,t)\right]=0;\quad t>0\end{aligned} \tag{6.180}$$

6.9.3 Derive the Wiener-Hopf Equations in Laplace Transform Region

Introduce the one-side Laplace transform $\bar f(x_1,x_2,p)$ with respect to time of $f(x_1,x_2,t)$ and its inverse transform:

$$\bar f(x_1,x_2,p)=\int_0^\infty f(x_1,x_2,t)\mathrm{e}^{-pt}\,\mathrm{d}t,\quad f(x_1,x_2,t)=\frac{1}{2\pi i}\int_{a-\mathrm{i}\infty}^{a+\mathrm{i}\infty}\bar f(x_1,x_2,p)\mathrm{e}^{pt}\,\mathrm{d}p \tag{6.181}$$

where $f(x_1,x_2,t)$ is called original function, $\bar{f}(x_1,x_2,p)$ is image function, and $p = \alpha + \mathrm{i}\beta$ is the Laplace transform complex parameter. $\bar{f}(x_1,x_2,p)$ is an analytic function in the plane $\mathrm{Re}\, p > \alpha_0$, where α_0 is the growth exponent of $f(t)$. The integral path in Eq. (6.181) is called Bromwich path. The two-side Laplace transform $\bar{f}^*(\varsigma,x_2,p)$ with respect to x_1 of $\bar{f}(x_1,x_2,p)$ is defined as

$$\begin{aligned} \bar{f}^*(\varsigma,x_2,p) &= \int_{-\infty}^{\infty} \bar{f}(x_1,x_2,p)\,\mathrm{e}^{-p\varsigma x_1}\mathrm{d}x_1 \\ f(x_1,x_2,p) &= \frac{p}{2\pi i}\int_{a'-\mathrm{i}\infty}^{a'+\mathrm{i}\infty} \bar{f}^*(\varsigma,x_2,p)\,\mathrm{e}^{p\varsigma x_1}\mathrm{d}\varsigma \end{aligned} \tag{6.182}$$

Applying Eqs. (6.181), and (6.175), using the integral by parts and the initial and radiation conditions we find

$$\bar{u}^*_{3,22} - p^2\alpha^2\bar{u}^*_3 = 0, \quad \bar{\psi}^*_{,22} - p^2\beta^2\bar{\psi}^* = 0; \quad \alpha(\varsigma) = \sqrt{L_s^{*2} - \varsigma^2}, \quad \beta(\varsigma) = \sqrt{L_e^2 - \varsigma^2} \tag{6.183}$$

To satisfy the boundary conditions at infinity, the solution is chosen in the following form:

$$\left.\begin{aligned} \bar{u}_3^{*+}(\varsigma,x_2,p) &= (1/p^2)A^+(\varsigma)\mathrm{e}^{-p\alpha x_2} \\ \bar{\psi}^{*+}(\varsigma,x_2,p) &= (1/p^2)B^+(\varsigma)\mathrm{e}^{-p\beta x_2} \end{aligned}\right\}, x_2 > 0; \quad \left.\begin{aligned} \bar{u}_3^{*-} &= -(1/p^2)A^-(\varsigma)\mathrm{e}^{p\alpha x_2} \\ \bar{\psi}^{*-} &= -(1/p^2)B^-(\varsigma)\mathrm{e}^{p\beta x_2} \end{aligned}\right\}, x_2 < 0 \tag{6.184}$$

where $\mathrm{Re}\alpha(\varsigma) \geq 0, \mathrm{Re}\beta(\varsigma) \geq 0$ in the ζ plane with branch cuts on the $\mathrm{Im}\varsigma = 0$:

$$\text{For } \alpha: \mathrm{Re}\varsigma < -L_s^* \quad \text{and} \quad \mathrm{Re}\varsigma > L_s^*; \quad \text{For } \beta: \quad \mathrm{Re}\varsigma < -L_e \quad \text{and} \quad \mathrm{Re}\varsigma > L_e \tag{6.185}$$

Li et al. (2005a) adopted the Wiener-Hopf technique (Noble 1958; Zhu and Kuang 1995) to solve above problem. Introduce unknown functions:

$$\begin{aligned} &\sigma_-(x_1,t) = \begin{cases} \sigma_{23}^{\pm}, & x_1 < 0 \\ 0, & x_1 \geq 0 \end{cases}, \qquad \varphi_-(x_1,t) = \begin{cases} \varphi^{\pm}, & x_1 < 0 \\ 0, & x_1 \geq 0 \end{cases}, \\ &\Delta w_+(x_1,t) = \begin{cases} 0, & x_1 < 0 \\ u_3^+ - u_3^-, & x_1 \geq 0 \end{cases}, \quad \Delta D_+(x_1,t) = \begin{cases} 0, & x_1 < 0 \\ D_2^+ - D_2^-, & x_1 \geq 0 \end{cases} \\ &\sigma_{23}^{\pm} = \sigma_{23}^{\pm}(x_1,0,t), \quad \varphi^{\pm} = \varphi^{\pm}(x_1,0,t), \quad D_2^{\pm} = D_2^{\pm}(x_1,0,t) \end{aligned} \tag{6.186}$$

So the boundary conditions can be expanded to the full range of the x_1-axis:

$$\begin{aligned} &\sigma_{23}^{\pm}(x_1,0,t) = \sigma_-(x_1,t) - \sigma_{23}^{(i)}(x_1,0,t), \quad \varphi^{\pm}(x_1,0,t) = \varphi_-(x_1,t) - \varphi^{(i)}(x_1,0,t), \\ &\quad -\infty < x_1 < \infty \\ &u_3^+(x_1,0,t) - u_3^-(x_1,0,t) = \Delta w_+(x_1,t), \quad D_2^+(x_1,0,t) - D_2^-(x_1,0,t) = \Delta D_+(x_1,t), \\ &\quad -\infty < x_1 < \infty \end{aligned} \tag{6.187}$$

The double Laplace transform of Eq. (6.187) is

$$\begin{aligned}
&\bar{\sigma}_{23}^{*\pm}(\varsigma,0,p)=\Sigma_{-}(\varsigma)/p-\bar{\sigma}_{23}^{*(i)}(\varsigma,0,p),\quad \bar{\varphi}^{*\pm}(\varsigma,0,p)=\Phi_{-}(\varsigma)/p^{2}-\bar{\varphi}^{*(i)}(\varsigma,0,p)\\
&\frac{1}{2}\left[\bar{u}_{3}^{*+}(\varsigma,0,p)-\bar{u}_{3}^{*-}(\varsigma,0,p)\right]=\frac{\Delta U_{+}(\varsigma)}{p^{2}},\quad \frac{1}{2}\left[D_{2}^{*+}(\varsigma,0,p)-D_{2}^{*-}(\varsigma,0,p)\right]=\frac{\Delta D_{+}(\varsigma)}{p^{2}}\\
&\Sigma_{-}(\varsigma)=p\int_{-\infty}^{0}\sigma_{-}^{*}(x_1,p)\mathrm{e}^{-p\varsigma x_1}\mathrm{d}x_1,\quad \Phi_{-}(\varsigma)=p^{2}\int_{-\infty}^{0}\Phi_{-}^{*}(x_1,p)\mathrm{e}^{-p\varsigma x_1}\mathrm{d}x_1\\
&\Delta U_{+}(\varsigma)=(p^{2}/2)\int_{0}^{\infty}\Delta w_{+}^{*}(x_1,p)\mathrm{e}^{-p\varsigma x_1}\mathrm{d}x_1,\quad \Delta D_{+}(\varsigma)=(p/2)\int_{0}^{\infty}\Delta D_{+}^{*}(x_1,p)\mathrm{e}^{-p\varsigma x_1}\mathrm{d}x_1
\end{aligned} \tag{6.188}$$

Substituting Eq. (6.184) and the transformed constitutive equation obtained from Eq. (6.176) into Eq. (6.188) we get

$$\begin{aligned}
&\bar{\sigma}_{23}^{*+}+\bar{\sigma}_{23}^{*-}:\quad -C_{44}^{*}\alpha(\varsigma)A_{s}(\varsigma)-e_{15}\beta(\varsigma)B_{s}(\varsigma)=\Sigma_{-}(\varsigma)-p\bar{\sigma}_{23}^{*(i)}\\
&\bar{\varphi}^{*+}-\bar{\varphi}^{*-}:\quad (e_{15}/\epsilon_{11})\hat{c}A_{s}(\varsigma)+B_{s}(\varsigma)=0\\
&\bar{u}_{3}^{*+}-\bar{u}_{3}^{*-}:\quad A_{s}(\varsigma)=\Delta U_{+}(\varsigma)\\
&\bar{\sigma}_{23}^{*+}-\bar{\sigma}_{23}^{*-}:\quad -C_{44}^{*}\alpha(\varsigma)A_{as}(\varsigma)-e_{15}\beta(\varsigma)B_{as}(\varsigma)=0\\
&\bar{\varphi}^{*+}+\bar{\varphi}^{*-}:\quad (e_{15}/\epsilon_{11})\hat{c}A_{as}(\varsigma)+B_{as}(\varsigma)=\Phi_{-}(\varsigma)-p^{2}\bar{\varphi}^{*(i)}\\
&D_{2}^{*+}-D_{2}^{*-}:\quad -e_{15}(1-\hat{c})\alpha(\varsigma)A_{as}(\varsigma)+\epsilon_{11}\beta(\varsigma)B_{as}(\varsigma)=\Delta D_{+}(\varsigma)\\
&A_{s}=(A^{+}+A^{-})/2,\quad A_{as}=(A^{+}-A^{-})/2;\quad B_{s}=(B^{+}+B^{-})/2,\quad B_{as}=(B^{+}-B^{-})/2
\end{aligned} \tag{6.189}$$

From Eq. (6.189) two decoupled Wiener-Hopf equations can be obtained:

$$-C_{44}^{*}\mathcal{K}(\varsigma)\Delta U_{+}(\varsigma)=\Sigma_{-}(\varsigma)-p\bar{\sigma}_{23}^{*(i)};\quad \mathcal{K}(\varsigma)=\alpha(\varsigma)-k_{e}^{2}\beta(\varsigma) \tag{6.190a}$$

$$\frac{C_{44}^{*}\mathcal{K}(\varsigma)\Delta D_{+}(\varsigma)}{\alpha(\varsigma)\beta(\varsigma)\left[e_{15}^{2}(1-\hat{c})+\epsilon_{11}C_{44}^{*}\right]}=\Phi_{-}(\varsigma)-p^{2}\bar{\varphi}^{*(i)};\quad k_{e}^{2}=\frac{e_{15}^{2}}{\epsilon_{11}C_{44}^{*}}\hat{c} \tag{6.190b}$$

The $\bar{\sigma}_{23}^{*(i)}$ and $\bar{\varphi}^{*(i)}$ in Eqs. (6.190a) and (6.190b) are the double Laplace transform of $\sigma_{23}^{(i)}$ and $\varphi^{(i)}$, respectively, and for an incident acoustic wave are equal to

$$\begin{aligned}
&\bar{\sigma}_{23}^{*(i)}(\varsigma,0,p)=-\frac{\sigma_0\bar{g}(p)}{p\left(\varsigma+L_{s}^{*}n_1\right)};\quad \bar{\varphi}^{*(i)}(\varsigma,0,p)=-\frac{\varphi_0\bar{g}(p)}{p^{2}\left(\varsigma+L_{s}^{*}n_1\right)}\\
&\sigma_0=C_{44}^{*}L_{s}^{*}n_2u_{30}^{(i)};\quad \varphi_0=-(e_{15}/\epsilon_{11})\hat{c}u_{30}^{(i)}
\end{aligned} \tag{6.191}$$

Fig. 6.19 Integration paths used for product decomposition of $H(\varsigma)$ in ζ plane

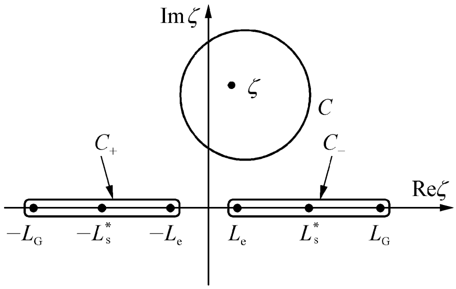

6.9.4 Decomposing of the Function $\mathcal{K}(\varsigma)$

In order to solve Eqs. (6.190) and (6.191), it is needed to factorize the function $\mathcal{K}(\xi)$ into sectionally analytic functions in the left and right half ς plane, respectively. Let (Li 2000)

$$\begin{aligned} &\mathcal{K}(\varsigma) = \alpha(\varsigma) - k_e^2\beta(\varsigma) = \left(1 - k_e^4\right)\frac{\left(L_G^2 - \varsigma^2\right)}{\alpha(\varsigma) + k_e^2\beta(\varsigma)}, \quad L_G = \sqrt{\frac{L_s^{*2} - k_e^4 L_e^2}{1 - k_e^4}} \\ &\alpha(\varsigma) + k_e^2\beta(\varsigma) = \left(1 + k_e^2\right)\sqrt{L_G^2 - \varsigma^2}\,\Omega(\varsigma), \quad \Omega(\varsigma) = \frac{\alpha(\varsigma) + k_e^2\beta(\varsigma)}{\left(1 + k_e^2\right)\sqrt{L_G^2 - \varsigma^2}} \end{aligned} \tag{6.192}$$

When $|\varsigma| \to \infty$, $\alpha \to \beta = \sqrt{-\varsigma^2}$ and $\Omega(\varsigma) \to 1$. Factorize $\Omega(\varsigma)$ into sectionally analytic functions $\Omega_+(\varsigma)$ and $\Omega_-(\varsigma)$ and $\Omega(\varsigma) = \Omega_+(\varsigma)\Omega_-(\varsigma)$. Let

$$\ln\,\Omega(\varsigma) = \ln\,\Omega_+(\varsigma) + \ln\,\Omega_-(\varsigma) = \frac{1}{2\pi \mathrm{i}}\oint_C \frac{\ln\,\Omega(z)}{z - \varsigma}\mathrm{d}z \tag{6.193}$$

where C is the integration path located in the ς plane with cuts C_+ and C_- (Fig. 6.19). There are three branch points inside C_+ or C_-.

Using the Cauchy principle value (PV) integration around C_+, it is obtained

$$\begin{aligned} &\Theta(\varsigma) = \arg[\Omega(\varsigma)] = \begin{cases} \pm\pi/2, & -L_G < \mathrm{Re}\varsigma < -L_s^*, \quad \mathrm{Im}\varsigma = \pm 0 \\ \pm\arctan\,\Xi(\varsigma), & -L_s^* < \mathrm{Re}\varsigma < -L_e, \quad \mathrm{Im}\varsigma = \pm 0 \end{cases} \\ &\Xi(\varsigma) = \frac{k_e^2\sqrt{(\varsigma - L_e)(\varsigma + L_e)}}{\sqrt{\left(L_s^* - \varsigma\right)\left(L_s^* + \varsigma\right)}} = \frac{k_e^2\sqrt{\left(\varsigma^2 - L_e^2\right)}}{\sqrt{\left(L_s^{*2} - \varsigma^2\right)}} \end{aligned} \tag{6.194}$$

By using the Cauchy's integral theorem, it is obtained

$$\Omega_\pm(\varsigma) = \sqrt{\frac{L_s^* \pm \varsigma}{L_G \pm \varsigma}}\exp\left\{-\frac{1}{\pi}\int_{L_e}^{L_s^*}\arctan[\Xi(\eta)]\frac{\mathrm{d}\eta}{\eta \pm \varsigma}\right\} \tag{6.195}$$

where $\Omega_{\pm}(\varsigma)$ is corresponding to the notations " $\pm$ " at right hand of the equality, respectively. Therefore, it yields

$$\begin{aligned}
&\alpha(\varsigma)+k_e^{\mathbf{2}}\beta(\varsigma)=\left(1+k_e^2\right)\sqrt{L_s^{*2}-\varsigma^2}M_+(\varsigma)M_-(\varsigma)\\
&\mathcal{K}(\varsigma)=\left(1-k_e^4\right)\frac{\left(L_G^2-\varsigma^2\right)}{\alpha(\varsigma)+k_e^{\mathbf{2}}\beta(\varsigma)}=\left(1-k_e^2\right)\frac{\left(L_G^2-\varsigma^2\right)}{\sqrt{L_s^{*2}-\varsigma^2}}S_+(\varsigma)S_-(\varsigma)\\
&M_{\pm}(\varsigma)=\exp\left[-\frac{1}{\pi}\int_{L_e}^{L_s^*}\arctan\Xi(\eta)\frac{\mathrm{d}\eta}{\eta\pm\varsigma}\right],\quad S_{\pm}(\varsigma)=\left[M_{\pm}(\varsigma)\right]^{-1}
\end{aligned}\tag{6.196}$$

6.9.5 Solutions of the Wiener-Hopf Equations

Substitution of Eqs. (6.196) and (6.191) into Eq. (6.190a) yields

$$-C_{44}^{**}\frac{\left(L_G^2-\varsigma^2\right)}{\sqrt{L_s^{*2}-\varsigma^2}}\Delta U_+(\varsigma)S_+(\varsigma)S_+(\varsigma)=\Sigma_-(\varsigma)+\frac{\sigma_0\bar{g}(p)}{\left(\varsigma+L_s^*n_1\right)},\quad C_{44}^{**}=C_{44}^*\left(1-k_e^2\right)\tag{6.197}$$

Introduce

$$R_-(\varsigma)=\frac{\sqrt{L_s^*-\varsigma}}{(L_G-\varsigma)S_-(\varsigma)},\quad \frac{R_-(\varsigma)}{\varsigma+L_s^*n_1}=\frac{R_-(\varsigma)-R_-\left(-L_s^*n_1\right)}{\varsigma+L_s^*n_1}+\frac{R_-\left(-L_s^*n_1\right)}{\varsigma+L_s^*n_1}\tag{6.198}$$

Equations (6.197) and (6.198) yield

$$\begin{aligned}
&-C_{44}^{**}\frac{(L_G+\varsigma)}{\sqrt{L_s^*+\varsigma}}\Delta U_+(\varsigma)S_+(\varsigma)-\frac{\sigma_0\bar{g}(p)R_-\left(-L_s^*n_1\right)}{\left(\varsigma+L_s^*n_1\right)}\\
&=\Sigma_-(\varsigma)R_-(\varsigma)+\frac{\sigma_0\bar{g}(p)\left[R_-(\varsigma)-R_-\left(-L_s^*n_1\right)\right]}{\left(\varsigma+L_s^*n_1\right)}
\end{aligned}\tag{6.199}$$

It is known that the functions at the left side in Eq. (6.199) are analytic in the right half-plane $\mathrm{Re}\varsigma>0$ and equal to zero at infinity, whereas those on the right side are analytic in the left half-plane $\mathrm{Re}\varsigma<0$ and they are continuous on $\mathrm{Im}\varsigma=0$. So according to Liouville theorem (Lavrenchive and Shabat 1951), these functions are analytic in whole plane and must be zero. So

$$\begin{aligned}
\Delta U_+(\varsigma)&=-\frac{\sigma_0\bar{g}(p)\sqrt{L_s^*+\varsigma}R_-\left(-L_s^*n_1\right)}{C_{44}^{**}(L_G+\varsigma)\left(\varsigma+L_s^*n_1\right)S_+(\varsigma)},\\
\Sigma_-(\varsigma)&=\frac{\sigma_0\bar{g}(p)}{\left(\varsigma+L_s^*n_1\right)}\left[\frac{R_-\left(-L_s^*n_1\right)}{R_-(\varsigma)}-1\right]
\end{aligned}\tag{6.200}$$

Analogously from Eqs. (6.196) and (6.190b), it can be obtained

$$\begin{aligned} \varDelta D_+(\varsigma) &= -\frac{\varphi_0 \bar{g}(p)\left(L_s^* + \varsigma\right)\sqrt{L_e + \varsigma} R'_-\left(-L_s^* n_1\right)\left[e_{15}^2(1-\hat{c}) + \epsilon_{11} C_{44}^*\right]}{C_{44}^{**}(L_G + \varsigma)\left(\varsigma + L_s^* n_1\right) S_+(\varsigma)} \\ \varPhi_-(\varsigma) &= \frac{\varphi_0 \bar{g}(p)}{\left(\varsigma + L_s^* n_1\right)}\left[\frac{R'_-\left(-L_s^* n_1\right)}{R'_-(\varsigma)} - 1\right]; \quad R'_-(\varsigma) = \frac{\left(L_s^* + \varsigma\right)\sqrt{L_e + \varsigma}}{(L_G + \varsigma) S_-(\varsigma)} \end{aligned} \tag{6.201}$$

Substituting Eqs. (6.200) and (6.201) into Eq. (6.189), one can obtain $A_s(\varsigma), B_s(\varsigma)$, $A_{as}, B_{as}(\varsigma)$ and $A^{\pm}(\varsigma), B^{\pm}(\varsigma)$:

$$\begin{aligned} A^{\pm}(\varsigma) &= -[\sigma_0 \pm \varphi_0 A_0(\varsigma)]\bar{g}(p)\varLambda(\varsigma) \\ B^{\pm}(\varsigma) &= [\sigma_0 \hat{c}(e_{15}/\epsilon_{11}) \pm \varphi_0 B_0(\varsigma)]\bar{g}(p)\varLambda(\varsigma) \\ A_0(\varsigma) &= \frac{e_{15}\sqrt{L_e + \varsigma}\sqrt{L_e + L_s^* n_1}\sqrt{L_s^* + L_s^* n_1}}{\sqrt{L_s^* - \varsigma}} \\ B_0(\varsigma) &= \frac{C_{44}^*\sqrt{L_s^* + \varsigma}\sqrt{L_s^* + L_t n_1}\sqrt{L_e + L_s^* n_1}}{\sqrt{L_e - \varsigma}} \\ \varLambda(\varsigma) &= \frac{(L_G - \varsigma)\sqrt{L_s^* + L_s^* n_1} S_-(\varsigma)}{\left(\varsigma + L_s^* n_1\right)\sqrt{L_s^* - \varsigma}(L_G + L_s^* n_1) S_-\left(-L_s^* n_1\right) C_{44}^* \mathcal{K}(\varsigma)} \end{aligned} \tag{6.202}$$

Substituting Eq. (6.202) into (6.184) and carrying out the inverse transform with ς we find

$$\begin{aligned} \bar{u}_3(x_1, x_2, p) &= -\frac{1}{2\pi \mathrm{i} p}\int_{\varsigma_\alpha - \mathrm{i}\infty}^{\varsigma_\alpha + \mathrm{i}\infty}\{[\sigma_0 + \varphi_0 A_0(\varsigma)\mathrm{sgn}(x_2)]\bar{g}(p)\varLambda(\varsigma)\} \\ &\quad \times \exp\{-p[\alpha(\varsigma)\mathrm{sgn}(x_2)x_2 - \varsigma x_{1,}]\}\mathrm{d}\varsigma \\ \bar{\psi}(x_1, x_2, p) &= \frac{1}{2\pi \mathrm{i} p}\int_{\varsigma_\beta - \mathrm{i}\infty}^{\varsigma_\beta + \mathrm{i}\infty}\left\{\left[\sigma_0 \hat{c}\frac{e_{15}}{\epsilon_{11}} + \varphi_0 B_0(\varsigma)\mathrm{sgn}(x_2)\right]\bar{g}(p)\varLambda(\varsigma)\right\} \\ &\quad \times \exp\{-p[\beta(\varsigma)\mathrm{sgn}(x_2)x_2 - \varsigma x_1]\}\mathrm{d}\varsigma \end{aligned} \tag{6.203}$$

6.9.6 Scattering Fields in Front of the Crack Tip

The one-side Laplace inversion with time can be obtained by replacing the original Bromwich path with deformed Cagniard-de Hoop inversion contours (Fig. 6.20) in the ς plane (Li et al. 2005a). The inversion procedure is given only for $x_2 > 0$; for $x_2 < 0$ the procedure is the same and is omitted. Along the Cagniard-de Hoop contours, the exponentials in Eq. (6.203) take the form e^{-pt}:

$$\alpha(\varsigma)x_2 - \varsigma x_1 = t, \quad \varsigma \epsilon \varGamma_\alpha, \varGamma_{\alpha\beta}; \quad \beta(\varsigma)x_2 - \varsigma x_1 = t, \quad \varsigma \epsilon \varGamma_\beta \tag{6.204}$$

A cut from $-L_s^*$ to $-L_e$ is needed due to two branch points $\varsigma = -L_s^*$ and $\varsigma = -L_e$. So a supplement path $\varGamma_{\alpha\beta}$ is needed to avoid the cut for $\varGamma_\alpha$. The physical

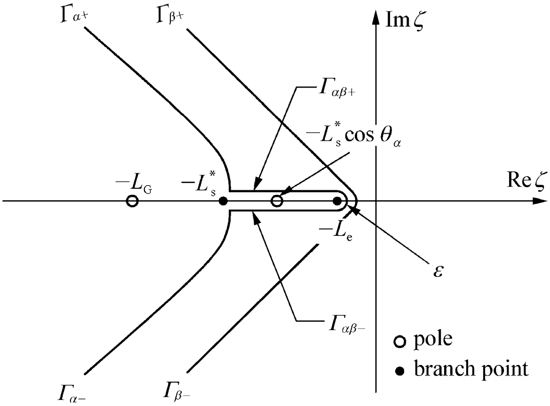

Fig. 6.20 The deformed Cagniard-de Hoop inversion paths $\Gamma_\alpha, \Gamma_\beta, \Gamma_{\alpha\beta}$

interpretation of $\Gamma_{\alpha\beta}$ is that the integral along $\Gamma_{\alpha\beta}\left(-L_s^* \cos\theta_\alpha \le \varsigma \le -L_e\right)$ represents an electroacoustic head wave, or a quasi-surface wave, which almost propagates in parallel with the boundary surface. The electroacoustic head wave in piezoelectric material was proved by experiments of Liu et al. (1989). The path Γ_β always avoids the cut. Let $x_1 = r\cos\theta,\ x_2 = r\sin\theta$ from Eq. (6.204) we get

$$\varsigma_{\alpha\pm} = -t\cos\theta \pm \mathrm{i}\sin\theta\sqrt{t^2 - L_s^{*2}r^2}/r;\quad L_s^* r \le t < \infty$$

$$\varsigma_{\beta\pm} = -t\cos\theta \pm \mathrm{i}\sin\theta\sqrt{t^2 - L_e^2 r^2}/r;\quad L_e r \le t < \infty$$

$$\varsigma_{\alpha\beta\pm} = -t\cos\theta \pm \sin\theta\sqrt{L_s^{*2}r^2 - t^2}/r \pm \mathrm{i}\varepsilon;\quad t_{\alpha 0} \le t < L_s^* r;\quad t_{\alpha 0} = \sqrt{L_s^{*2} - L_e^2}x_2 + L_e x_1$$

Finally, the exact inversions are found:

$$\begin{aligned} u_3^{(s)}(x_1, x_2, t) &= \int_0^t G(t-\tau)u_{3\delta}^{(s)}(x_1, x_2, \tau)\mathrm{d}\tau + u_{3r}^{(s)}(x_1, x_2, t) \\ \psi^{(s)}(x_1, x_2, t) &= \int_0^t G(t-\tau)\psi_\delta^{(s)}(x_1, x_2, \tau)\mathrm{d}\tau + \psi_r^{(s)}(x_1, x_2, t) \end{aligned} \tag{6.205}$$

where $u_{3\delta}^{(s)}, \psi_\delta^{(s)}$ denote the scattering fields due to the impulsive incident wave and $u_{3r}^{(s)}, \psi_r^{(s)}$ represent the reflective and transmission waves:

$$\begin{aligned} u_{3\delta}^{(s)} &= -\frac{1}{\pi}\mathrm{Re}\left\{(\sigma_0 + \varphi_0 A_0(\varsigma_{\alpha+})\mathrm{sgn}(x_2))\Lambda(\varsigma_{\alpha+})\frac{\alpha(\varsigma_{\alpha+})}{\sqrt{t^2 - L_s^{*2}r^2}}\right\}H\left(t - L_s^* r\right) \\ &\quad + \frac{1}{\pi}\mathrm{Im}\left\{\left(\sigma_0 + \varphi_0 A_0(\varsigma_{\alpha\beta+})\mathrm{sgn}(x_2)\right)\Lambda(\varsigma_{\alpha\beta+})\frac{\alpha(\varsigma_{\alpha\beta+})}{\sqrt{t^2 - L_s^{*2}r^2}}\right\}\left[H(t-t_0) - H\left(t - L_s^* r\right)\right] \\ \psi_\delta^{(s)} &= \frac{1}{\pi}\left\{\left(\sigma_0 \hat{c}\frac{e_{15}}{\epsilon_{11}} + \varphi_0 B_0(\varsigma_{\beta+})\mathrm{sgn}(x_2)\right)\Lambda(\varsigma_{\beta+})\frac{\beta(\varsigma_{\beta+})}{\sqrt{t^2 - L_e^2 r^2}}\right\}H(t - L_e r) \\ t_0 &= \sqrt{L_s^{*2} - L_e^2}x_2 + L_e x_1, \quad r = \sqrt{x_1^2 + x_2^2} \end{aligned} \tag{6.206}$$

$$
\begin{aligned}
&u_{3r}^{(s)} = \begin{cases} [\mathrm{Re}\varPi(\theta_\alpha)]U_0^{(i)}G(t_*) - [\mathrm{Im}\varPi(\theta_\alpha)]U_0^{(i)}\left\{\dfrac{1}{\pi}PV\displaystyle\int_{-\infty}^{\infty}\dfrac{G(t_*)}{\tau - t}\mathrm{d}\tau\right\}, & 0 \le \theta < \theta_\alpha \\ 0, & \theta_\alpha \le \theta < 2\pi - \theta_\alpha \\ -U_0^{(i)}G(t_*), & 2\pi - \theta_\alpha \le \theta < 2\pi \end{cases} \\
&\varphi_r^{(s)}(x_1, x_2, t) = (e_5/\epsilon_{11})\hat{c}u_3^{(r)}(x_1, x_2, t), \qquad 0 \le \theta < 2\pi \\
&\varPi(\theta_\alpha) = \frac{L_s^* n_2 - k_e\sqrt{L_e^2 - L_s^{*2}n_1^2}}{L_s^* n_2 + k_e\sqrt{L_e^2 - L_s^{*2}n_1^2}}, \quad t_* = t - L_s^*(n_1x_1 - n_2x_2)
\end{aligned}
\tag{6.207}
$$

For an incident shear wave with $\cos\theta_\alpha < L_e/L_s^*$ through a semi-infinite conducting crack in a transversely isotropic piezoelectric material, in front of the crack tip except the incident acoustic wave, there have been electroacoustic reflection, transmission, scattering and head waves, and electric scattering wave. Because in the "quasi-hyperbolic approximation" the Faraday's electric induction by a changing magnetic field is not considered, it cannot be used to solve the problem for $-L_s^*\cos\theta_\alpha > -L_e$ and the electric incident wave.

6.10 Transient Response of a Mode-I Crack

6.10.1 Fundamental Equations

Figure 6.21 shows a transverse isotropic piezoelectric strip of width $2h$ with a central crack of length $2a$ subjected to loadings $-\sigma_0 H(t), -D_0 H(t)$ on the crack surface, where $H(t)$ is the Heaviside step function. Axis x_1 is along the crack direction and the polarized axis x_3 is perpendicular to the crack. In plane x_1x_3 there are generalized displacements (u_1, u_3, φ) and stresses $(\sigma_1, \sigma_3, \sigma_5, D_1, D_3)$. Applying the Voigt notations the constitutive equations are

$$
\begin{aligned}
&\sigma_1 = C_{11}\varepsilon_1 + C_{13}\varepsilon_3 - e_{31}E_3, \quad \sigma_3 = C_{13}\varepsilon_1 + C_{33}\varepsilon_3 - e_{33}E_3, \quad \sigma_5 = C_{44}\varepsilon_5 - e_{15}E_1 \\
&D_1 = \epsilon_{11}E_1 + e_{15}\varepsilon_5, \quad D_3 = \epsilon_{33}E_3 + e_{31}\varepsilon_1 + e_{33}\varepsilon_3
\end{aligned}
\tag{6.208}
$$

The generalized momentum equations in displacements are

$$
\begin{aligned}
&C_{11}u_{1,11} + C_{44}u_{1,33} + (C_{13} + C_{44})u_{3,13} + (e_{31} + e_{15})\varphi_{,13} = \rho\ddot{u}_1 \\
&(C_{13} + C_{44})u_{1,13} + C_{44}u_{3,11} + C_{33}u_{3,33} + e_{15}\varphi_{,11} + e_{33}\varphi_{,33} = \rho\ddot{u}_3 \\
&(e_{31} + e_{15})u_{1,13} + e_{15}u_{3,11} + e_{33}u_{3,33} - \epsilon_{11}\varphi_{,11} - \epsilon_{33}\varphi_{,33} = 0
\end{aligned}
\tag{6.209}
$$

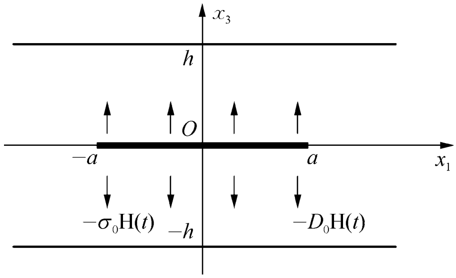

Fig. 6.21 A piezoelectric strip with a crack

The mechanical and electric impermeable conditions are

$$\begin{aligned}
&\sigma_3(x_1,0,t) = -\sigma_0 H(t), \quad D_3(x_1,0,t) = -D_0 H(t), \quad -a < x_1 < a \\
&u_3(x_1,0,t) = \varphi(x_1,0,t) = 0, \quad a < |x_1| < \infty, \quad \sigma_5(x_1,0,t) = 0, \quad -\infty < x_1 < \infty \\
&\sigma_3(x_1 \pm h/2,t) = \sigma_5(x_1,\pm h/2,t) = D_3(x_1,\pm h/2,t) = 0, \quad -\infty < x_1 < \infty
\end{aligned} \tag{6.210}$$

When the derivatives of variables are zeros at the initial time, the Laplace transform (Eq. 6.181) of governing equations (6.208), (6.209), and (6.210) are

$$\begin{aligned}
&\bar{\sigma}_1 = C_{11}\bar{\varepsilon}_1 + C_{13}\bar{\varepsilon}_3 - e_{31}\bar{E}_3, \quad \bar{\sigma}_3 = C_{13}\bar{\varepsilon}_1 + C_{33}\bar{\varepsilon}_3 - e_{33}\bar{E}_3, \quad \bar{\sigma}_5 = C_{44}\bar{\varepsilon}_5 - e_{15}\bar{E}_1 \\
&\bar{D}_1 = \epsilon_{11}\bar{E}_1 + e_{15}\bar{\varepsilon}_5, \quad \bar{D}_3 = \epsilon_{33}\bar{E}_3 + e_{31}\bar{\varepsilon}_1 + e_{33}\bar{\varepsilon}_3
\end{aligned} \tag{6.211}$$

$$\begin{aligned}
&C_{11}\bar{u}_{1,11} + C_{44}\bar{u}_{1,33} + (C_{13}+C_{44})\bar{u}_{3,13} + (e_{31}+e_{15})\bar{\varphi}_{,13} = \rho p^2 \bar{u}_1 \\
&(C_{13}+C_{44})\bar{u}_{1,13} + C_{44}\bar{u}_{3,11} + C_{33}\bar{u}_{3,33} + e_{15}\bar{\varphi}_{,11} + e_{33}\bar{\varphi}_{,33} = \rho p^2 \bar{u}_3 \\
&(e_{31}+e_{15})\bar{u}_{1,13} + e_{15}\bar{u}_{3,11} + e_{33}\bar{u}_{3,33} - \epsilon_{11}\bar{\varphi}_{,11} - \epsilon_{33}\bar{\varphi}_{,33} = 0
\end{aligned} \tag{6.212}$$

$$\begin{aligned}
&\bar{\sigma}_3 = -\sigma_0/p, \quad \bar{D}_2 = -D_0/p, \quad -a < x_1 < a, \quad x_3 = 0 \\
&\bar{u}_3 = \bar{\varphi} = 0, \quad a < |x_1| < \infty, \quad x_3 = 0, \quad \bar{\sigma}_5 = 0, \quad -\infty < x_1 < \infty, \quad x_3 = 0 \\
&\bar{\sigma}_3 = \bar{\sigma}_5 = \bar{D}_2 = 0, \quad -\infty < x_1 < \infty, \quad x_3 = \pm h/2
\end{aligned} \tag{6.213}$$

6.10.2 Reduction to Singular Integration Equations

Because the problem is symmetric with respect to $x_3 = 0$, it is only needed to consider the upper part. In the Laplace transform region, Wang and Yu (2001) adopted the solutions in the following Fourier integrals:

$$\begin{aligned}
\bar{u}_1 &= (2/\pi)\sum_{j=1}^{6}\int_0^\infty q_j A_j(\xi) e^{-\gamma_j x_3} \sin(\xi x_1)\,\mathrm{d}\xi \\
\bar{u}_3 &= (2/\pi)\sum_{j=1}^{6}\int_0^\infty a_j A_j(\xi) e^{-\gamma_j x_3} \cos(\xi x_1)\,\mathrm{d}\xi \\
\bar{\varphi} &= (2/\pi)\sum_{j=1}^{6}\int_0^\infty b_j A_j(\xi) e^{-\gamma_j x_3} \cos(\xi x_1)\,\mathrm{d}\xi
\end{aligned} \tag{6.214}$$

where $A_j(\xi)(j = 1-6)$ are unknown functions. Substitution of Eq. (6.214) into Eq. (6.212) yields

$$\begin{aligned}
&\frac{2}{\pi}\sum_{j=1}^{6}\int_0^\infty A_j(\xi)e^{-\gamma_j x_3}\sin(\xi x_1)\\
&\quad\times\left[\left(-C_{11}\xi^2 + C_{44}\gamma_j^2 - \rho p^2\right)q_j + (C_{13}+C_{44})\xi\gamma_j a_j + (e_{31}+e_{15})\gamma_j b_j\xi\right]\mathrm{d}\xi = 0\\
&\frac{2}{\pi}\sum_{j=1}^{6}\int_0^\infty A_j(\xi)e^{-\gamma_j x_3}\cos(\xi x_1)\\
&\quad\times\left[-(C_{13}+C_{44})\xi\gamma_j q_j + \left(C_{33}\gamma_j^2 - C_{44}\xi^2 - \rho p^2\right)a_j + \left(e_{33}\gamma_j^2 - e_{15}\xi^2\right)b_j\right]\mathrm{d}\xi = 0\\
&\frac{2}{\pi}\sum_{j=1}^{6}\int_0^\infty A_j(\xi)e^{-\gamma_j x_3}\cos(\xi x_1)\\
&\quad\times\left[-(e_{31}+e_{15})\xi\gamma_j q_j + \left(e_{33}\gamma_j^2 - \xi^2 e_{15}\right)a_j + \left(\epsilon_{11}\xi^2 - \epsilon_{33}\gamma_j^2\right)b_j\right]\mathrm{d}\xi = 0
\end{aligned} \tag{6.215}$$

From Eq. (6.215) it is obtained

$$\begin{aligned}
&\left(-C_{11}\xi^2 + C_{44}\gamma_j^2 - \rho p^2\right)q_j + (C_{13}+C_{44})\xi\gamma_j a_j + (e_{31}+e_{15})\gamma_j b_j\xi = 0\\
&\quad-(C_{13}+C_{44})\xi\gamma_j q_j + \left(C_{33}\gamma_j^2 - C_{44}\xi^2 - \rho p^2\right)a_j + \left(e_{33}\gamma_j^2 - e_{15}\xi^2\right)b_j = 0\\
&\quad-(e_{31}+e_{15})\xi\gamma_j q_j + \left(e_{33}\gamma_j^2 - \xi^2 e_{15}\right)a_j + \left(\epsilon_{11}\xi^2 - \epsilon_{33}\gamma_j^2\right)b_j = 0
\end{aligned} \tag{6.216}$$

So the coefficient determinant of q_j, a_j, b_j must be zero, i.e.,

$$\begin{vmatrix}
C_{44}\gamma^2 - C_{11}\xi^2 - \rho p^2 & (C_{13}+C_{44})\xi\gamma & (e_{31}+e_{15})\gamma\xi\\
-(C_{13}+C_{44})\xi\gamma & C_{33}\gamma^2 - C_{44}\xi^2 - \rho p^2 & e_{33}\gamma^2 - e_{15}\xi^2\\
-(e_{31}+e_{15})\xi\gamma & e_{33}\gamma^2 - \xi^2 e_{15} & \epsilon_{11}\xi^2 - \epsilon_{33}\gamma^2
\end{vmatrix} = 0 \tag{6.217}$$

From Eq. (6.217) it can be obtained $\gamma_j(j = 1-6)$. For convenience let $q_j = 1$ in Eq. (6.214), which has not lost the generality, and a_j, b_j can be determined from Eq. (6.216):

$$\begin{aligned}
&a_j = \frac{\Delta_a(\gamma_j)}{\Delta_0(\gamma_j)},\quad b_j = \frac{\Delta_b(\gamma_j)}{\Delta_0(\gamma_j)}\\
&\Delta_a(\gamma_j) = \left(C_{11}\xi^2 - C_{44}\gamma_j^2 + \rho p^2\right)\left(e_{33}\gamma_j^2 - e_{15}\xi^2\right) - (C_{13}+C_{44})(e_{31}+e_{15})\xi^2\gamma_j^2\\
&\Delta_b(\gamma_j) = (C_{13}+C_{44})^2\xi^2\gamma_j^2 - \left(C_{11}\xi^2 - C_{44}\gamma_j^2 + \rho p^2\right)\left(C_{33}\gamma_j^2 - C_{44}\xi^2 - \rho p^2\right)\\
&\Delta_0(\gamma_j) = \left[(C_{13}+C_{44})\left(e_{33}\gamma_j^2 - e_{15}\xi^2\right) - (e_{31}+e_{15})\left(C_{33}\gamma_j^2 - C_{44}\xi^2 - \rho p^2\right)\right]\xi\gamma_j
\end{aligned} \tag{6.218}$$

$A_j(\xi)(j = 1-6)$ is determined by the boundary conditions.

Introduce the half of the generalized dislocation density:

$$f(x_1,p)=\begin{cases}\bar{u}^{+}_{3,1}, & -a<x_1<a\\ 0, & a\le|x_1|<\infty\end{cases},\quad g(x_1,p)=\begin{cases}\bar{\varphi}^{+}_{,1}, & -a<x_1<a\\ 0, & a\le|x_1|<\infty\end{cases}\tag{6.219a}$$

Around the crack the single-valued conditions are

$$\int_a^b\left(\bar{u}^{+}_{3,1}-\bar{u}^{-}_{3,1}\right)\mathrm{d}u\Rightarrow\int_a^b f(u,p)\mathrm{d}u=0,\quad \int_a^b g(u,p)\mathrm{d}u=0\tag{6.219b}$$

Substituting Eq. (6.214) into (6.211), then into the boundary conditions (6.213), and applying conditions (6.219), in the interval $0<x_1<a$, the following singular integral equations are obtained (Erdogan and Gupta 1972; Erdogan 1975; Lu 1984):

$$\begin{aligned}&\frac{\alpha_1}{\pi}\int_0^a\frac{f(u,p)}{u-x_1}\mathrm{d}u+\frac{\alpha_2}{\pi}\int_0^a\frac{g(u,p)}{u-x_1}\mathrm{d}u+\frac{1}{\pi}\int_0^a[Q_{11}(u,x_1)f(u,p)+Q_{12}(u,x_1)g(u,p)]\mathrm{d}u=-\frac{\sigma_0}{p}\\&\frac{\alpha_3}{\pi}\int_0^a\frac{f(u,p)}{u-x_1}\mathrm{d}u+\frac{\alpha_4}{\pi}\int_0^a\frac{g(u,p)}{u-x_1}\mathrm{d}u+\frac{1}{\pi}\int_0^a[Q_{21}(u,x_1)f(u,p)+Q_{22}(u,x_1)g(u,p)]\mathrm{d}u=-\frac{D_0}{p}\end{aligned}\tag{6.220}$$

where

$$\begin{aligned}&Q_{ij}(u,x_1)=\int_0^\infty 2\left[P_{ij}(\xi,p)-\alpha_{ij}\right]\cos(\xi x_1)\sin(\xi u)\,\mathrm{d}\xi+\frac{\alpha_{ij}}{u+x_1},\quad i,j=1,2\\&\alpha_{11}=\alpha_1,\quad \alpha_{12}=\alpha_2,\quad \alpha_{21}=\alpha_3,\quad \alpha_{22}=\alpha_4\end{aligned}\tag{6.221}$$

And

$$\begin{aligned}&P_{11}(\xi,p)=\sum_{j=1}^{6}\frac{C_{33}\gamma_j a_j+e_{33}\gamma_j b_j-C_{13}\xi}{\xi\Delta(\xi,p)}\Delta_{j1}(\xi,p)\\&P_{12}(\xi,p)=\sum_{j=1}^{6}\frac{C_{33}\gamma_j a_j+e_{33}\gamma_j b_j-C_{13}\xi}{\xi\Delta(\xi,p)}\Delta_{j2}(\xi,p)\\&P_{21}(\xi,p)=\sum_{j=1}^{6}\frac{e_{33}\gamma_j a_j+\epsilon_{33}\gamma_j b_j-e_{13}\xi}{\xi\Delta(\xi,p)}\Delta_{j1}(\xi,p)\\&P_{22}(\xi,p)=\sum_{j=1}^{6}\frac{e_{33}\gamma_j a_j+\epsilon_{33}\gamma_j b_j-e_{13}\xi}{\xi\Delta(\xi,p)}\Delta_{j2}(\xi,p)\\&\Delta(\xi,p)=\det[M_{ij}],\quad M_{1j}=a_j,\quad M_{2j}=b_j\\&M_{3j}=-\left[C_{44}(\gamma_j+a_j\xi)+e_{15}b_j\xi\right],\quad M_{4j}=-\left[C_{44}(\gamma_j+a_j\xi)+e_{15}b_j\xi\right]e^{-\gamma_j h}\\&M_{5j}=\left[C_{31}\xi-C_{33}\gamma_j a_j-e_{33}\gamma_j b_j\right]e^{-\gamma_j h},\quad M_{6j}=\left[e_{31}\xi-e_{33}\gamma_j a_j+\epsilon_{33}\gamma_j b_j\right]e^{-\gamma_j h}\end{aligned}\tag{6.222}$$

where $\Delta_{jn}(j=1-6,n=1,2)$ is the complementary minor of matrix $|M_{ij}|$ with respect to the component M_{nj}.

6.10.3 Solutions

In order to use the standard numerical method, introduce the dimensionless variables:

$$\frac{u}{a} = \frac{\rho + 1}{2}, \quad \frac{x_1}{a} = \frac{r + 1}{2} \tag{6.223}$$

Equation (6.220) is rewritten as

$$\begin{aligned}
&\frac{\alpha_1}{\pi}\int_{-1}^{1}\frac{F(\rho,p)}{\rho - r}\mathrm{d}\rho + \frac{\alpha_2}{\pi}\int_{-1}^{1}\frac{V(\rho,p)}{\rho - r}\mathrm{d}\rho + \frac{1}{\pi}\int_{0}^{a}\left[\hat{Q}_{11}(\rho,r)F(\rho,p) + \hat{Q}_{12}(\rho,r)V(\rho,p)\right]\mathrm{d}\rho = -\frac{\sigma_0}{p}\\
&\frac{\alpha_3}{\pi}\int_{-1}^{1}\frac{F(\rho,p)}{\rho - r}\mathrm{d}\rho + \frac{\alpha_4}{\pi}\int_{-1}^{1}\frac{V(\rho,p)}{\rho - r}\mathrm{d}\rho + \frac{1}{\pi}\int_{0}^{a}\left[\hat{Q}_{21}(\rho,r)F(\rho,p) + \hat{Q}_{22}(\rho,r)V(\rho,p)\right]\mathrm{d}\rho = -\frac{D_0}{p}\\
&-1 < r < 1
\end{aligned} \tag{6.224}$$

where

$$\begin{aligned}
&F(\rho,p) = f\left(\frac{\rho+1}{2}a, p\right), \quad V(\rho,p) = \mathrm{g}\left(\frac{\rho+1}{2}a, p\right),\\
&\hat{Q}_{ij}(\rho,r) = \frac{a}{2}Q_{ij}\left(\frac{\rho+1}{2}a, \frac{r+1}{2}a\right)
\end{aligned} \tag{6.225}$$

Let

$$\begin{aligned}
&F(\rho,p) = \frac{R(\rho,p)}{\sqrt{1-\rho^2}}, \quad V(\rho,p) = \frac{T(\rho,p)}{\sqrt{1-\rho^2}}\\
&R(\rho,p) = \sum_{i=0}^{\infty} C_i \mathrm{T}_i(\rho), \quad T(\rho,p) = \sum_{i=0}^{\infty} D_i \mathrm{T}_i(\rho)
\end{aligned} \tag{6.226}$$

where $T_k(\rho)$ $(U_k(\rho))$ is the first (second) kind of the Chebyshev polynomials. Using the Gauss-Chebyshev formula yields a linear algebraic equation system

$$\begin{aligned}
&\sum_{k=1}^{n}\left\{\left[\frac{\alpha_1}{\rho_k - r_m} + \hat{Q}_{11}(\rho_k, r_m)\right]\frac{R(\rho_1,p)}{n} + \left[\frac{\alpha_2}{\rho_k - r_m} + \hat{Q}_{12}(\rho_k, r_m)\right]\frac{T(\rho_1,p)}{n}\right\} = -\frac{\sigma_0}{p}\\
&\sum_{k=1}^{n}\left\{\left[\frac{\alpha_3}{\rho_k - r_m} + \hat{Q}_{21}(\rho_k, r_m)\right]\frac{R(\rho_1,p)}{n} + \left[\frac{\alpha_4}{\rho_k - r_m} + \hat{Q}_{22}(\rho_k, r_m)\right]\frac{T(\rho_1,p)}{n}\right\} = -\frac{D_0}{p}
\end{aligned} \tag{6.227}$$

where

$$\mathrm{T}_n(\rho_k)=0,\quad \rho_k=\cos\left(\frac{2k-1}{2n}\pi\right);\quad \mathrm{U}_n(r_k)=0,$$
$$r_k=\cos\left(\frac{k}{n+1}\pi\right);\quad k=1,2,\ldots,n \tag{6.228}$$

Because $f(x_1,p),\mathrm{g}(x_1,p)$ are the odd functions of x_1, $f(0,p)=\mathrm{g}(0,p)=0$, or $R(-1,p)=T(-1,p)=0$. So $R(\rho_n,p)=T(\rho_n,p)=0$, since ρ_n is the closest to -1 in all ρ_k in the limit sense $n\to\infty$ (Erdogan and Gupta 1972; Achenbach et al. 1980). So Eq. (6.227) is a $2(n-1)\times 2(n-1)$ linear algebraic equations with $2(n-1)\times 2(n-1)$ variables $R(\rho_k,p),T(\rho_k,p)$. It is solvable.

Applying the following behavior of the Chebyshev polynomials

$$\frac{1}{\pi}\int_{-1}^{1}\frac{\mathrm{T}_n(u)\,\mathrm{d}u}{(u-x_1)\sqrt{1-u^2}}=-\frac{|x_1|}{x_1\sqrt{x_1^2-1}}\left(x_1-\frac{|x_1|\sqrt{x_1^2-1}}{x_1}\right)^n,$$
$$|x_1|>1,\quad n=0,1,\ldots \tag{6.229}$$

in the Laplace transform region, the dynamic stress factors can be expressed as

$$\bar{K}_{\mathrm{I}}(p)=\lim_{x\to a^+}\sqrt{2\pi(x_1-a)}\bar{\sigma}_3(x_1,0,p)=-\sqrt{\frac{\pi a}{2}}[\alpha_1R(1,p)+\alpha_2T(1,p)]$$
$$\bar{K}_D(p)=\lim_{x\to a^+}\sqrt{2\pi(x_1-a)}\bar{D}_3(x_1,0,p)=-\sqrt{\frac{\pi a}{2}}[\alpha_3R(1,p)+\alpha_4T(1,p)] \tag{6.230}$$

The dynamic stress factors $K_{\mathrm{I}}(t),K_D(t)$ in the physical plane are obtained by the Laplace inverse transform using the numerical method. The asymptotic generalized stresses and displacements are

$$\sigma_3(x_1,0,t)=\frac{1}{\sqrt{2\pi(x_1-a)}}K_{\mathrm{I}}(t),\quad D_3(x_1,0,t)=\frac{1}{\sqrt{2\pi(x_1-a)}}K_D(t)$$
$$\begin{Bmatrix}u_3(x_1,0,t)\\ \varphi(x_1,0,t)\end{Bmatrix}=\frac{\sqrt{2\pi(a-x_1)}}{\alpha_2\alpha_3-\alpha_1\alpha_4}\begin{bmatrix}-\alpha_4 & \alpha_2\\ \alpha_3 & -\alpha_1\end{bmatrix}\begin{Bmatrix}K_{\mathrm{I}}(t)\\ K_D(t)\end{Bmatrix} \tag{6.231}$$

And the energy release rate with the electric enthalpy is

$$\tilde{G}\mathrm{d}a=2\int_a^{a+\mathrm{d}a}\frac{1}{2}[\sigma_3(x_1,0,t),\quad D_3(x_1,0,t)]\begin{Bmatrix}u_3(x_1-\mathrm{d}a,0,t)\\ \varphi(x_1-\mathrm{d}a,0,t)\end{Bmatrix}\mathrm{d}x_1$$
$$G=[\pi/2(\alpha_2\alpha_3-\alpha_1\alpha_4)]\left[-\alpha_4K_{\mathrm{I}}^2(t)+2\alpha_2\alpha_3K_{\mathrm{I}}(t)K_D(t)-\alpha_1K_D^2(t)\right] \tag{6.232}$$

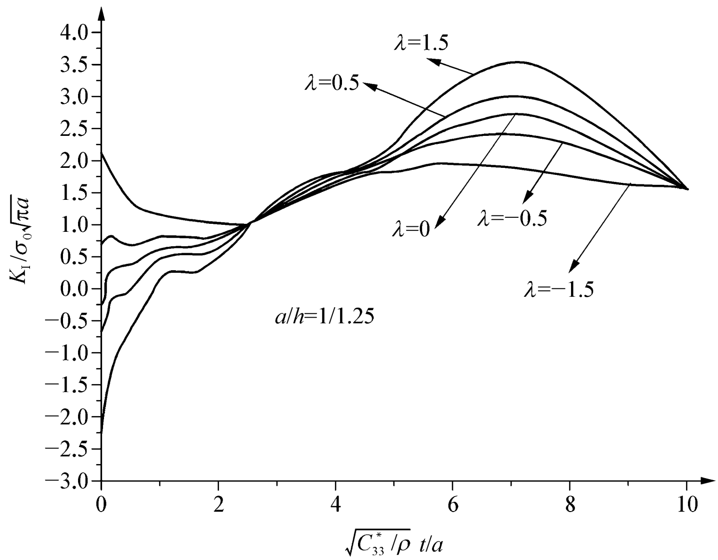

Fig. 6.22 Variation of $K_I/\sigma_0\sqrt{\pi a}$ with $\sqrt{C_{33}^*/\rho}\ t/a$ for various λ under $h/a = 1.25$ (Reprinted from Wang and Yu 2001, with permission from Mechanics of materials)

6.10.4 Numerical Example

In the numerical analysis the material is taken PZT-5H with material constants:

$$C_{11} = 12.6 \times 10^{10}, \quad C_{13} = 5.3 \times 10^{10}, \quad C_{33} = 11.7 \times 10^{10}, \quad C_{44} = 3.53 \times 10^{10}(\mathrm{N/m^2})$$
$$e_{31} = -6.5\,(\mathrm{C/m^2}), \quad e_{33} = 23.3\,(\mathrm{C/m^2}), \quad e_{21} = 17.0\,(\mathrm{C/m^2})$$
$$\epsilon_{11} = 15.1 \times 10^{-9}\,(\mathrm{C/Vm}), \quad \epsilon_{11} = 13.0 \times 10^{-9}\,(\mathrm{C/Vm}), \quad \rho = 7,500\,\mathrm{kg/m^3}$$

The solved values of α_k are

$$\alpha_1 = 5.094 \times 10^{10}, \quad \alpha_2 = 14.216, \quad \alpha_3 = 14.216, \quad \alpha_4 = -178.769 \times 10^{-10}$$

Figures 6.22 and 6.23 show the variations of the dimensionless generalized dynamic stress intensity factors $(K_I, K_D)/\sigma_0\sqrt{\pi a}$ with the dimensionless time $\sqrt{C_{33}^*/\rho}\ t/a$, $C_{33}^* = C_{33} + e_{33}^2/\epsilon_{33}$ under $h/a = 1.25$ and the different loading parameters $\lambda = -D_0\alpha_2/\sigma_0\alpha_4$. It can be seen that the dynamic intensity factors are increased at first and then decreased and after a long time they approach the static values.

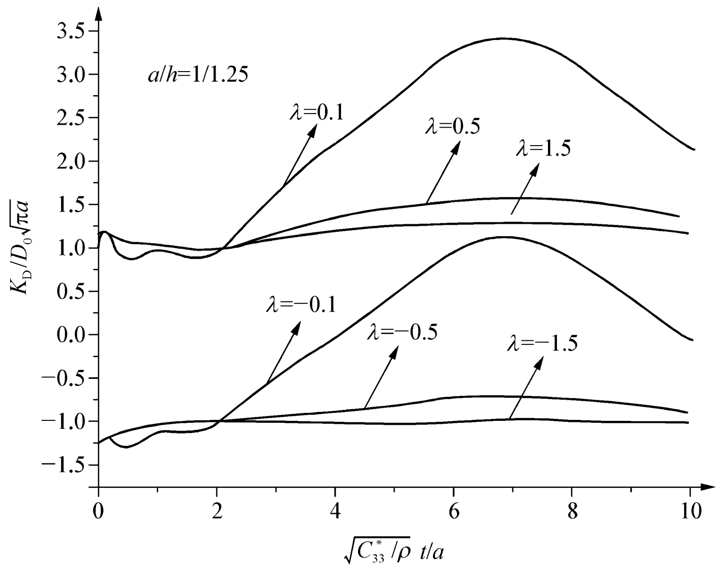

Fig. 6.23 Variation of $K_D/\sigma_0\sqrt{\pi a}$ with $\sqrt{C^*_{33}/\rho}\ t/a$ for various λ under $h/a = 1.25$ (Reprinted from Wang and Yu 2001, with permission from Mechanics of materials)

6.11 On the General Dynamic Analyses of Interface Cracks

6.11.1 *Governing Equations in Laplace-Fourier Transform Region*

In this section the electrically quasi-static assumption is adopted. The generalized momentum and constitutive equations are shown in Eqs. (3.2) and (6.1) or

$$\begin{aligned} &C_{ijkl}u_{l,kj} + e_{kij}\varphi_{,kj} = \rho\ddot{u}_i, \quad e_{ikl}u_{l,ki} - \epsilon_{ij}\varphi_{,ji} = 0 \\ &\sigma_{ij} = C_{ijkl}\epsilon_{kl} - e_{kij}E_k, \quad D_i = \epsilon_{ij}E_j + e_{ikl}\varepsilon_{kl} \end{aligned} \tag{6.233}$$

Shen et al. (1999) applied the Laplace-Fourier transform, i.e., at first adopted the Laplace transform (Eq. (6.181)) with respect to time and then used the Fourier transform (Eq. (4.242)) with respect to time x_1, to solve the problem. When the initial derivatives of variables are zero, the Laplace transform of the Eq. (6.233) is

$$\begin{aligned} &\bar{\sigma}_{ij} = C_{ijkl}\bar{u}_{k,l} + e_{kij}\bar{\varphi}_{,k}, \quad \bar{D}_i = -\epsilon_{ik}\bar{\varphi}_{,k} + e_{ikl}\bar{u}_{k,l} \\ &\left(C_{ijkl}\bar{u}_l + e_{kij}\bar{\varphi}\right)_{,ki} = \rho p^2\bar{u}_j, \quad \left(-\epsilon_{ik}\bar{\varphi} + e_{ikl}\bar{u}_l\right)_{,ki} = 0 \end{aligned} \tag{6.234}$$

Denote the Fourier transform of $\bar{u}_i(x_1, x_2, p)$ as $\bar{u}_i^*(s, x_2, p)$ and let

$$x = x_1. \quad y = \mathrm{i}sx_2 \tag{6.235}$$

By using $\bar{u}_{l,1}^* = \mathrm{i}s\bar{u}_l^*, \quad \bar{u}_{l,11}^* = (\mathrm{i}s)^2\bar{u}_l^*$, the Fourier transform of the second equation in Eq. (6.234) with respect to x_1 is

$$\begin{aligned}
&\left[C_{1jk1}^* + (C_{1jk2} + C_{2jk1})\partial/\partial y + C_{2jk2}\partial^2/\partial y^2\right]\bar{u}_k^* \\
&\quad + \left[e_{1j1} + (e_{1j2} + e_{2j1})\partial/\partial y + e_{2j2}\partial^2/\partial y^2\right]\bar{\varphi}^* = 0 \\
&\left[e_{1k1} + (e_{1k2} + e_{2k1})\partial/\partial y + e_{2k2}\partial^2/\partial y^2\right]\bar{u}_k^* \\
&\quad - \left[\epsilon_{11} + (\epsilon_{12} + \epsilon_{21})\partial/\partial y + \epsilon_{22}\partial^2/\partial y^2\right]\bar{\varphi}^* = 0 \\
&C_{1jk1}^* = C_{1jk1}^*(p, s) = C_{1jk1} + \rho(p^2/s^2)\delta_{jk}
\end{aligned} \tag{6.236}$$

Introduce notations

$$\boldsymbol{Q} = \begin{bmatrix} C_{1jk1}^* & e_{1j1} \\ e_{1k1} & -\epsilon_{11} \end{bmatrix}, \quad \boldsymbol{R} = \begin{bmatrix} C_{1jk2} & e_{2j1} \\ e_{1k2} & -\epsilon_{12} \end{bmatrix}, \quad \boldsymbol{T} = \begin{bmatrix} C_{2jk2} & e_{2j2} \\ e_{2k2} & -\epsilon_{22} \end{bmatrix}, \quad \bar{\boldsymbol{U}}^* = \begin{Bmatrix} \bar{u}_k^* \\ \bar{\varphi}^* \end{Bmatrix} \tag{6.237}$$

where $\boldsymbol{Q}$, $\boldsymbol{T}$ are positive definite. Applying Eq. (6.237), Eq. (6.236) becomes

$$\left[\boldsymbol{T}\partial^2/\partial y^2 + (\boldsymbol{R} + \boldsymbol{R}^{\mathrm{T}})\partial/\partial y + \boldsymbol{Q}\right]\bar{\boldsymbol{U}}^* = \boldsymbol{0} \tag{6.238}$$

Assume

$$\bar{\boldsymbol{U}}^*(s, y, p) = \boldsymbol{a}(s, p)\mathrm{e}^{\mu y(s,p)}, \quad \partial\bar{\boldsymbol{U}}^*/\partial y = \mu\bar{\boldsymbol{U}}^* \tag{6.239}$$

Substitution of Eq. (6.239) into Eq. (6.238) yields

$$\left[\boldsymbol{T}\mu^2 + (\boldsymbol{R} + \boldsymbol{R}^{\mathrm{T}})\mu + \boldsymbol{Q}\right]\boldsymbol{a} = \boldsymbol{0}, \quad |\boldsymbol{D}(\mu)| = \left|\boldsymbol{T}\mu^2 + (\boldsymbol{R} + \boldsymbol{R}^{\mathrm{T}})\mu + \boldsymbol{Q}\right| = 0 \tag{6.240}$$

Equations (6.237) and (6.240) are identical in the form with Eqs. (3.13) and (3.14), respectively, if use C_{1jk1}^* instead of C_{1jk1}. Analogous to Eq. (3.15), from $|\boldsymbol{D}(\mu)| = 0$ eight roots $\mu_j (j = 1 \sim 8)$ can be obtained. When $s \to \pm\infty$, Eq. (6.239) and μ_i approach the static solutions. The general solution of Eq. (6.239) is

$$\bar{\boldsymbol{U}}^*(s, y, p) = \sum_{k=1}^{4}\left[C_k\boldsymbol{a}_k(s, y, p)\mathrm{e}^{y\mu_k(s,p)} + C_{k+4}\boldsymbol{a}_{k+4}(s, y, p)\mathrm{e}^{y\mu_{k+4}(s,p)}\right] \tag{6.241}$$

The Fourier transform of the first equation in Eq. (6.234) is

$$\bar{\boldsymbol{\Sigma}}_2^* = \mathrm{i}s\left(\boldsymbol{R}^{\mathrm{T}} + \boldsymbol{T}\partial/\partial y\right)\bar{\boldsymbol{U}}^* \tag{6.242}$$

6.11.2 Dynamical Interface Crack

The material I is located at the upper half-plane $S^+, x_2 > 0$; the material II is located at the lower half-plane S^-, $x_2 < 0$; $x_1 = 0$ is the interface and there is a crack of length $2a$ on it. The coordinate origin is selected at the center of the crack (Fig. 4.2b). For the materials I and II, Eqs. (6.238) and (6.242) are all held. The boundary conditions are

$$\begin{aligned}
&\boldsymbol{\Sigma}_2^{(\mathrm{I})} = \left[\sigma_{21}^{(\mathrm{I})}, \sigma_{22}^{(\mathrm{I})}, \sigma_{23}^{(\mathrm{I})}, D_2^{(\mathrm{I})}\right]^{\mathrm{T}} = \boldsymbol{\Sigma}_2^{(\mathrm{II})} = \boldsymbol{\tau}_0 H(t), \quad |x_1| < a \\
&\Sigma_{ij}^{(\mathrm{I})}(x_1, x_2, t) = \Sigma_{ij}^{(\mathrm{II})} = 0, \quad \text{when} \quad \left|\sqrt{x_1^2 + x_2^2}\right| \to \infty \\
&\boldsymbol{U}^{(\mathrm{I})}(u_1, u_2, u_3, \varphi) = \boldsymbol{U}^{(\mathrm{II})}, \quad \boldsymbol{\Sigma}_2^{(\mathrm{I})}(x_1) = \boldsymbol{\Sigma}_2^{(\mathrm{II})}(x_1) = \boldsymbol{\Sigma}_2(x_1, 0, t), \quad |x_1| > a, \quad x_2 = 0
\end{aligned} \tag{6.243}$$

where $\boldsymbol{\tau}_0$ is a constant vector. The initial conditions are

$$\boldsymbol{U}^{(\mathrm{I})}(x_1, x_2, 0) = \boldsymbol{U}^{(\mathrm{II})} = \mathbf{0}, \quad \dot{\boldsymbol{U}}^{(\mathrm{I})}(x_1, x_2, 0) = \dot{\boldsymbol{U}}^{(\mathrm{II})} = \mathbf{0} \tag{6.244}$$

The jump value of the generalized displacements on $x_2 = 0$ is defined as

$$\Delta\boldsymbol{U}(x_1) = \boldsymbol{U}^{(\mathrm{I})}(x_1, 0) - \boldsymbol{U}^{(\mathrm{II})}(x_1, 0), \quad \boldsymbol{\psi}(x_1) = \mathrm{d}\Delta\boldsymbol{U}(x_1)/\mathrm{d}x_1 \tag{6.245}$$

where $\boldsymbol{\psi}(x_1)$ is the dislocation density. The single-valued condition around the crack is

$$\int_{-a}^{a} \boldsymbol{\psi}(x_1, t)\mathrm{d}x_1 = 0, \quad \boldsymbol{\psi} = [\psi_1, \psi_2, \psi_3, \psi_4] \tag{6.246}$$

The Laplace-Fourier transform of Eqs. (6.245) and (6.246) is

$$\begin{aligned}
&\Delta\bar{\boldsymbol{U}}^*(s, p) = \bar{\boldsymbol{U}}^{*(\mathrm{I})}(s, 0, p) - \bar{\boldsymbol{U}}^{*(\mathrm{II})}(s, 0, p) = -(\mathrm{i}/s)\bar{\boldsymbol{\psi}}^* = -(\mathrm{i}/s)\int_{-a}^{a} \bar{\boldsymbol{\psi}}(x_1, p)\mathrm{e}^{-\mathrm{i}sx_1}\mathrm{d}x_1 \\
&\int_{-a}^{a} \bar{\boldsymbol{\psi}}^*(x_1, p)\mathrm{d}x_1 = 0; \quad \int_{-a}^{a} \bar{\boldsymbol{\psi}}(x_1, p)\mathrm{d}x_1 = 0
\end{aligned} \tag{6.247}$$

The Laplace transform of Eq. (6.243) is

$$\begin{aligned}
&\bar{\boldsymbol{\Sigma}}_2(x_1, 0) = \boldsymbol{\tau}_0/p, \quad |x_1| < a; \quad \bar{\boldsymbol{U}}^{(\mathrm{I})}(x_1, 0, t) = \bar{\boldsymbol{U}}^{(\mathrm{II})}(x_1, 0, t), \quad a < |x_1| < \infty \\
&\bar{\boldsymbol{\Sigma}}_2^{(\mathrm{I})}(x_1, 0) = \bar{\boldsymbol{\Sigma}}_2^{(\mathrm{II})}(x_1, 0) = \bar{\boldsymbol{\Sigma}}_2(x_1, 0), \quad |x_1| < \infty; \quad \bar{\boldsymbol{\Sigma}}_2^{(\mathrm{I})} = \bar{\boldsymbol{\Sigma}}_2^{(\mathrm{II})} = 0, \quad |\boldsymbol{x}| \to \infty
\end{aligned} \tag{6.248}$$

6.11.3 Reduced to the Singular Integral Equation

In order to make $\bar{\boldsymbol{U}}^*$ finite when $|s| \to \infty$, the solution of Eq. (6.241) is expressed as

$$\begin{gathered}
\bar{\boldsymbol{U}}^{*(\mathrm{I})}(s,y,p) = \begin{cases} \boldsymbol{A}_1^{(\mathrm{I})}\boldsymbol{E}_1^{(\mathrm{I})}\boldsymbol{C}_1^{(\mathrm{I})}, & s<0 \\ \boldsymbol{A}_2^{(\mathrm{I})}\boldsymbol{E}_2^{(\mathrm{I})}\boldsymbol{C}_2^{(\mathrm{I})}, & s>0 \end{cases}; \quad \bar{\boldsymbol{U}}^{*(\mathrm{II})}(s,y,p) = \begin{cases} \boldsymbol{A}_1^{(\mathrm{II})}\boldsymbol{E}_1^{(\mathrm{II})}\boldsymbol{C}_1^{(\mathrm{II})}, & s>0 \\ \boldsymbol{A}_2^{(\mathrm{II})}\boldsymbol{E}_2^{(\mathrm{II})}\boldsymbol{C}_2^{(\mathrm{II})}, & s<0 \end{cases} \\
\boldsymbol{A}_1^{(\mathrm{N})} = \left[\boldsymbol{a}_1^{(\mathrm{N})},\boldsymbol{a}_2^{(\mathrm{N})},\boldsymbol{a}_3^{(\mathrm{N})},\boldsymbol{a}_4^{(\mathrm{N})}\right], \quad \boldsymbol{A}_2^{(\mathrm{N})} = \left[\boldsymbol{a}_5^{(\mathrm{N})},\boldsymbol{a}_6^{(\mathrm{N})},\boldsymbol{a}_7^{(\mathrm{N})},\boldsymbol{a}_8^{(\mathrm{N})}\right]; \quad \boldsymbol{E}_1^{(\mathrm{I})} = \left\langle \mathrm{e}^{-\mathrm{i}s\mu_j x_2}\right\rangle \\
\boldsymbol{E}_2^{(\mathrm{N})} = \left\langle \mathrm{e}^{-\mathrm{i}s\mu_{j+4} x_2}\right\rangle; \quad \boldsymbol{C}_1^{(N)} = \left[C_1^{(N)},C_2^{(N)},C_3^{(N)},C_4^{(N)}\right], \quad \boldsymbol{C}_2^{(\mathrm{N})} = \left[C_5^{(\mathrm{N})},C_6^{(\mathrm{N})},C_7^{(\mathrm{N})},C_8^{(\mathrm{N})}\right]
\end{gathered} \tag{6.249}$$

where $\mathrm{N} = \mathrm{I}, \mathrm{II}$. Equation (6.249) can be rewritten as

$$\begin{gathered}
\bar{\boldsymbol{U}}^{*(\mathrm{I})} = \boldsymbol{A}_1^{(\mathrm{I})}\boldsymbol{E}_1^{(\mathrm{I})}\boldsymbol{C}_1^{(\mathrm{I})} + \boldsymbol{A}_2^{(\mathrm{I})}\boldsymbol{E}_2^{(\mathrm{I})}\boldsymbol{C}_2^{(\mathrm{I})}; \quad \bar{\boldsymbol{U}}^{*(\mathrm{II})} = \boldsymbol{A}_1^{(\mathrm{II})}\boldsymbol{E}_1^{(\mathrm{II})}\boldsymbol{C}_1^{(\mathrm{II})} + \boldsymbol{A}_2^{(\mathrm{II})}\boldsymbol{E}_2^{(\mathrm{II})}\boldsymbol{C}_2^{(\mathrm{II})} \\
\boldsymbol{C}_2^{(\mathrm{I})} = \boldsymbol{C}_1^{(\mathrm{II})} = \boldsymbol{0}, \quad \text{when} \quad s<0; \quad \boldsymbol{C}_1^{(\mathrm{I})} = \boldsymbol{C}_2^{(\mathrm{II})} = \boldsymbol{0}, \quad \text{when} \quad s>0
\end{gathered} \tag{6.250}$$

From Eq. (6.242) it is obtained

$$\begin{gathered}
\bar{\boldsymbol{\Sigma}}_2^{*(\mathrm{I})}(s,y,p) = \begin{cases} \mathrm{i}s\boldsymbol{B}_1^{(\mathrm{I})}\mathbf{E}_1^{(\mathrm{I})}\boldsymbol{C}_1^{(\mathrm{I})} = \mathrm{i}s\boldsymbol{B}_1^{(\mathrm{I})}\boldsymbol{A}_1^{(\mathrm{I})^{-1}}\bar{\boldsymbol{U}}^{*(\mathrm{I})} = -s\boldsymbol{Y}_1^{(\mathrm{I})-1}\bar{\boldsymbol{U}}^{*(\mathrm{I})}, & s<0 \\ \mathrm{i}s\boldsymbol{B}_2^{(\mathrm{I})}\mathbf{E}_2^{(\mathrm{I})}\boldsymbol{C}_2^{(\mathrm{I})} = \mathrm{i}s\boldsymbol{B}_2^{(\mathrm{I})}\boldsymbol{A}_2^{(\mathrm{I})^{-1}}\bar{\boldsymbol{U}}^{*(\mathrm{I})} = -s\boldsymbol{Y}_2^{(\mathrm{I})^{-1}}\bar{\boldsymbol{U}}^{*(\mathrm{I})}, & s>0 \end{cases} \\
\bar{\boldsymbol{\Sigma}}_2^{*(\mathrm{II})}(s,y,p) = \begin{cases} \mathrm{i}s\boldsymbol{B}_1^{(\mathrm{II})}\mathbf{E}_1^{(\mathrm{II})}\boldsymbol{C}_1^{(\mathrm{II})} = \mathrm{i}s\boldsymbol{B}_1^{(\mathrm{II})}\boldsymbol{A}_1^{(\mathrm{II})^{-1}}\bar{\boldsymbol{U}}^{*(\mathrm{II})} = -s\boldsymbol{Y}_1^{(\mathrm{II})-1}\bar{\boldsymbol{U}}^{*(\mathrm{II})}, & s>0 \\ \mathrm{i}s\boldsymbol{B}_2^{(\mathrm{II})}\mathbf{E}_2^{(\mathrm{II})}\boldsymbol{C}_2^{(\mathrm{II})} = \mathrm{i}s\boldsymbol{B}_2^{(\mathrm{II})}\boldsymbol{A}_2^{(\mathrm{II})^{-1}}\bar{\boldsymbol{U}}^{*(\mathrm{II})} = -s\boldsymbol{Y}_2^{(\mathrm{II})^{-1}}\bar{\boldsymbol{U}}^{*(\mathrm{II})}, & s<0 \end{cases} \\
\boldsymbol{B}_1^{(N)} = \left[\boldsymbol{b}_1^{(\mathrm{N})},\boldsymbol{b}_2^{(\mathrm{N})},\boldsymbol{b}_3^{(\mathrm{N})},\boldsymbol{b}_4^{(\mathrm{N})}\right], \quad \boldsymbol{B}_2^{(\mathrm{N})} = \left[\boldsymbol{b}_5^{(\mathrm{N})},\boldsymbol{b}_6^{(\mathrm{N})},\boldsymbol{b}_7^{(\mathrm{N})},\boldsymbol{b}_8^{(\mathrm{N})}\right], \\
\boldsymbol{b}^{(\mathrm{N})} = \left(\boldsymbol{R}^{(\mathrm{N})\mathrm{T}} + \boldsymbol{T}^{(\mathrm{N})}\partial/\partial y\right)\boldsymbol{a}^{(\mathrm{N})}; \quad \mathrm{N} = \mathrm{I}, \mathrm{II}
\end{gathered} \tag{6.251}$$

On the crack surface Eq. (6.251) becomes

$$\begin{gathered}
\bar{\boldsymbol{\Sigma}}_2^{*(\mathrm{I})}(s,0,p) = \boldsymbol{R}^{(\mathrm{I})}\bar{\boldsymbol{U}}^{*(\mathrm{I})}; \quad \bar{\boldsymbol{\Sigma}}_2^{*(\mathrm{II})}(s,0,p) = \boldsymbol{R}^{(\mathrm{II})}\bar{\boldsymbol{U}}^{*(\mathrm{II})} \\
\boldsymbol{R}^{(\mathrm{I})} = \begin{cases} \mathrm{i}s\boldsymbol{B}_1^{(\mathrm{I})}\boldsymbol{A}_1^{(\mathrm{I})-1} = -s\boldsymbol{Y}_1^{(I)-1}, & s<0 \\ \mathrm{i}s\boldsymbol{B}_2^{(\mathrm{I})}\boldsymbol{A}_2^{(\mathrm{I})-1} = -s\boldsymbol{Y}_2^{(I)^{-1}}, & s>0 \end{cases}; \quad \boldsymbol{R}^{(\mathrm{II})} = \begin{cases} \mathrm{i}s\boldsymbol{B}_1^{(\mathrm{II})}\boldsymbol{A}_1^{(\mathrm{II})-1} = -s\boldsymbol{Y}_1^{(\mathrm{II})-1}, & s>0 \\ \mathrm{i}s\boldsymbol{B}_2^{(\mathrm{II})}\boldsymbol{A}_2^{(\mathrm{II})-1} = -s\boldsymbol{Y}_2^{(\mathrm{II})^{-1}}, & s<0 \end{cases}
\end{gathered} \tag{6.252}$$

where $\boldsymbol{Y}^{(\mathrm{N})} = \mathrm{i}\boldsymbol{A}^{(\mathrm{N})}\boldsymbol{B}^{(\mathrm{N})^{-1}}$. Because on the whole interface $\boldsymbol{\Sigma}_2^{(\mathrm{I})}(x_1) = \boldsymbol{\Sigma}_2^{(\mathrm{II})}(x_1)$, so

$$\boldsymbol{R}^{(\mathrm{I})}\bar{\boldsymbol{U}}^{*(\mathrm{I})} = \boldsymbol{R}^{(\mathrm{II})}\bar{\boldsymbol{U}}^{*(\mathrm{II})} \tag{6.253}$$

From Eqs. (6.247) and (6.253) it is obtained

$$\bar{\boldsymbol{U}}^{*(\mathrm{I})}=\boldsymbol{R}^{(\mathrm{II})}\boldsymbol{R}^{-1}\Delta\bar{\boldsymbol{U}}^{*},\quad \bar{\boldsymbol{U}}^{*(\mathrm{II})}=\boldsymbol{R}^{(\mathrm{I})}\boldsymbol{R}^{-1}\Delta\bar{\boldsymbol{U}}^{*};\quad \boldsymbol{R}=\boldsymbol{R}^{(\mathrm{II})}-\boldsymbol{R}^{(\mathrm{I})} \tag{6.254}$$

Combining Eqs. (6.242), (6.247), (6.252), (6.253), and (6.254) and performing the Fourier inverse transform, it is obtained

$$\begin{aligned}&\bar{\boldsymbol{\Sigma}}_2(x_1,0,p)=-(\mathrm{i}/2\pi)\int_{-a}^{a}\bar{\boldsymbol{\psi}}(\xi,p)\mathrm{d}\xi\int_{-\infty}^{\infty}(1/s)\boldsymbol{M}\mathrm{e}^{-\mathrm{i}s(\xi-x_1)}\mathrm{d}s,\quad |x_1|<\infty\\&\boldsymbol{M}=\boldsymbol{R}^{(\mathrm{II})}\boldsymbol{R}^{(\mathrm{I})}\boldsymbol{R}^{-1}=\boldsymbol{R}^{(\mathrm{I})}\boldsymbol{R}^{(\mathrm{II})}\boldsymbol{R}^{-1}\end{aligned} \tag{6.255}$$

Equation (6.255) is a singular integral equation, and its singular behavior is determined by the asymptotic behavior at infinity of the kernel function $s^{-1}\boldsymbol{M}(s,p)$. When $s\to\infty,\boldsymbol{Y}_j^{(\mathrm{N})},\boldsymbol{Y}_j^{(\mathrm{N})-1}$ approach the static values, so are finite. At the static case $\boldsymbol{A}_2^{(\mathrm{N})}=\bar{\boldsymbol{A}}_1^{(\mathrm{N})},\quad \boldsymbol{B}_2^{(\mathrm{N})}=\bar{\boldsymbol{B}}_1^{(\mathrm{N})}$. It is noted that for a constant, $\bar{\boldsymbol{A}}$ is not the Laplace transform of $\boldsymbol{A}$, but is the conjugate value of $\boldsymbol{A}$. From Eq. (6.252) it is obtained

$$\begin{aligned}&\lim_{s\to\infty}(1/s)\boldsymbol{R}^{(\mathrm{I})}=-\boldsymbol{Y}_{2\ \mathrm{static}}^{(\mathrm{I})-1}=\bar{\boldsymbol{Y}}_{1\ \mathrm{static}}^{(\mathrm{I})-1};\quad \lim_{s\to\infty}(1/s)\boldsymbol{R}^{(\mathrm{II})}=-\boldsymbol{Y}_{1\ \mathrm{static}}^{(\mathrm{II})-1}\\&\lim_{s\to-\infty}(1/s)\boldsymbol{R}^{(\mathrm{I})}=-\boldsymbol{Y}_{1\ \mathrm{static}}^{(\mathrm{I})-1};\quad \lim_{s\to-\infty}(1/s)\boldsymbol{R}^{(\mathrm{II})}=-\boldsymbol{Y}_{2\ \mathrm{static}}^{(\mathrm{II})-1}=\bar{\boldsymbol{Y}}_{1\ \mathrm{static}}^{(\mathrm{II})-1}\end{aligned} \tag{6.256}$$

So

$$\begin{aligned}&\lim_{s\to\infty}(1/s)\boldsymbol{M}=\bar{\boldsymbol{Y}}_{1\ \mathrm{static}}^{(\mathrm{I})-1}\left(-s\boldsymbol{Y}_{1\ \mathrm{static}}^{(\mathrm{II})-1}\right)\left[s\left(-\boldsymbol{Y}_{1\ \mathrm{static}}^{(\mathrm{II})-1}-\bar{\boldsymbol{Y}}_{1\ \mathrm{static}}^{(\mathrm{I})-1}\right)\right]^{-1}=\boldsymbol{M}_\infty\\&\lim_{s\to-\infty}(1/s)\boldsymbol{M}=-\boldsymbol{Y}_{1\ \mathrm{static}}^{(\mathrm{I})-1}s\bar{\boldsymbol{Y}}_{1\ \mathrm{static}}^{(\mathrm{II})-1}\left[s\left(\bar{\boldsymbol{Y}}_{1\ \mathrm{static}}^{(\mathrm{II})-1}+\boldsymbol{Y}_{1\ \mathrm{static}}^{(\mathrm{I})-1}\right)\right]^{-1}=-\bar{\boldsymbol{M}}_\infty\\&\boldsymbol{M}_\infty=\bar{\boldsymbol{Y}}_{1\ \mathrm{static}}^{(\mathrm{I})-1}\boldsymbol{Y}_{1\ \mathrm{static}}^{(\mathrm{II})-1}\left(\boldsymbol{Y}_{1\ \mathrm{static}}^{(\mathrm{II})-1}+\bar{\boldsymbol{Y}}_{1\ \mathrm{static}}^{(\mathrm{I})-1}\right)\end{aligned} \tag{6.257}$$

or

$$\lim_{s\to\pm\infty}(1/s)\boldsymbol{M}=(s/|s|)\mathrm{Re}\,\boldsymbol{M}_\infty+\mathrm{i}\mathrm{Im}\,\boldsymbol{M}_\infty. \tag{6.258}$$

By separating the singular part in Eq. (6.255) and then substituting the result into the boundary condition Eq. (6.248), the following singular integral equation can be obtained:

$$\mathrm{Im}\,\boldsymbol{M}_\infty\bar{\boldsymbol{\psi}}+\frac{\mathrm{Re}\,\boldsymbol{M}_\infty}{\pi}\int_{-a}^{a}\xi\frac{\bar{\boldsymbol{\psi}}(\xi,p)}{t-x_1}\mathrm{d}\xi-\frac{\mathrm{i}}{2\pi}\int_{-a}^{a}\bar{\boldsymbol{\psi}}(t,p)\mathrm{d}t\int_{-\infty}^{\infty}\left(\frac{1}{s}\boldsymbol{M}+\boldsymbol{M}_\infty\right)\mathrm{e}^{-\mathrm{i}s(\xi-x_1)}\mathrm{d}s=\boldsymbol{\tau}_0 \tag{6.259}$$

Let λ_i be the eigenvector of $(\mathrm{Re}\,\boldsymbol{M}_\infty)^{-1}\mathrm{Im}\,\boldsymbol{M}_\infty$ and $\boldsymbol{\Lambda}$ be the matrix constituted of λ_i, then we get

$$\boldsymbol{\Lambda}(\mathrm{Re}\,\boldsymbol{M}_\infty)^{-1}(\mathrm{Im}\,\boldsymbol{M}_\infty)\boldsymbol{\Lambda}^{-1} = \mathrm{diag}(\boldsymbol{\Lambda}) = \langle\lambda_i\rangle \tag{6.260}$$

Multiplying both sides of Eq. (6.259) by $(\mathrm{Re}\,\boldsymbol{M}_\infty)^{-1}$, introducing the dimensionless variable $x = x_1/a, \eta = \xi/a$ and using Eq. (6.260), Eq. (6.259) can be reduced to

$$\begin{aligned}&\lambda_i\bar{\Psi}_{\lambda i}(x,p) + \frac{1}{\pi}\int_{-1}^{1}\frac{\bar{\Psi}_{\lambda i}(\eta,p)}{\eta - x}\mathrm{d}\eta + \int_{-1}^{1}\sum_{k=1}^{4}F_{ik}\bar{\Psi}_{\lambda i}(\eta,p)\mathrm{d}\eta = \bar{T}_{0i}(x,p)\\ &[F_{ik}] = -\frac{\mathrm{i}a}{2\pi}\boldsymbol{\Lambda}(\mathrm{Re}\,\boldsymbol{M}_\infty)^{-1}\left\{\int_{-\infty}^{\infty}\left(\frac{1}{s}\boldsymbol{M} + \boldsymbol{M}_\infty\right)e^{-isa(\eta - x)}\mathrm{d}s\right\}\boldsymbol{\Lambda}^{-1}, \boldsymbol{T}_0 = \boldsymbol{\Lambda}(\mathrm{Re}\,\boldsymbol{M}_\infty)^{-1}\bar{\boldsymbol{\tau}}_0\end{aligned} \tag{6.261}$$

The solution of Eq. (6.261) can be expressed by the series of the Jacobi polynomials. Let

$$\begin{aligned}&\bar{\Psi}_{\lambda i}(x,p) = \sum_{n=0}^{\infty}C_{ni}(p)P_n^{(\alpha,\beta)}(x)w_i(x), \quad |x| < 1\\ &w_i(x) = (1-x)^{\alpha_i}(1+x)^{\beta_i}, \quad \alpha_k = \frac{\mathrm{i}}{2\pi\mathrm{i}}\ln\frac{1-\lambda_k\mathrm{i}}{1+\lambda_k\mathrm{i}} - \frac{1}{2}, \quad \beta_k = -\frac{\mathrm{i}}{2\pi\mathrm{i}}\ln\frac{1-\lambda_k\mathrm{i}}{1+\lambda_k\mathrm{i}} - \frac{1}{2}\end{aligned} \tag{6.262}$$

where $P_n^{(\alpha,\beta)}$ is the Jacobi polynomial, C_{ni} is unknown constant, and α_k, β_k determined by Eq. (6.262) are the singular indexes of the dynamical problem and usually are complex numbers. As in usual elastic problem, in the front of the crack tip, there is a small region in which the displacements of the upper and the lower surfaces may be imbedded to each other. Substituting Eq. (6.262) into Eqs. (6.261) and (6.247) in terms of the dimensionless length x, using the orthogonal relation of the Jacobi polynomials and $P_0^{(\alpha,\beta)}(t) = 1$ and the following relations

$$\begin{aligned}&\lambda_k P_n^{(\alpha_k,\beta_k)}(x)w_k(x) + \frac{1}{\pi}\int_{-1}^{1}P_n^{(\alpha,\beta)}(t)\frac{w_k(t)}{t-x}\mathrm{d}t\\ &= \begin{cases}\frac{1}{2}\sqrt{1+\lambda_k^2}P_n^{(\alpha_k,\beta_k)}(x), & |x| < 1\\ \frac{1}{2}\sqrt{1+\lambda_k^2}\left[(x-1)^{\alpha_k}(x-1)^{\beta_k}P_n^{(\alpha_k,\beta_k)}(x) + G_{kn}^{\infty}(x)\right], & |x| > 1\end{cases},\end{aligned} \tag{6.263}$$

the linear algebraic equations of C_n^k ($C_0^k = 0$) can be obtained. Where $G_{kn}^{\infty}(x)$ is the principle part of $P_n^{(\alpha_k,\beta_k)}(x)w_k(x)$ at infinity and is finite at $x = 1$, it is no contribution on the stress intensity factors. Take the first $N+1$ terms. The following $4N$ equations determined by C_n^k can be obtained:

$$
\begin{aligned}
&\frac{1}{2}\sqrt{1+\lambda_k^2}\theta_{j-1}^{(-\alpha_k,-\beta_k)}C_j^k+\sum_{n=1}^{\infty}\sum_{m=1}^{4}Y_{jn}^{km}C_n^m=q_{jk},\quad k=1-4,\quad j=1-N\\
&q_{jk}=\int_{-1}^{1}\bar{T}_{0k}P_{j-1}^{(-\alpha_k,-\beta_k)}(x)w_k(x)\mathrm{d}x,\quad Y_{jn}^{km}=\int_{-1}^{1}H_n^{km}P_{j-1}^{(-\alpha_k,-\beta_k)}(x)w_k(x)\mathrm{d}x\\
&H_n^{km}(x,p)=\int_{-1}^{1}F_{km}(x,t,p)P_n^{(\alpha_k,\beta_k)}(t)w_k(t)\mathrm{d}t\\
&\theta_k^{(\alpha,\beta)}=\frac{2^{\alpha+\beta+1}\Gamma(k+\alpha+1)(k+\beta+1)}{(2k+\alpha+\beta+1)(k+\alpha+\beta+1)k!},\quad \theta_0^{(\alpha,\beta)}=\frac{2^{\alpha+\beta+1}\Gamma(\alpha+1)(\beta+1)}{\Gamma(\alpha+\beta+2)}
\end{aligned}
\tag{6.264}
$$

The singular part of the generalized traction in front of the crack tip $|x|>a$ can be obtained from Eq. (6.255):

$$
\bar{\boldsymbol{\Sigma}}_2(x,0,p)=\mathrm{Re}\,\boldsymbol{M}_\infty\boldsymbol{\Lambda}^{-1}\sum_{n=1}^{N}\begin{bmatrix}(1/2)\sqrt{1+\lambda_k^2}(x-1)^{\alpha_k}(x+1)^{\beta_k}P_n^{(\alpha_k,\beta_k)}(x)C_n^k\\ \cdots\cdots\cdots\cdots\cdots\cdots\cdots\cdots\cdots\cdots\\ \cdots\cdots\cdots\cdots\cdots\cdots\cdots\cdots\cdots\cdots\\ (1/2)\sqrt{1+\lambda_4^2}(x-1)^{\alpha_4}(x+1)^{\beta_4}P_n^{(\alpha_4,\beta_4)}(x)C_n^4\end{bmatrix}
\tag{6.265}
$$

The generalized stress intensity factors in the Laplace transform region are

$$
\bar{\boldsymbol{K}}=[\bar{K}_{\mathrm{II}},\bar{K}_{\mathrm{I}},\bar{K}_{\mathrm{III}},\bar{K}_D]^{\mathrm{T}}=\lim_{x\to1^+}\sqrt{2\pi}\langle(x-1)^{\alpha}\rangle\bar{\boldsymbol{\Sigma}}_2(x,0,p)
\tag{6.266}
$$

After solving $\bar{\boldsymbol{K}}$ in the Laplace transform region, the stress intensity factors in the physical region are obtained by the numerical Laplace inverse transform.

There are many papers to discuss the wave propagation in a piezoelectric material with defects, e.g., Li and Mataga (1996) discussed the semi-infinite crack propagation; Chen et al. (1998) discussed a Griffith moving crack along the interface of two dissimilar piezoelectric materials; Li and Weng (2002) discussed the Yoffe-type moving crack in a functionally graded piezoelectric material; and Ing and Wang (2004a, b) discussed the transient response of a semi-infinite propagating crack subjected to dynamic antiplane concentrated loading on the crack faces. Chen and Liu (2005) discussed the dynamic behavior of a functionally graded piezoelectric strip with periodic cracks vertical to the boundary. Shen et al. (2000) discussed the dynamics mode-III interfacial crack in nonlinear piezoelectric materials. Meikumyan (2007) discussed the diffraction of acoustic and electric waves in piezoelectric medium by an absorbent half-plane electrode.

References

Achenbach J, Keer L, Mendelsohn D (1980) Elastodynamic analysis of an edge crack. J Appl Mech 47:551–556

Assour MB, Elmazria O, Rioboo RJ, Sarry PA (2000) Modelling of SAW filter based on ZnO/diamond/Si layered structure including velocity dispersion. Appl Surf Sci 164:200–204

Auld BA (1973) Acoustic fields and waves in solids. Wiley, New York

Babich VM, Lukyanov VV (1998) Wave propagation along a curved piezoelectric layer. Wave Motion 28:1–11

Banerjee DK, Bao YH (1974) Thermoelastic waves in anisotropic solids. J Acoust Soc Am 56:1444–1454

Biryukov SV, Gulyaev YV, Kryiov VV, Plessky VP (1995) Surface acoustic waves in inhomogeneous media. Springer, New York

Bleustein JL (1968) A new surface wave in piezoelectric materials. Appl Phys Lett 13:412–413

Borcherdt RD (1973) Energy and plane waves in linear viscoelastic media. J Geophys Res 78:2442–2453

Buchen PW (1971) Plane waves in linear viscoelastic media. Geophys J R Astron Soc 23:531–542

Cattaneo C (1958) Sur une forme de l'équation de la chaleur éliminant le paradoxe d'une propagation instantanee. Comptes Rendus de l'Académie des Sciences Paris 247:431–433

Chen J, Liu Z-X (2005) On the dynamic behavior of a functionally graded piezoelectric strip with periodic cracks vertical to the boundary. Int J Solids Struct 42:3133–3146

Chen Z-T, Karihaloo BL, Yu S-W (1998) A Griffith moving crack along the interface of two dissimilar piezoelectric materials. Int J Fract 91:197–203

Cho Y, Yamanouchi K (1987) Nonlinear, elastic, piezoelectric, electrostrictive and dielectric constants of Lithium niobate. J Appl Phys 61:875–886

Danoyan ZN, Pilliposian GT (2007) Surface electro-elastic Love waves in a layered structure with a piezoelectric substrate and a dielectric layer. Int J Solids Struct 44:5829–5847

Darinskii AN, Le Clezio E, Feuillard G (2008) The role of electromagnetic waves in the reflection of acoustic waves in piezoelectric crystals. Wave Motion 45:428–444

Dieulesaint E, Royer D (1980) Elastic waves in solids. Translated by Bastin A, Motz M. Wiley, New York

Du J, Xian K, Wang J, Young Y-K (2008) Propagation of Love waves in prestressed piezoelectric layered structures loaded with viscous liquid. Acta Mech Solida Sin 21:542–548

Erdogan F (1975) Complex function technique. In: Continuum physics, vol II. Academic, New York

Erdogan F, Gupta GD (1972) On the numerical solution of singular integral equations. Q Appl Math 32:525–553

Every AG, Neiman VI (1992) Reflection of electroacoustic waves in piezoelectric solids: mode conversion into four bulk waves. J Appl Phys 71:6018–6024

Ezzat MA, Otman MI, Ei-Karamany AS (2002) State space approach to generalized thermo-viscoelasticity with two relaxation times. Int J Eng Sci 40:283–302

Fischer FA (1955) Fundamentals of electroacoustics. Interscience, New York

Green AE, Lindsay KA (1972) Thermoelasticity. J Elast 2:1–7

Gulyaev YV (1969) Electroacoustic surface waves in solids. Soviet Phys-JETP (A translation of the "J Exp Theor Phys Acad Sci USSR") 9:37–38

Ing Y-S, Wang M-J (2004a) Explicit transient solutions for a mode-III crack subjected to dynamic concentrated loading in a piezoelectric medium. Int J Solids Struct 41:3849–3864

Ing Y-S, Wang M-J (2004b) Transient analysis of a mode-III crack propagating in a piezoelectric medium. Int J Solids Struct 41:6197–6214

Jackson HE, Walker CT (1971) Thermal conductivity, second sound and phonon-phonon interactions in NaF. Phys Rev B 3:1428–1439

Jin F, Wang Z-K, Wang T-J (2001) The Bleustein-Gulyaev (B-G) Wave in a piezoelectric layered half-space. Int J Eng Sci 39:1271–1285

Joseph DD, Preziosi L (1989) Heat waves. Rev Mod Phys 61:41–73
Joseph DD, Preziosi L (1990) Addendum to the paper: heat waves. Rev Mod Phys 62:375–391
Joshi SG, Jin Y (1991) Propagation of ultrasonic lamb waves in piezoelectric plates. J Appl Phys 70:4113–4120
Kaliski S (1965) Wave equation of thermoelasticity. Bulletin de l'Académie Polonaise des Sciences, Série des Sciences Techniques 13:211–219
Khuri-Yakub BT, Kino GS (1974) A monolithic zinc-oxide-silicon convolver. Appl Phys Lett 25:188–193
Krebes ES (1983) The viscoelastic reflection/transmission problem: two special cases. Bull Seismol Soc Am 73:1673–1683
Kuang Z-B (2002) Nonlinear continuum mechanics. Shanghai Jiaotong University Press, Shanghai (in Chinese)
Kuang Z-B (2009) Variational principles for generalized dynamical theory of thermopiezoelectricity. Acta Mech 203:1–11
Kuang Z-B (2011) Some thermodynamic problems in continuum mechanics. In: Piraján JCM (ed) Thermodynamics – kinetics of dynamic systems. Intech Open Access Publisher, Croatia
Kuang Z-B, Yuan X-G (2011) Reflection and transmission theories of waves in pyroelectric and piezoelectric materials. J Sound Vib 330:1111–1120
Kuang Z-B, Zhou Z-D (2012) Waves in pyroelectric materials. ICTAM, Beijing
Kyame JJ (1949) Wave propagation in piezoelectric crystals. J Acoust Soc Am 21:159–167
Landau L (1941) The theory of superfluidity of helium II. J Phys 5:71–90
Laurent T, Bastien FO, Pommier J, Cachard A, Remiens D, Cattan E (2000) Lamb wave and plate mode in ZnO/Silicon and AIN/Silicon membrane application to sensors able to operate in contact with liquid. Sens Actuators 87:26–37
Lavrenchive MA, Shabat VA (1951) Method and theory of complex functions. National Technical and Theoretical Literature Press, Moscow; Лаврентьев МА, Шабат ВА (1951) Метод теории фукций коплексснго переменого. Государственное издадельство. технико – теоретический литературы. Москва
Li S (1996) The electromagneto-acoustic surface wave in a piezoelectric medium: the Bleustein-Gulyaev mode. J Appl Phys 80:5264–5269
Li S (2000) Transient wave propagation in a transversely isotropic piezoelectric half space. Z Angew Math Phys 51:236–266
Li S, Mataga PA (1996) Dynamic crack propagation in piezoelectric materials-part I. electrode solution, J Mech Phys Solids 44:1799–1830
Li C, Weng GJ (2002) Yoffe-type moving crack in a functionally graded piezoelectric material. Proc R Soc Lond A 458:381–399
Li S, To AC, Glaser SD (2005a) On scattering in a piezoelectric medium by a conducting crack. J Appl Mech 72:943–954
Li X-F, Yang JS, Jiang Q (2005b) Spatial dispersion of short surface acoustic waves in piezoelectric ceramics. Acta Mech 180:11–20
Lionetto F, Montagna F, Maffezzoli A (2005) Ultrasonic dynamic mechanical analysis of polymers. Appl Rheol 15:326–335
Liu Y, Wang C-h, Ying CF (1989) Electromagnetic acoustic head waves in piezoelectric media. Appl Phys Lett 55:434–436
Liu H, Wang Z-K, Wang T-J (2001) Effect of initial stress on the propagation behavior of Love waves in a layered piezoelectric structure. Int J Solids Struct 38:37–51
Liu H, Wang T-J, Wang Z-K, Kuang Z-B (2002a) Effect of a biasing electric field on the propagation of antisymmetric Lamb waves in piezoelectric plates. Int J Solids Struct 39:1777–1790
Liu H, Wang T-J, Wang Z-K, Kuang Z-B (2002b) Effect of a biasing electric field on the propagation of symmetric Lamb waves in piezoelectric plates. Int J Solids Struct 39:2031–2049
Liu H, Kuang Z-B, Cai Z-M (2003a) Propagation of Bleustein-Gulyaev waves in a prestressed layered piezoelectric structure. Ultrasonics 41:397–405
Liu H, Kuang Z-B, Cai Z-M (2003b) Application of transfer matrix method in analyzing the inhomogeneous initial stress problem in prestressed layered piezoelectric media. In: Watanabe K,

Ziegler F (eds) IUTAM symposium on dynamics of advanced materials and smart structures. Kluwer Academic Publishers, Dordrecht/Boston/London

Liu H, Kuang Z-B, Cai Z-M (2003c) Love wave in non-homogeneous layered structures. Acta Mech Sin 35:485–488

Liu H, Kuang Z-B, Cai Z-M (2003d) Propagation of surface acoustic waves in prestressed anisotropic layered piezoelectric structures. Acta Mech Solida Sin 16:16–23

Lord HW, Shulman Y (1967) A generalized dynamical theory of thermoelasticity. J Mech Phys Solids 15:299–309

Lu C-K (1984) A class of quadrature formulas of Chebyshev type for singular integrals. J Math Anal Appl 100:416–435

Ma XJ, Liu FS, Zhang MJ, Sun YY (2011) Viscosity of aluminum under shock-loading conditions. Chin Phys B 20:068301–068304

Meikumyan A (2007) On diffraction of acoustic and electric waves in piezoelectric medium by an absorbent half-plane electrode. Int J Solids Struct 44:3811–3827

Mindlin RD (1968) Polarization gradient in elastic dielectrics. Int J Solids Struct 4:637–642

Mineev VN, Mineev AV (1997) Viscosity of metals under shock-loading conditions. J De Phys IV 7(C3):583–585

Nayfen A (1995) Wave propagation in layered anisotropic media. Elsevier, Amsterdam

Noble B (1958) Methods based on the wiener-Hopf technique. Pergamon Press, New York

Ogden RW (1984) Nonlinear elastic deformations. Ellis Horwood/Halsted Press, Chichester/New York

Pang Y, Wang Y-S, Liu J-X, Fang D-N (2008) Reflection of plane waves at the interface between piezoelectric piezomagnetic media. Int J Eng Sci 46:1098–1110

Sharma JN, Pal M (2004) Propagation of Lamb waves in a transversely isotropic piezo-thermoelastic plate. J Sound Vib 270:587–610

Sharma JN, Walia V, Gupta SK (2008) Reflection of piezothermoelastic waves from the charge and stress free boundary of a transversely isotropic half space. Int J Eng Sci 46:131–146

Shen S-P, Nishioka T, Kuang Z-B (1999) Impact interfacial fracture for piezoelectric ceramic. Mech Res Commun 26:347–352

Shen S-P, Kuang Z-B, Nishioka T (2000) Dynamics mode-III interfacial crack in nonlinear piezoelectric materials. Int J Appl Electromagn Mech 11:211–222

Sinha AK, Tanski WJ, Lukaszek T, Ballato A (1985) Influence of biasing stress on the propagation of surface waves. J Appl Phys 57:767–776

Stewart JT, Yong YK (1994) Exact analysis of the propagation of acoustic waves in multilayered anisotropic piezoelectric plate. IEEE Trans Ultrason Ferroelectr Freq Control 41:375–390

Su J, Liu H, Kuang Z-B (2005) Love wave in $ZnO/SiO_2/Si$ structure with initial stresses. J Sound Vib 286:981–999

Thomson WT (1950) Transmission of elastic waves through a stratified solid medium. J Appl Phys 21:89–93

Tiersten HF (1978) Perturbation theory for linear electroelastic equations for small fields superposed on a bias. J Acoust Soc Am 64:832–837

Vernotte P (1958) Les paradoxes de la théorie continue de l'equation de la chaleeur. Comptes Rendus de l'Académie des Sciences Paris 246:3154–3155

Wang X-Y, Yu S-W (2001) Transient response of a crack in piezoelectric strip subjected to the mechanical and electrical impacts: mode-I problem. Mech Mater 33:11–20

Yuan X-G, Kuang Z-B (2008) Waves in pyroelectrics. J Therm Stress 31:1190–1211

Yuan X-G, Kuang Z-B (2010) The inhomogeneous waves in pyroelectrics. J Therm Stress 33:172–186

Zhou Z-D, Yang F-P, Kuang Z-B (2012) Reflection and transmission of plane waves at the interface of pyroelectric bi-materials. J Sound Vib 331:3558–3566

Zhu J-J, Kuang Z-B (1995) On interface crack propagation with variable velocity for longitudinal shear problems. Int J Fract 72:121–144